Technische Universität München
Fakultät für Medizin

The Role of Stem Cell Marker Aldehyde Dehydrogenase 1A3 in Chemoresistance and Ferroptosis in the C6 Glioma Model

Julian Nissen Allgeier

Vollständiger Abdruck der von der Fakultät für Medizin der Technischen Universität München zur Erlangung des akademischen Grades eines Doktors der Medizin genehmigten Dissertation.

Vorsitz: Prof. Dr. Florian Eyer

Prüfer*innen der Dissertation:

1. Prof. Dr. Jürgen Schlegel
2. Priv.-Doz. Dr. Friederike Schmidt-Graf

Die Dissertation wurde am 07.03.2022 bei der Technischen Universität München eingereicht und durch die Fakultät für Medizin am 12.07.2022 angenommen.

Institut für Neuropathologie der Medizinischen Fakultät der
Technischen Universität München

DISSERTATION

The Role of Stem Cell Marker Aldehyde Dehydrogenase 1A3 in Chemoresistance and Ferroptosis in the C6 Glioma Model

zur Erlangung des akademischen Grades Doctor medicinae (Dr.med.)

vorgelegt der Medizinischen Fakultät der Technischen Universität München

von

Julian Nissen Allgeier

aus Ratingen

Gutachter/-in

1. Prof. Dr. med. Florian Eyer
2. Prof. Dr. med. Jürgen Schlegel
3. PD Dr. med. Friederike Schmidt-Graf

Datum der Promotion: 20.09.2022

Für Lara und meine Eltern

Vielen Dank für deine tatkräftige Unterstützung, Jürgen

Glück auf

Contents

Abbreviations

AACR	American Association for Cancer Research
ACSL4	Acyl-CoA synthetase long-chain family member 4
ALDH	Aldehyde Dehydrogenase
AML	Acute Myeloid Leukemia
ASCO	American Society of Clinical Oncology
ATP	Adenosine Triphosphate
BCL-2	B-cell lymphoma 2
bFGF	Basic fibroblast-like Growth Factor
BH	BCL-2 homology motifs
BRCA-1	Breast Cancer Antigen-1
BTSC	Brain Tumor stem cells
BV	Bevacizumab
CD	Cluster of Differentiation
Cdk	Cyclin-dependent kinases
CFA	Colony Forming Assay
CNS	Central Nervous System
CRC	Colorectal Cancer
CRISPR	clustered regularly interspaced short palindromic repeats
CSC	Cancer Stem Cell
CT	Computer Tomography
CT	Chemotherapy
CTLA-4	Cytotoxic T-Lymphocyte Antigen-4
D2GH	D-2-hydroglutarate
DC	Dendritic Cells
DEAB	N,N-diethylaminobenzaldehyde
DFX	Defuroxamine
DGN	Deutsche Gesellschaft für Neurologie
DIMATE	4-dimethylamino-4-methyl-pent-2-ynthioic acid-S-methylester
DMEM	Dulbecco's Modified Eagle Medium
DNA	Deoxyribonucleic Acid
EANO	European Association of Neuro-Oncology
EGFR	Epidermal Growth Factor Receptor
FACS	Fluorescence associated Cell Sorting
FDA	Food and Drug Administration

FLAIR	Fluid-attenuated Inversion Recovery
GBM	Glioblastoma multiforme
GFAP	Glial fibrillary acidic protein
GFP	Glial fibrillary protein
GLUT	Glucose Transporter
Gpx4	Glutathione peroxidase 4
GSH	Glutathione
GTR	Gross Total Resection
Gy	Gray
HCC	Hepatocellular Carcinoma
HSC	Hematopoetic Stem Cell
ICMD	Intracerebral Microdialysis
IDH	Isocitrate Dehydrogenase
IPI	Ipilimumab
KPS	Karnofsky Performance Scale
Lip-1	Liproxstatin-1
LPO	Lipid Peroxidation
MGMT	O6-methylguanine-DNA-methyltransferase
MRI	Magnetic Resonance Imaging
MTIC	Cis 5-(3-N-methyltriazene-1-yl)-imidazole-4-carboxamide
NADPH	Nicotinamide adenine dinucleotide phosphate
NIV	Nivolumab
NSC	Neural Stem Cells
OS	Overall Survival
PCR	Polymerase Chain Reaction
PD-1	Programmed Death-1
PDGF	Platelet-derived Growth Factor
PE	Plating Efficiency
PFS	Progression-free Survival
PI3K/Akt/mTOR	Phosphatydilinositol-3-kinase/Akt/mammalian target of rapamycin
RA	Retinoic Acid
RB	Retinoblastoma
RNA	Ribonucleic Acid
ROS	Reactive oxygen species
RSL-3	RAS-selective ligand-3
RT	Radiotherapy

RTK	receptor tyrosine kinase
SCLC	Small Cell Lung Cancer
SF	Surviving Fraction
sgRNA	Single guided Ribonucleic Acid
SGZ	Subgranular zone
shRNA	Short hairpin ribonucleic acid
SLC7A11	System X_c^-
SP	Side Population
STR	Subtotal Resection
SVZ	Ventricular-subventricular zone
TCGA	Total Cancer Genome Atlas
TGF-β	Transforming Growth Factor-β
TMZ	Temozolomide
TTF	Tumor-treating fields
VDAC	Voltage-dependent anion channel
VEGF	Vascular Endothelial Growth Factor
WHO	World Health Organization

1 Introduction

Glioblastoma multiforme (GBM) is the most common malignant tumor entity of the brain and spinal cord and makes up 14.7% of all central nervous system tumors (Ostrom et al., 2018). It is also its deadliest, with a median survival of about 15 months, despite conventional treatment options including surgery if anatomically feasible, chemotherapy and radiotherapy. The addition of the chemotherapeutical agent Temozolomide in 2005 brought with it some improvement in survival rates compared to the previous standard treatment regimen of surgery and radiotherapy only. Nevertheless, overall prognosis remains poor and a diagnosis with GBM is a death sentence. Its resistance to chemotherapy has been the subject of intense research both in the present and in the past, and numerous attempts have been made to explain why GBM particularly is so resistant and always recurs.

An approach to explain this phenomenon is the cancer stem cell (CSC) theory. It first gained traction in 1997 when Bonnet and Dick identified a primitive leukemic stem cell constantly replenishing non-cycling leukemic blasts in AML (Bonnet & Dick, 1997). By now cancer stem cells have been studied extensively in almost every type of cancer tissue, including glioma. In 2003, brain tumor stem cells (BTSC) were first identified in pediatric brain tumor tissue samples and isolated from the rest of the tumor mass by their differentiation marker CD 133 (Singh et al., 2003). They were found to be integral in maintaining processes such as proliferation and self-renewal of the tumor mass. It is not a stretch to assume that their presence and their lack of expression of common biomarkers of differentiated cells that are otherwise part of the tumor bulk contribute to their ability to bypass or survive conventional therapeutic strategies. Especially relevant for this set of laboratory work is the observation that tumor subpopulations classified as BTSCs not only exist in primary human brain tumor tissues but also in established cultured cell lines. In the C6 glioma cell line, despite having been cultured in laboratories across the world for many years, tumor stem cell subpopulations have been assessed by use of traditional stem cell markers and have been estimated between 0.4-4%. (Kondo et al., 2004; Zhou et al., 2009). Over the course of the last 10 years, biomedical research has continued its search for a better understanding of these stem cell-like subpopulations. In the pursuit for the identification of bio markers, the enzyme aldehyde dehydrogenase (ALDH) has been implicated in many different types of tumors, including gliomas (Rasper et al., 2010; Schafer et al., 2012). ALDHs oxidize aldehydes to carboxylic acids and are vital for cellular processes of detoxification. As such, their expression in tumor tissues could be an integral part of mediating resistance to therapy.

Furthermore, the description of another regulated form of cell death, ferroptosis, has opened up a multitude of questions aimed at better understanding the pathophysiology of a variety

of diseases, among them neurodegenerative diseases and cancer. Ferroptosis is an oxidative form of regulated cell death coupled to accumulation of intracellular iron and inhibition of cellular antioxidant strategies leading to cell destruction that resembles necrotic cell death (Dixon et al., 2012; Tang et al., 2020). Its induction has been implicated in a variety of tumor cell models; notably, scientists were able to induce ferroptosis in hepatocellular carcinoma cells, subsequently decreasing cancer cell viability and improving survival (Nie et al., 2018).

Characterizing glioma stem cells (GSC) in all models used in in vitro research is vital for comprehensive understanding, meaning that while some have shown promising results regarding the use of certain ALDH1 isotypes for characterization of GSCs and even implied relevance for mediating therapy resistance, results need to be validated in other disease models as well. The same is true for the evaluation of ferroptosis in the setting of gliomatous tumors; enhancing tumor therapy by invoking ferroptotic cell death in tumor tissue would pose an exciting new approach for future therapies. Investigating the role of ALDH1A3 in the established glioma cell line C6 will contribute essential information to the relevance and function of glioma stem cells in the tumor microenvironment.

1.1 Glioblastoma multiforme

1.1.1 Epidemiology

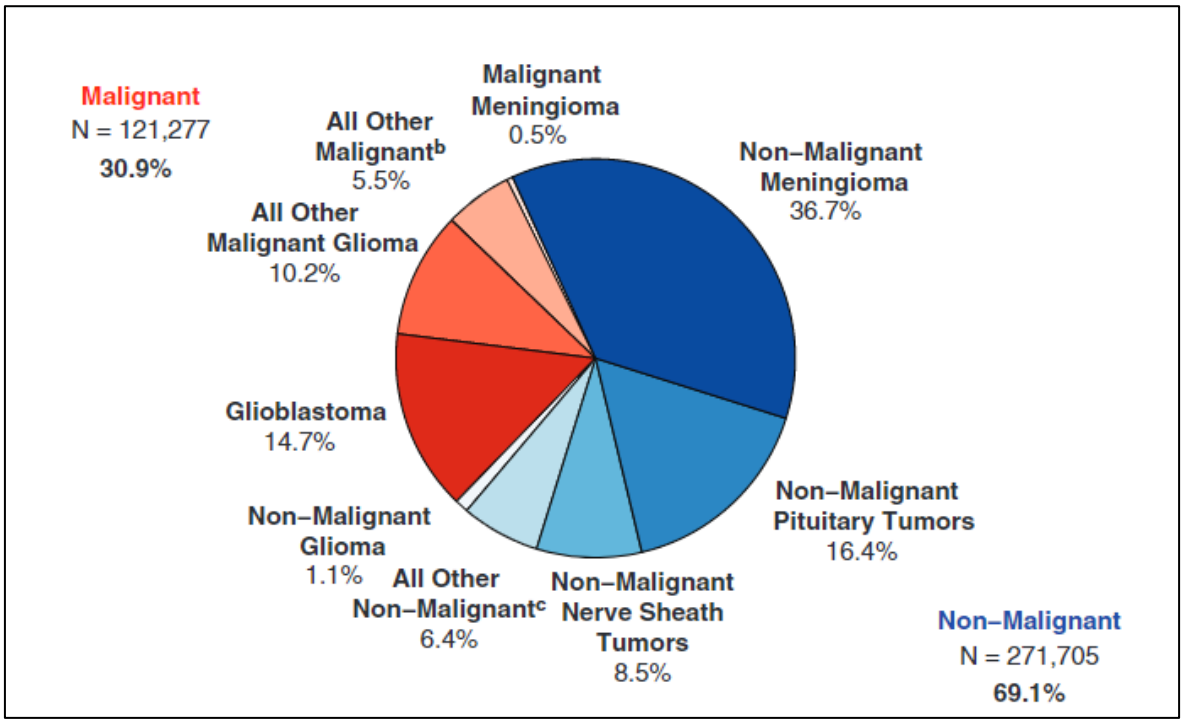

Figure 1. Distribution of primary brain and other CNS tumors in adults (N=392,982) according to the CBTRUS statistical report (Ostrom et al., 2018).

In the United States, Glioblastoma is the third most common tumor of the central nervous system with 14.7% after meningioma (37.1%) and tumors of the pituitary gland (16.5%), while being the most common malignant (47.7%) and gliomatous (57%) tumor entity (Ostrom et al., 2018). The average age at diagnosis of GBM is 64.0 years with an age-adjusted incidence rate of 3.13 per 100,000. Survival in GBM patients is remarkably low, with 1, 2, 5, and 10-year survival rates at 40.2%, 17.4%, 5.6%, 1.4% respectively (Ostrom et al., 2018).

1.1.2 Classification

The 2016 WHO Classification brought about a paradigm shift in the method by which brain tumors are organized and categorized. Prior to 2016, CNS tumors were categorized only according to histopathological markers and clinical parameters such as average survival on a sort of malignancy scale rather than a strict histopathological grading. The publication of the 2016 classification introduced molecular parameters as means by which to grade CNS tumors, revolutionizing classification in the process. These improvements brought about a narrowing of the diagnostic categories. For the classification of GBM, IDH mutation status

was introduced as a subclassification due to its association with primary/secondary GBM status. The entity ‘epitheloid glioblastoma’ joins ‘gliosarcoma’ and ‘giant cell glioblastoma’ as histopathological subtypes under the umbrella of IDH-WT GBM (Louis et al., 2016). Since then, the Consortium to Inform Molecular and Practical Approaches to CNS Tumor Taxonomy (cIMPACT -NOW) has reacted to recent developments in the histopathological and molecular diagnostics including ATRX loss, several Histone H3 mutations, TERT promotor methylation, +7/-10 cytogenetic signature and $BRAF^{V600E}$ mutation, now reflected in the current EANO guidelines (Weller et al., 2020). Most recently, alterations in the MYB-/MYBL1, the MAPK pathway or the H3 gene were included as essential in the proper characterization of tumors of glial origin (Louis et al., 2021).

1.1.3 Molecular Markers

The following is a summary of the molecular markers introduced to further classify GBM and other important molecular markers playing a role, for example, in evaluating prognosis in GBM patients.

1.1.3.1 Isocitrate Dehydrogenase (IDH)

Isocitrate Dehydrogenase (IDH) physiologically acts as enzyme in the oxidative decarboxylation of isocitrate to alpha-ketoglutarate (α-KG) during catalysis and in the citric acid cycle, consuming NAPD+ and generating NAPDH in the process. There are currently three known isotypes of IDH with IDH 1 being localized for intracellular processes in the cytosol and peroxisomes and IDH 2 in the mitochondria respectively (Waitkus et al., 2016). The last isotype, IDH 3, exclusively generates α-KG for the citric acid cycle. IDH enzymes have been implicated in a variety of pathologic processes, including lipogenesis during hypoxia in melanoma cells (Filipp et al., 2012), insulin secretion in pancreatic beta cells (MacDonald et al., 2013) and existence of fatty streaks in murine liver tissue (Koh et al., 2004). IDH 1/2 mutations eventually result in the increased production of D-2-hydroglutarate (D2HG). Accumulation of D2HG inhibits various signaling and metabolic pathways within glial cells, disrupting normal energy production pathways, especially in situations of hypoxia.

In 2008, a full-scale genomic analysis of 105 tissue samples of Glioblastoma multiforme found point mutations in IDH genes associated with tumors of glial origin and an improved overall survival. IDH wild type samples (n=79) provided showed an average overall survival of 1.1 years compared to an IDH mutant (n=11) average overall survival of 3.8 years (Hazard Ratio 3.7) (Parsons et al., 2008), the basis for its inclusion in the newest edition of the WHO classification.

1.1.3.2 MGMT Promoter Methylation

O6-methylguanine-DNA-methyltransferase (MGMT) is located on Chromosome 10q26 and encodes O6-alkylguanine DNA alkyltransferase (AGT), a repair enzyme responsible for removing a methyl group from the O6-Position of Guanine. Generally, chemotherapeutic agents that methylate DNA do so at the N7-position of Guanine. However, about 7% prefer the O6-Position, among them Temozolomide, Dacarbazine, and Procarbazine (Gerson, 2004). Functional AGT activity then predisposes to more effective repair of alkylated DNA segments, thus providing more effective protection from chemotherapeutic side effects in normal cells. On the other side, mutations render cells, specifically cancer cells, more prone to DNA damage and apoptosis (Gerson, 2004). Hegi et al. showed that epigenetic methylation of the MGMT promoter conferred an improved overall survival of 21.7 months (n=46) in a study arm treated with Temozolomide (TMZ) and radiotherapy as compared to radiotherapy alone (overall survival 15.3 months, n=45) (Hegi et al., 2005). Regardless of therapy, MGMT status was a prognostically relevant marker. No statistically significant difference could be concluded between the two treatment arms in patients with unmethylated MGMT promoter status (Hegi et al., 2005).

1.1.3.3 Tp53

Tp53 is a transcription factor dubbed ‘guardian of the genome’ as early as 1992 (Lane, 1992) for its essential role in preventing cells with DNA damage from further proliferation. Molecular alterations of the Arf-MDM2-p53 pathway are implicated in 84% of all GBM and about 94% of all GMB cell lines. Individual mutations of p53 are deregulated in 22% of those cases (Zhang et al., 2018).

1.1.3.4 PI3K/Akt/mTOR Pathway

The Phosphatydilinositol-3-kinase/Akt/mammalian target of rapamycin (PI3K/Akt/mTOR) pathway is crucial in cell cycle regulation and is involved in a variety of cell growth signals that are enacted by mTOR at the end of the signal transduction chain (X. Li et al., 2016) and activated through membrane-spanning receptor tyrosine kinase (RTK) complexes. Phosphorylation of Phosphatidylinositol-4,5-biphosphate (PIP_2) to Phosphatidylinositol-3,4,5-triphosphate (PIP_3) by PI3K enables activation of Akt and subsequently inhibition of tuberous sclerosis complex (TSC) 1/2, thereby activating mTOR, causing cell growth. The PIK3CA gene, encoding for p110α, the catalytically active protein of the complex, and was found in a significant amount of investigated GBM tissue samples. As part of Cancer Genome Atlas (TCGA) research, the PIK3R1 gene, encoding for p85α, a protein with inhibitive capability when bound to p110α, has also been found mutated in a significant part of GBM tissue samples assessed, mediating constitutive activation of p110α and therefore

mTOR activation further downstream (Cancer Genome Atlas Research, 2008). The most commonly mutated RTK in glioblastoma is the epidermal growth factor receptor (EGFR), with approximately 60% of glioblastomas harboring mutations resulting in activation of cell signaling cascades such as the PI3K pathway (Brennan et al., 2013). Furthermore, mutations in the phosphatase tensin homologue (PTEN) gene, a tumor suppressor that dephosphorylates PIP_3 to PIP_2, have been associated with GBM metastasis and with resistance to common therapy options (Jiang et al., 2007; Zhang et al., 2015).

1.1.3.5 Retinoblatoma (RB) and Cyclin-dependent kinases (Cdk)

The retinoblastoma (RB) pathway is essential for DNA replication and cell proliferation. Rb thereby exhibits an inhibitory function, preventing continuity of the cell cycle by prevention of S phase activation. Type D cyclins are enzymes that are responsible for assembling enzymatic complexes that, after G1 phase, initiate entry into S phase where DNA replication takes place. Cyclin-dependent kinases (Cdk), specifically Cdk4 and Cdk6, accumulate in the nucleus and through collaboration with Cyclin E-dependent kinase 2 (Cdk2) cause phosphorylation of Rb and therefore activation of S-phase and proliferation (Sherr & McCormick, 2002). The TGCA has revealed ~78% of glioblastoma tissue samples to have mutations including Cdk4/6 amplification or Rb mutation, making this pathway an attractive target for researching additional therapy options.

1.1.3.6 Histone H3 Mutations

Histone H3 mutations are commonly found in glioma, including those of childhood and early adulthood. The variant H3.3K-27M was found in pediatric patients (36%) and rarely in young adults (3%) while variant H3.3-G34V occurred mostly in older patients with a median age of 20 (Schwartzentruber et al., 2012). The fourth edition of the WHO classification in 2016 included H3-mutant glioma as its own entity independent of GBM (Louis et al., 2016).

1.1.3.7 TERT Promotor Methylation

Activating mutations of telomerase reverse transcriptase (TERT) result in telomerase activation and occur frequently (70%) in primary GBM and are associated with 1p19q loss and IDH1/2 mutations (Arita et al., 2013). Prognostic relevance is attributed to the combination of TERT mutation and MGMT-unmethylated status where overall survival compared to MGMT-methylated status was poorer (Arita et al., 2016).

1.1.4 Clinical Presentation

The array of clinical symptoms a patient might experience varies depending on the pathogenesis and the location of the tumor. Initial symptoms are unspecific and include

headaches, nausea and vomiting, gait imbalance, seizures, or other focal neurological deficits (Omuro & DeAngelis, 2013). Most commonly, seizures, cognitive disorder and aphasia are observed (Posti et al., 2015). Seizures often commence as focal seizures and headaches tend to correlate with macroscopic location of the tumor bulk (Alexander & Cloughesy, 2017).

1.1.5 Diagnostics

The guidelines of the Deutsche Gesellschaft für Neurologie (DGN) specifying the diagnostic process for glioma are currently under revision with the latest edition having been released in 2015. As it stands, Magnetic Resonance Imaging (MRI) with contrast is the diagnostic modality of choice when GBM, or, more generally, brain tumor, is suspected due to superior contrast and more precise tissue differentiation. MRI sequences used most commonly include pre- and post-Gadolinium T1, T2, FLAIR. Computer tomography (CT) is indicated when MRI is unavailable or contraindicated, for example due to patient characteristics such as a pacemaker. CT information is less valuable but has its niche, for example when differential diagnosis is Oligodendroglioma due to its tendency to show intratumoral calcifications (Mabray et al., 2015). In MRI, GBM appears as a contrast-enhancing lesion with irregularly-enhancing margins, heterogeneous interior signal and the possibility of central necrosis and hemorrhage. Considerable diagnostic difficulty is associated with the phenomenon of pseudoprogression, an imaging curiosity seen in patients after adjuvant radiochemotherapy with TMZ. In these patients, during their first follow-up MRI, the lesion appeared as increasingly contrast-enhanced and indicated tumor progression but stabilized afterwards (de Wit et al., 2004). Notably, Brandes et al. found that in a cohort with diagnosed GBM and concomitant radiochemotherapy status of MGMT-Methylation correlated with pseudoprogression and later clinical stabilization (Brandes et al., 2008).

Pseudoprogression might cause physicians to alter therapy that is actually effective due to the assumption that increase of contrast-enhancing lesions on MRI equals actual progression of disease. This dilemma is illustrated by Chamberlain et al., finding that in a cohort where 26 of 51 GBM patients were judged to have failed radiochemotherapy based on both clinical evaluation and neuroimaging and proceeded to surgery with histopathology for 7 of them (13.7%) merely revealing tumor necrosis without evidence of live tumor cells (Chamberlain et al., 2007).

Lastly, tissue diagnosis is essential in order to classify the lesion and enable further planning of therapy. Less frequently used diagnostic modalities like EEG and spinal taps are mainly used to exclude differential diagnoses and manage complications.

1.1.6 Therapy

1.1.6.1 Surgery

Current standard of care is the resection of the tumor. Surgery is beneficial not only for its obvious role in removing the tumor but also because tissue diagnosis is necessary to confirm the diagnosis of GBM and provide the patient with an accurate prognostic outlook. Gross total resection (GTR) is preferred over subtotal resection (STR). In a large meta-analysis, Brown et al. concluded that GBM patients undergoing GTR were 61% more likely to survive 1 year, 19% more likely to survive 2 years and 51% more likely to be progression free after 12 months (Brown et al., 2016). Regardless, when GTR is not an option due to location of the tumor or individual patient characteristics, STR promises improved overall survival compared to biopsy alone.

In recurrent GBM, similar standards apply. Small center studies have shown that resection of tumor tissue enables the physician to confirm a relapse of GBM and, regardless of extent, improves progression-free survival (PFS) (Bloch et al., 2012).

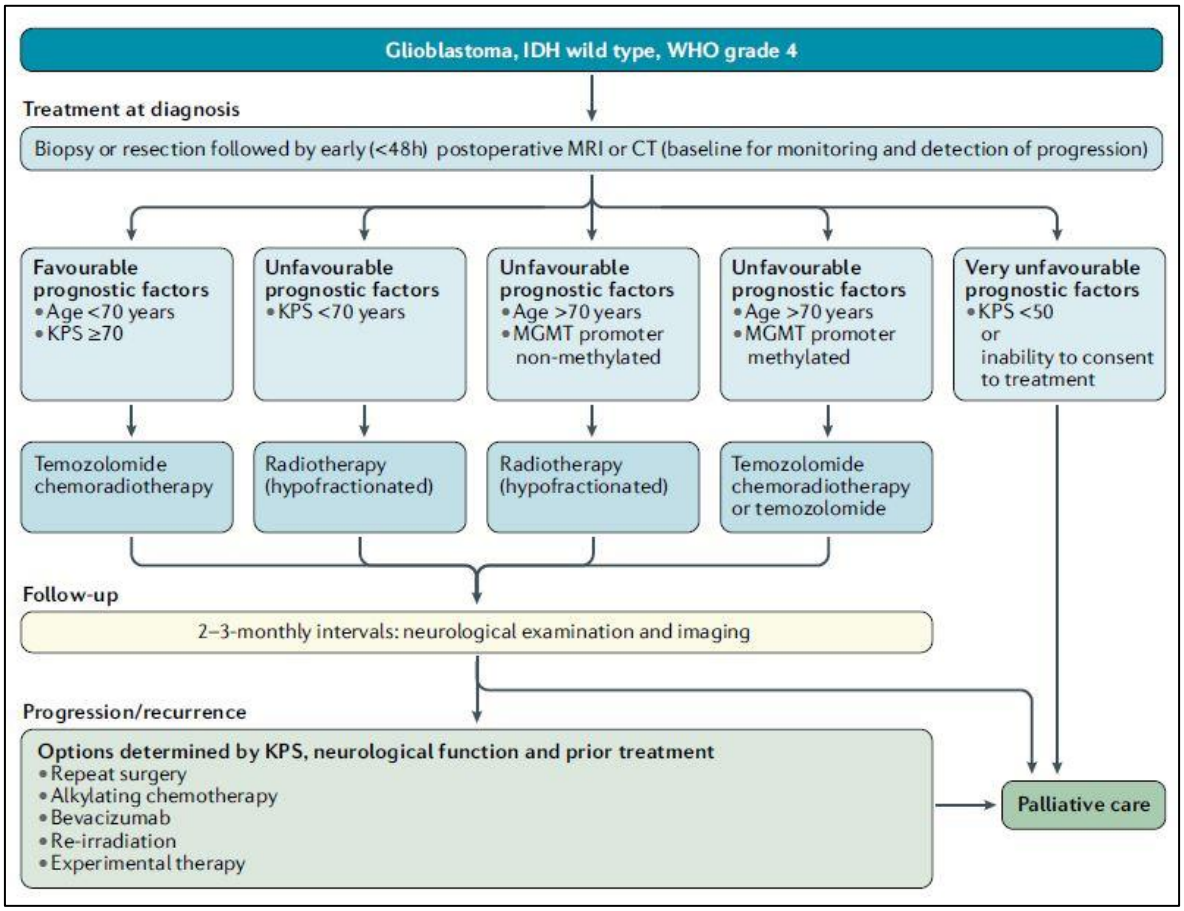

Figure 2. GBM treatment algorithm according to European Association of Neuro-Oncology (EANO) (Weller et al., 2020).

1.1.6.2 Radiotherapy (RT)

Before the introduction of other treatment modalities in the therapy of GBM, resection alone offered a median survival of only 3-6 months. Around 1980, the benefit of radiotherapy post-surgical intervention was first elucidated and subsequently became standard of care as it was found to improve average survival up to a year (Walker et al., 1980). The current RT regimen as stated in the 2017 ASCO guidelines includes fractionated radiotherapy as soon as safely permissible, but generally 3-6 weeks post-surgery (Sulman et al., 2017). The dose to be administered is 60Gy in 2Gy portions over 30 days, or 6 weeks. This applies for patients <70 years and in generally good health. Elderly patients and those with a Karnofsky Performance Scale (KPS) <50 show no benefit with the fractionation mentioned above and are recommended hypo fractionated radiotherapy (i.e. 40Gy in 15 sessions) or external beam RT (Sulman et al., 2017).

1.1.6.3 Chemotherapy (CT)

Chemotherapeutical agents were regarded as largely ineffective in the early 2000s. In 2005, however, research now regarded as a modern landmark in glioma therapy concluded that Temozolomide, a DNA-methylating agent given concomitantly with radiotherapy after surgical resection, gave patients a significant benefit in overall survival (Stupp et al., 2005). Other chemo- or immunotherapeutic agents that have been tested in clinical trials in the recent past include Bevacizumab, Cilengitide, Rindopepimut (Gilbert et al., 2014; Nabors et al., 2015; Zussman & Engh, 2015). Prior to TMZ, platins and Nitrosureas like Carmustine had been under investigation for use in GBM therapy and showed no significant survival benefit but caused severe, mostly hematologic, side effects, and were thus abandoned.

1.1.6.3.1 Temozolomide (TMZ)

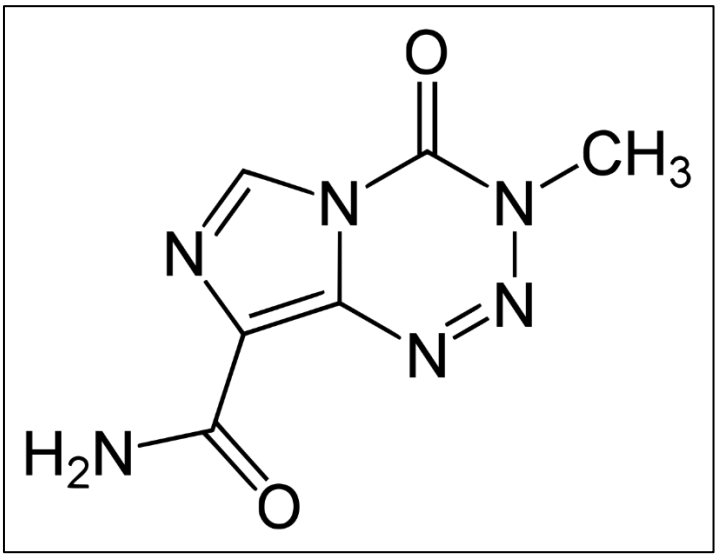

Figure 3. Molecular structure of temozolomide

Temozolomide is an imidazotetrazinone and a derivative of Mitozolomide, a drug used in preclinical trials for small cell lung carcinoma (SCLC) and melanoma which were precluded due to severe myelosuppressive side effects (Gundersen et al., 1987). FDA approved in 1997, Temozolomide first showed promise in Phase I trials and stood apart from Mitozolomide specifically due to its significantly improved side effect profile (Newlands et al., 1992). Temozolomide is a prodrug, the active metabolite is 5-(3-N-methyltriazene-1-yl)-imidazole-4-carboxamide (MTIC). This chemical conversion occurs readily at physiologic pH in the presence of water. Temozolomide, when administered orally, has a plasma availability of 98% and a half-life of roughly 1.81 hours (Newlands et al., 1997). Temozolomide is a methylating agent, adding methyl groups most prominently at the N7-Position of Guanine. Upwards of 70% of methylation reactions occur here, with about 9.2% and 5% occurring at N3-Adenine and O6-Guanine, the site usually employed by other methylating agents, respectively (Newlands et al., 1997). In the early 2000s, TMZ became the first oral chemotherapeutic agent to effectively increase overall survival in Glioblastoma patients. First given concomitantly with radiotherapy and after completion of RT courses adjuvantly for six weeks, TMZ increased median survival from 12.1 months to 14.6 months (Stupp et al., 2005). The Comprehensive Cancer Center Munich recommends TMZ be given at doses of 75mg/m² body surface area concomitantly to radiotherapy and after completion of RT for 5 days per week for 6 weeks at a dose of 150-200mg/m2 body surface area.

1.1.6.3.2 Bevacizumab

An Anti-VEGF antibody, Bevacizumab (BV), effectively inhibits neoangiogenesis. While this is useful for example in patients with diabetic retinopathy, where neovascularizations of the retina inhibit vision concomitantly with other inhibiting factors, Bevacizumab has also become a useful therapeutic agent in the treatment of several cancers expressing high levels of VEGF. Tumor cells in tumor entities, especially fast-growing ones like GBM, regularly become subject to hypoxic conditions; thus, tumors that have the ability to deal with those conditions by overexpressing VEGF can easily resupply all affected areas with oxygen.

Bevacizumab was first reported to provide improved outcome combined with a manageable side effect profile in colorectal cancer and metastatic renal cell carcinoma (Kabbinavar et al., 2003). Bevacizumab was found to provide an average median survival of 9.2 and 8.7 months in treatments groups receiving BV and BV+ Irinotecan, a Topoisomerase-Inhibitor, respectively (Friedman et al., 2009). A study targeting BV in newly diagnosed GBM compared BV, RT, and TMZ with RT and TMZ, finding an increase in progression-free survival (PFS) of 10.6 months compared to 6.2 months but no significant differences in overall survival, 72.4% vs. 66.3% at 1 year, respectively (Chinot et al., 2014).

1.1.6.4 Immunotherapy

The advent of immunotherapy, most notably inhibition or blockade of cytotoxic-T-lymphocyte antigen-4 (CTLA-4) and programmed cell death protein 1 (PD-1) and its ligand, PD-L1, has caused significant stir in the GBM research community.

Currently, trials with mono- or combined check point inhibition are ongoing in glioblastoma research. Most notably, the CHECKMATE 143 trial in phase I enrolled 40 patients to assess tolerability of Nivolumab (NIV) with or without Ipilimumab (IPI). While noting a tolerable side effect profile, all cohorts (NIV mono, NIV1/IPI3 and NIV3/IPI1) showed comparable overall survival (OS) at 7.3 -10.4 months (Omuro et al., 2018). Unfortunately, phase III of the study could not produce significantly improved survival compared BV in patients with recurrent GBM (Reardon et al., 2020).

Pembrolizumab, another PDL-1 inhibitor finding extensive therapeutical use in other tumor entities, has also been shown to have therapeutic relevance in GBM; specifically, Pembrolizumab showed significant increase of overall (OS) (417d vs. 228,5d, Hazard Ratio (HR) 0,39) and progression-free survival (PFS) (99,5d vs 77,5d, HR 0,43) when administered prior to surgical resection as opposed to the more conventional adjuvant approach (Cloughesy et al., 2019).

1.1.6.5 Tumor Vaccines and Other Therapeutic Approaches.

Rindopepimut is a 13-amino acid sequence vaccine spanning the length of the EGFR-variant III which is amplified in in 25-30% of GBM patients (Pelloski et al. (2007). Preliminary single arm studies showed some promise but a Phase III-study was terminated early for futility after an interim analysis revealed no significant differences in overall survival between the study arms (Weller et al., 2017).

Dendritic cells (DC), as antigen-presenting cells, have a substantial role in presenting tumor antigens and initiating an immune response. The process of using those cells for tumor therapy, however, requires extraction of autologous DC, loading with tumor antigen and reintroduction to the patient (Oh et al., 2015). A recently concluded Phase III-trial investigating the addition of the DC vaccine DCVax-L to standard therapy has cautiously reported improved overall survival, implicating there may be light at the end of the tunnel (Stepanenko & Chekhonin, 2018).

Tumor-treating fields (TTF) inhibit cell division by causing mitotic arrest and apoptosis of rapidly dividing cells through delivery of low intensity, medium frequency electrical fields (Kirson et al., 2007). Recent research has found an increase of PFS in patients treated with TTF and adjuvant TMZ compared to adjuvant TMZ alone, 6.1 vs. 4.0 months respectively, and an increase in overall survival of 20.9 vs. 16.0 months, respectively (Stupp et al., 2017). Patients had a 1/8 chance to be alive at the 5-year point, compared with 1/20 for the control group.

1.2 Cancer and the Evolution of Cancer Theory

The transformation of a physiologically functioning cell into one that is capable of forming a tumor is tissue-dependent and subject to environmental conditions and genetic alterations. Scientific approaches to understanding the biology of cancerous transformation have been subject of intense research for over 50 years.

In 2000, a true “hallmark” review written by D. Hanahan and R. Weinberg introduced the scientific community to six “hallmarks of cancer”, an attempt to classify the capabilities a cell must have to transform into one capable of forming a tumor into six distinct categories. These include self-sufficiency from growth signals, colorfully illustrated by GBM through the production of PDGF, insensitivity to anti-growth signals, often mediated by expression and secretion of TGFβ, means of evading apoptosis, for example by inactivation of p53, a breach of the mortality barrier enabling them with endless replicative potential, tissue invasion and metastasis, and sustained angiogenesis through expression of VEGF

(Hanahan & Weinberg, 2000). These hallmarks still provide an important foundation to understanding the evolution of cancer in human beings. In 2011, with more than a decade of additional research under their belt, Hanahan and Weinberg amended their initial hallmarks to include others, now featuring tumor-growth enabling characteristics and other emerging hallmarks. They suggest that genome instability and increase of mutational frequency in the face of an already genomically-deranged tumor cell population further promote selection of more tumorigenic cells; further, they review innate inflammation within tumor populations not only as an immune response by the host to a pathological process, but rather also as a means by which this tumor promotes its growth, even from microscopic neoplastic processes to full-blown macroscopic tumors (Hanahan & Weinberg, 2011). Hanahan and Weinberg also chose to include a reprogrammed energy metabolism as an emerging hallmark, paying their dues to the comparatively ancient observation by Otto Warburg in the 1930s that cancer cells commonly reprogram their energy metabolism from the considerably more efficient way of generating ATP by oxidative phosphorylation in the mitochondria to aerobic glycolysis along with upregulation of GLUT1 transporters to increase access of the cell to Glucose. Lastly, immunoevasion is proposed as an emerging hallmark in an effort to include knowledge gained from various studies investigating tumorigenesis in immunodeficient mice as compared to immunocompetent mice and the ability of a immunocompetent host to suppress tumor growth after transplantation (Hanahan & Weinberg, 2011). While these conceptual reviews have certainly shaped our approach to understanding how tumors grow, it is important to ponder its limitations as well. As Lazebnik points out, with the exception of invasion and metastasis, these suggested criteria of malignancy are shared by benign tumors as well, thus not necessarily hallmarking cancer per se (Lazebnik, 2010).

Emerging in the last decade, the investigation of the microenvironment of tumors has contributed to an increasing amount of evidence that microscopic tumoral conditions such as hypoxia in the setting of rapid growth of the tumor mass selects for cells with increased MGMT expression and thus increased resistance to chemoradiotherapy in human glioblastoma cell populations (Okada et al., 2014).

1.2.1 Competing Cancer Initiation Theories

Generally, research in cancer biology has focused on two different and competing theories as to the mechanisms behind tumor growth. The stochastic model of tumorigenesis has historically proposed that every cell in a tumor mass has the ability to dissociate, invade, and form a new tumor mass on its own. Cancer stem cell (CSC) theories, however, postulate that a smaller subpopulation of cells within the tumor mass drives growth,

invasion, and metastasis while the rest of the cells are responsible for maintenance and homeostasis of tumor. Historically, the CSC theory gained track on the back of foundational hematologic studies where primitive leukemic stem cells were found to constantly replenish leukemic blast cycles in AML (Bonnet & Dick, 1997). A workshop held in 2006 by the American Association for Cancer Research (AACR) set out to address the emerging concept of CSC defining them as cells within a tumor with the capability to self-renew and to cause the heterogeneous lineages of cancer cells that comprise that tumor. This is in contrast to initially circulating definitions in which a CSC was defined as a stem-like progenitor cell that acquired oncogenic mutations thereby causing it to be able to growth into a tumor (Fialkow et al., 1977). Recent clinical studies specifically on CSC in breast cancer have found increased relative sizes of CSC population after conventional chemotherapy, indicating its active role in selecting for cancer stem cells (Creighton et al., 2009; Li et al., 2008).

Conventional cancer therapy, specifically chemotherapy, targets cells that are rapidly proliferating. Assuming that most cells within a tumor population are within such a phase of the cell cycle, therapy generally results in elimination of such cells and reduction of tumor size, thereby mimicking a response seemingly successful in eliminating the tumor. In different tumor populations, however, researchers have addressed cell cycle states in CSC populations. In HCC, CD13 was identified as a marker for dormant CSC in the G0 phase of the cell cycle (Haraguchi et al., 2010). Thus, if CSC are dormant and non-proliferating, they evade chemotherapeutic effects and if they are responsible for driving tumor growth, the tumor will resubstantiate and will result in local recurrence of the tumor. Dormancy in cancer is not a novel concept. Patient groups with different cancer entities experience metastatic relapse up to decades after remission. It is thought that cells that have disseminated from the initial tumor mass and extravasated in a different location with a different microenvironment enter a G0-G1 cell arrest, truly inactive, only to resurface years later after acclimatization to their new environment (Aguirre-Ghiso, 2007).

CSC in solid tumors were found to be small side populations identified by assay selecting for Hoechst-Dye excluding cells that could be sorted for (Clarke et al., 2006). Similar observations were made in research identifying minor (0.4%) cell populations in glioma cells in vitro that were able to be sustained on serum-free growth medium with PDGF/bFGF alone and over the course of the experiments, expressed markers for both neural and glial cell populations (Kondo et al., 2004). The preface “small” sparked controversy and questions regarding the legitimacy of the CSC theory considering that other groups had claimed to identify with the same methods side populations with stemness properties of up to 25%. Furthermore, other research groups have since established that within tumor populations

there can be significantly less than just a minor SP of cells that drive tumor growth. In Eμ-myc mice, pre-B/B lymphoma could be initiating by injection of as little as one cell (Kelly et al., 2007) regardless of that cell's progeny, suggesting that possibly any cell within a tumor mass can spark tumor growth. While in the ensuing time, the definition of the CSC theory and CSC per se has been adjusted to allow for reportedly widely varying sizes of stem cell population within different kinds of tumors, these early definitory difficulties illustrate a need for continuous efforts going towards characterization of tumor stem cell subpopulations specific for all tumor entities.

1.2.2 The CSC Hypothesis in Neuro-Oncology

In 2003, investigation of tumor stem cell populations within CNS neoplasms gained significant ground. Singh et al. used CD 133 to isolate brain tumor stem cell (BTSC) populations not expressing Nestin or GFAP as neural and astrocytic cell markers, respectively (Singh et al., 2003). Pediatric brain tumors were shown to preferentially express genes known to be expressed in neural stem cells (NSC), including musashi-1, Sox2, bmi-1, and CD133 (Hemmati et al., 2003). A significant adduct to understanding the importance of stem cells in the formation of CNS tumors and specifically GBM is understanding that regular stem cells are generally not found everywhere within a certain tissue but rather reside within a specific microenvironment, the stem cell niche. These niches are zones in which the body retains stem cells for possibility of tissue restitution after completion of developmental stages. There, they are located in close proximity to endothelial cells and vascular cells and generally regulated by a variety of vascular-derived growth factors (Gilbertson & Rich, 2007). This is important information not only in making the link to stem cell populations within GBM but to those in a variety of different cancers. Supplying nutrients to a rapidly expanding colony of cells is vital for its continued growth and thus angiogenesis has long been known to play a significant role in the formation and sustenance of a tumor. As has already been stated, VEGF-Inhibitors like Bevacizumab have proven effective in the right setting in cancer therapy, even for GBM. Research has, however, shown a specific link not only to the viability of the tumor bulk as a whole but also to the viability of CSC. Bao demonstrated that CD133+ GBM cells but not CD133- GBM cells freshly resected have the ability to readily form highly-vascularized, hemorrhagic tumors in a mouse model (Bao et al., 2006). Thus, gaining an increased understanding of the microenvironment of tumors and specifically that of the stem cells within is a vital step towards identifying new targets for therapeutic approaches.

In the brain, stem cells can be found in the ventricular-subventricular zone (SVZ) and the subgranular zone (SGZ) at the interface of the hilus and dentate gyrus (Fuentealba et al.,

2012). A subpopulation of stem cells with astroglial properties named B1 cells exemplify the highly specialized architecture of CNS stem cells, with long processes contacting surrounding blood vessels and a single cilium directly contacting the ventricle itself (Mirzadeh et al., 2008; Shen et al., 2008).

1.2.3 Traditional Stem Cell Markers

Understanding and defining markers specific to cancer stem cells is a daunting but essential task, not only because identifying adequate markers or combination or markers will enable the research community to study specific stem cell populations more accurately, but also because they might pose specific therapeutic targets.

Historically, CD 133 and CD 44, among others, have been used to isolate stem cell populations from tumor cells in vivo and in vitro (Ishimoto et al., 2011; Miraglia et al., 1997). Up to this point, CD133 remains the most used marker for isolation of stem cell populations. However, since these markers are shared by normal stem cells and even other non-stem cell-like cells, it is likely that isolation of stem cells by any one marker is inadequate. In vitro research with different colorectal cancer (CRC) cell lines showed differential expression of stem cell markers within their population (Wang et al., 2012) and thus confirms the observation that, to be certain a true cancer stem cell population is actually isolated, a combination of markers needs to be identified in said cell population.

The enzyme Aldehyde Dehydrogenase (ALDH) has gained significant traction within the scientific community as a reliable cancer stem cell marker.

1.2.4 Aldehyde Dehydrogenases

Aldehyde Dehydrogenases are a group of 19 enzymes located ubiquitously throughout the various tissues and with varying target substrates and metabolites. Depending on the isotype, ALDHs can be found in virtually every compartment of the cell and even in several different compartments at once. Several ALDHs play pivotal roles in developmental processes through producing retinoic acid (RA) from retinal. Deficiencies in ALDH enzymes have consequently been implicated in a variety of diseases, including Sjögren-Larsson Syndrome, Type II hyperprolinemia, hyperammonemia, and Alzheimer's types (Marchitti et al., 2008). ALDH enzymes furthermore play an important role in maintaining cell homeostasis through detoxification. In the body, this is needed most prominently in the accumulation of aldehydes during breakdown of cellular membranes through a process called lipid peroxidation (LPO). Aldehydes created during LPO cause accumulation of DNA damage and DNA adducts and are implicated in carcinogenesis, justifying interest in their status as biomarkers for different cancers (O'Brien et al., 2005). Aldehyde production is

associated with the metabolism of alcohols, amino acids, certain chemotherapeuticals (Cyclophosphamide), and the breakdown of neurotransmitters such as GABA, Serotonine, Adrenalin and Noradrenalin. During LPO, the most common toxic aldehydes produced are 4-hydroxy-2-nonenal (4-HNE), malondialdehyde (MDA) and methyglyoxal, among others (Singh et al., 2013).

1.2.5 ALDH Isotypes and their Role as Prognostic Markers

During tumor growth, cell growth resulting in oxidative stress, breakdown of cell membranes and accumulation of aldehyde metabolites are a common occurrence, indicating that readily available ALDH enzymes yield distinct survival benefits for tumor cells in need of detoxification. Thus, it is reasonable to investigate whether ALDH enzymes can serve as prognostic markers for different cancers. ALDH1A3 has been shown to be associated with poorer prognosis, including more undifferentiated, larger tumors in gallbladder cancer (Yang et al., 2013). In gastric cancer of both the intestinal and diffuse type, ALDH1A3 and ALDH1L1 were found to correlate with poorer OS while no significant correlation could be evaluated for ALDH1A1 (K. Li et al., 2016). In some subgroups of ovarian cancer, ALDH1A2 expression is associated with worse prognosis and OS; in contrast, other subgroups show strong correlation of ALDH1A3 and better OS, once again reiterating that associations are isotype, tissue, and, moreover, cancer genotype-specific (Ma & Zhao, 2016).

1.2.6 ALDH Isotypes and CSC

With the advent of the Aldefluor Assay, it has become increasingly easy to identify and isolate ALDH1-hi cell populations. Using conventional stem cell markers, hematopoietic stem cells (HSC) have been isolated and shown to possess high ALDH1 activity (Burger et al., 2009). Breast cancer research has repeatedly shown that cells that express stem cell marker CD44 and have high ALDH1 activity are significantly more metastatic than those CD44- and ALDH-lo (Croker et al., 2009). Furthermore, there is evidence that within tissues, ALDH-hi cells reside in locations in which stem-like and other progenitor cells are commonly located, further fueling the practicality of ALDH1 as a CSC marker (Deng et al., 2010). To be fair, the authors of this publication do conclude that if this localization were to become an important criterion, then it could only act as such in tissue that have otherwise weak ALDH1-expression. ALDH1 expression in CSC is so intriguing not only because ALDH plays a role in marginalizing oxidative stress and cellular breakdown in tumor masses undergoing therapy but also because it plays an active role in retinoic acid metabolism, thereby enabling the cell to remain in an undifferentiated, stem cell-like state. Investigation of ALDH expression with the Aldefluor Assay must be done with caution, however; Marcato et al. note that based on an analysis of available literature, Aldefluor activity is not specific

to ALDH1A1 activity and that, specifically in breast cancer models, the only isoform that reliably correlated with ALDH activity in the Aldefluor Assay was ALDH1A3 (Marcato et al., 2011).

In glioma models, early experiments in our laboratory indicated that ALDH1 expression positively correlated with an ability to form neurospheres, indicative of a stem cell-like cell capabilities, while ALDH1- cell populations were unable to do so (Rasper et al., 2010). Later, isotype-specific evaluation revealed ALDH1A1 as a mediator of TMZ resistance in a selected group of human glioma cell lines and also as a predictor of poorer outcome in vivo, with patient in GBM relapse expressing significantly higher ALDH1A1 levels than during initial treatment (Schafer et al., 2012).

In short, ALDH expression has been routinely used to isolate CSC populations from tumors and there is an obvious correlation with poorer prognosis in many different cancer entities. This ALDH expression is isotype specific, however, and in order to help validate these results, the generation of stable models to investigate ALDH activity in all popular cell culture models is necessary.

1.3 Cell Death

In the recent decade, there has been a paradigm shift as to the mechanisms by which a cell ceases to exist. Historically, the differentiation between necrosis, an unprogrammed type of cell death that leads to breakage of cell membrane and spilling its intracellular contents, causing damage to the surrounding tissue, and apoptosis, a regulated type of cell death that enables the body to dispose of damaged cells without compromising surrounding tissues, has been the basis for understanding the differences in how compromised tissues go under. Recently, new players have appeared on the horizon.

1.3.1 Necrosis

Necrosis is an unregulated cell death due to an outside stimulus and results in breakage of cells with release of its contents in its entirety. Swelling of the cell as a response to this outside stimulus, e.g. a bacterial pathogen or mechanical insult of tissue, results in loss of membrane integrity, causing spillage of content of the cells. These contents themselves and the inflammatory response they induce, subsequently cause damage to the surrounding tissues (Rock & Kono, 2008).

1.3.2 Apoptosis

In contrast, apoptosis is a signal-regulated sort of cell death with specific mediators and receptors that induce death of the cell with minimal damage to the surrounding cells. First observed in nematodes, a specific cell death gene, CED-3, was discovered, encoding for a group of proteases called caspases (cysteine-dependent aspartate-specific proteases). These enzymes act as initiators and executioners of the process and cause degradation of the cell with minimal collateral damage (Kerr et al., 1972). This can be caused intrinsically, through the cell sensing damage to itself or extrinsically, through mediators binding to cell surface receptors. After the cell becomes aware of damage to its DNA for example, activation of tumor suppressor proteins like p53 leads to activation of the BCL-2 protein group, an assortment of molecules that can have either pro or anti-death capabilities. Within the group, these molecules are sorted according to their BCL homology (BH) motifs (Ashkenazi & Salvesen, 2014). A cell damage signal causes the inactivation of the anti-death proteins and activation of the pro-death counter parts, leading to BH-2 motif proteins creating pores in the outer mitochrondial membrane by activation of Bax/Bak, facilitating the release of cytochrome c into the cytoplasm. Cytochrome c binds Apaf1 (apoptotic protease activating factor) and ATP, forming the apoptosome, an intracellular oligomeric protein complex which binds the zymogenic form of caspase-9, cleaving it and letting its active form activate caspase-3 and caspase-7, committing the cell to apoptotic cell death (Hardwick & Youle, 2009).

Extrinsically, this machinery can be activated through specific death ligands. The receptors responsible for mediation of the signal belong to the tumor necrosis factor superfamily. Commonly found death receptors include Fas, DR4, DR5, common ligands are FasL and Apo2L/TRAIL. They induce the formation of a death inducing signaling complex (DISC); this complex includes the Fas-associated death domain (FADD) and caspase-8 as well as caspase-10, recruited through a FADD incorporated death effector domain (DED). TNF-alpha binding to the TNF-alpha receptor causes assembly of a similar cytoplasmatic complex termed Complex I. Proapoptotic signals are mediated by RIPK-1 in both complexes. If RIPK-1 is polyubiquinated, the result is a proinflammatory and prosurvival response mediated by activation of Necrosis-factor kappa B (NF-kB), JNK, and ERK (Ashkenazi & Salvesen, 2014). Deubiquination of RIPK-1 by CYLD results in RIPK-1 activation of RIPK-3 through phosphorylation and in subsequent formation of a complex called necrosome. The necrosome is a complex containing RIPK-1, RIPK-3, Fas-associated death domain (FADD) and caspase-8. RIPK-3 phosphorylates the pseudokinase mixed lineage kinase like (MLKL) which translocates to the cell membrane causing rapid sodium and calcium influx through Na+ channels thereby osmotically rupturing the cell (Seifert &

Miller, 2017). This process of regulated yet necrotic cell death is called necroptosis and is especially useful in situations in which pathogens or cancerous cells can inhibit apoptosis at the sub cellular level.

1.3.3 Autophagy

Another intracellular process called autophagy exhibits important functions in maintaining (sub)cellular homeostasis by formation of an autophagosome from products of highly conserved atg genes to, at baseline level, serve as a garbage deposal of the cell and, when activated during starvation and after depletion of other common energy storage mechanisms, recycles intracellular organelles and other components of the cytoplasm to fuel mechanisms of energy generation. After formation of autophagosomes around organelles to be sequestered, they fuse with lysosomes for degradation of autophagosomal contents. Autophagy is activated and propelled by a variety of signals that are involved in maintaining cellular homeostasis. In mammals, this role is played by the ULK1 complex, which is regulated, among others, by the mTORC1 complex. In the setting of abundance of nutrients including lipids, amino acids and carbohydrates, signal transduction through the mTORC1 complex inhibits autophagy and maintains its role as garbage disposal (Rabinowitz, 2010). Another major player, mammalian Beclin-1, induces formation of the autophagosome; its genomic proximity to the BRCA-1 tumor suppressor gene implicates the loss of its function in breast cancer tumorigenesis (Qu, 2003). Interestingly, there is crosstalk between the apoptotic and the autophagy signaling cascades, as caspase-8 inhibition induces Beclin-1 signaling and therefore autophagy, acting as a safeguard mechanism in the presence of caspase-inhibiting pathogens or cancer cells.

1.3.4 Ferroptosis

As is becoming evident, within the last decade the interpretation that all kinds of regulated cell death are of an apoptotic nature has shifted and new forms of regulated cell death have arisen. Another mechanism that has surfaced is called ferroptosis. The discovery of two small molecules, erastin and RAS-selective ligand-3 (RSL-3) and their lethal potential in the presence of cancer tissue with known RAS-mutation (Dolma S, 2003; Yang & Stockwell, 2008) lead to further questions regarding their mechanism of action. Ferroptosis has since become known as a form of iron-dependent necrotic cell death in which accumulation of ROS mediated by the presence of Fe^{2+} and inactivation of the cell's antioxidant machinery lead to the breakage of cell membranes through the process of lipid peroxidation. Destruction of the cell through such mechanisms is most prominently hindered by the Glutathione (GSH) -Gluthathione peroxidase-4 (Gpx4) pathway. Gpx4 reduces a variety of peroxides including lipid peroxides at the expense of GSH, which is in turn reduced back to

its active form by Gluthathione reductase, thereby preventing LPO. (Yang et al., 2014). Production of GSH is Cysteine-dependent and its delivery to the cell is mediated by System X^{c-}, a cysteine-glutamate antiporter (Lu, 2009). Inactivation of Gpx4 was shown prominently to induce ferroptosis and acute renal injury in $Gpx4^{-/-}$ mice (Friedmann Angeli et al., 2014). Furthermore, tp53 suppresses expression of System X^{c-}, thus resensitizing the cell to ferroptostic cell death (Jiang et al., 2015). Acyl-CoA synthetase long-chain family member 4 (ACSL-4), an enzyme that controls intracellular levels of poly-unsaturated fatty acids such as arachidonic acid, also plays a pivotal role in enabling ferroptosis in the cell as $ACSL\text{-}4^{-/-}$ mice show high resistance to ferroptotic cell death (Doll et al., 2017).

Iron metabolism obviously presents as a key regulator of ferroptosis as well. Inactivation of Transferrin leads to decreased ferroptotic activity and reduced cell death (Gao et al., 2015).

In hepatocellular carcinoma (HCC), the p62-Keap1-NRF2 pathway has also been indicated in ferroptosis, as Keap-1 mediated inactivation of NRF-2 contributes to reduced activation of heme-oxygenase 1 (HO-1) and thus reduced availability of iron ions throughout the body while Erastin or Sorafenib-mediated inactivation of the pathway promotes ferroptosis through increased intracellular iron availability (Sun et al., 2016).

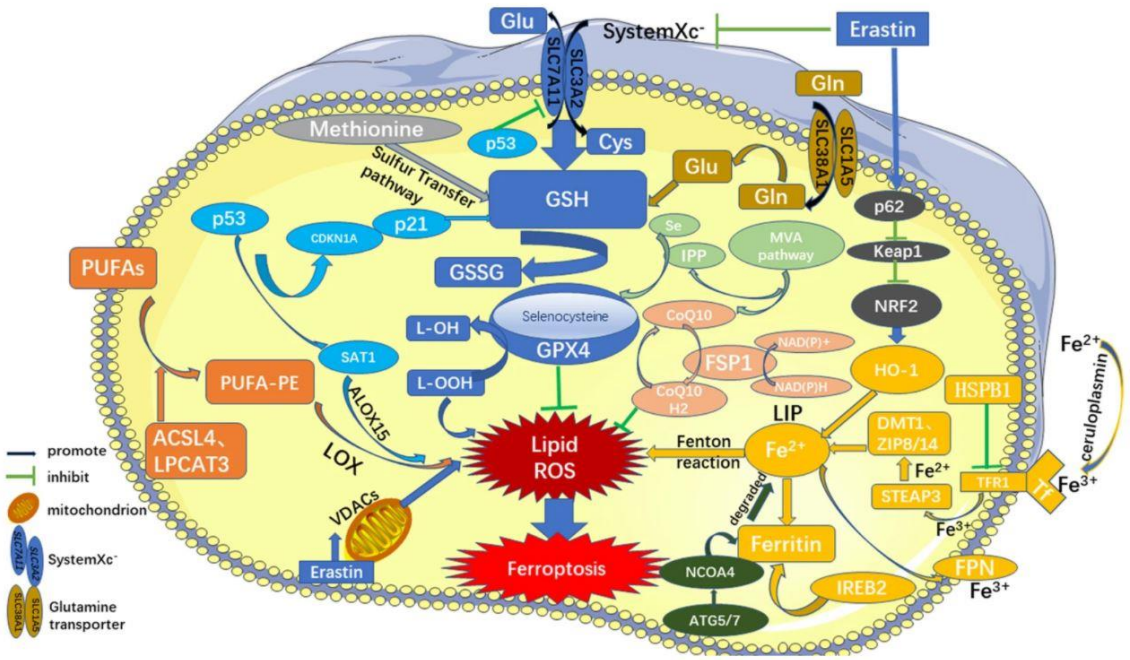

Figure 4. Cellular mechanisms in ferroptosis (Li et al., 2020)

1.3.4.1 Ferroptosis Inducers

1.3.4.1.1 Erastin

Treatment of ras-mutant cell lines with Erastin increased the presence of reactive oxygen species (ROS) and leads to rapid cell death, potentiated by the presence of Fe^{2+} ions (but not other metal ions) and inhibited by the iron chelator Deferoxamin (Dixon et al., 2012). Morphologically, the subcellular changes seen were not similar to those in other forms of cell death, e.g. necrosis, apoptosis, and autophagy, the only marked morphological change seen manifested in the density of the mitochondrial membrane, consistent with the identified targets of Erastin, VDAC2 and VDAC3, anion selective voltage-dependent channels involved in the energy production metabolism by transporting adenosine-containing molecules to the interior mitochondrial space (Dixon et al., 2012). Genetically, ferroptosis was found to cause cell death independently of prominent signaling pathways indicated in other forms of cell death, further cementing its place as an individual type of cell death (Dixon et al., 2012; Dolma S, 2003; Yang & Stockwell, 2008).

The effect or Erastin is propelled through System X_c^- , a sodium-independent cysteine/glutamate antiporter, and is exhibited by inhibition and withholding of cysteine, a precursor for gluthathione synthesis, to the cell, thus accounting for loss of intracellular antioxidant capacity (Yang & Stockwell, 2016); glutamate cell membrane receptors can typically also induce cell death by calcium influx but this is not the mechanism by which Erastin acts, as use of calcium chelators has no effect of cell death (Wolpaw et al., 2011).

1.3.4.1.2 RSL-3

RSL3 does not exhibit its effect through System X_c^- but rather by binding and inhibition of glutathione peroxidase 4 (GPX4), the only intracellular enzyme that reduces lipid hydroperoxides; its inhibition results in an inability to clear reactive oxygen species and therefore induction of ferroptosis (Yang et al., 2014).

1.4 In Vitro Glioma Models

Using cell lines in vitro to study a particular tumor is an essential step in increasing understanding of the tumor biology of a specific tumor type or in the preclinical evaluation of potential therapeutic approaches. However, certain prerequisites have to be in place in order to draw conclusions from cell culture experiments. This rings true particularly in the setting of studying gliomas in vitro. Requirements that need to be met include similarity of genetic background to at least a subset of human gliomas, a similar degree of genetic,

epigenetic, and phenotypic intratumoral heterogeneity (Lenting et al., 2017), and a tumor microenvironment that resembles that of human gliomas in terms of immunocompetence, cell-cell interactions and, if possible, also of the blood-brain-barrier (Lenting et al., 2017). Lastly, the model needs proven stability over time (Lenting et al., 2017).

The most commonly used cell lines for glioma cell culture research are U87 and U251, both derived from human glioblastoma specimens (Ponten & Macintyre, 1968; Westermark et al., 1973); murine and rat models that are represented frequently in cell culture include the C6, F98, 9L, T9 cell lines, among others (Barth & Kaur, 2009).

1.4.1 The C6 Glioma Model

Initially created in Wistar-Furth rats by exposition to N,N'-nitroso-methylurea, the C6 glioma cell is one of the most commonly used models to study glioma in vitro and in vivo (Benda et al., 1968). C6 gliomas are moderately invasive, can be injected into syngeneic animal models and have been shown to be similar to human GBM in invasiveness and immune evasion strategies (Doblas et al., 2010; Gieryng et al., 2017). C6 cells have high mitotic index and nuclear polymorphism, are highly angiogenic, present as p53, PTEN, p14 wild type and with p16 mutation and EGFR overexpression (Giakoumettis et al., 2018). Well characterized, they represent an excellent model for evaluation of tumor resistance and susceptibility to potential novel therapeutic agents. Additionally, various attempts have been made to characterize its stem cell subpopulation (Kondo et al., 2004; Zheng et al., 2007). The ability to translate potential in vitro findings to an in vivo model in an immunocompetent host make the C6 glioma model an excellent choice for the study of mechanisms of glioma tumor resistance. Unfortunately, since C6 glioma cells were induced in outbred Wistar-Furth rats, their injection will only grow to invasive tumors in the outbred Wistar and not in the common type (Beutler et al., 1999). This represents a significant limitation to their in vivo use as they cannot be used for the evaluation of immunotherapy (Barth & Kaur, 2009).

2 Objective

As glioma remains incurable, continuous evaluation and investigation of known in vitro models, taking into account any recent adjustments to previously accepted scientific standards, is paramount. Glioblastoma multiforme remains essentially incurable with no therapies that can significantly boost overall or progression free survival. For this purpose, the heterogeneity of glioma and the nature of its cell populations needs further investigation to identify possible unknown molecular mechanisms that can be targeted for future therapies. As such, the tumor stem cell population in the C6 glioma model needs to be further characterized; the suitability of ALDH1A3 as a biomarker for this subpopulation could enable easier targeting of the GSC population and its role in detoxification of cell processes could also resemble a target for upcoming therapies. As stated, the rat glioma cell line C6 has been well characterized in the past and can also be assessed in vivo. Lastly, there is currently insufficient evidence investigating the role of ferroptotic cell death and its induction as a possibility to invoke cell death in glial tumors. Thus, we evaluated the following concepts as part of this scientific work:

1. Suitability of ALDH1A3 as a marker for the C6 tumor stem cell population.
2. The impact of ALDH1A3 reduction/knockout on therapy resistance in the setting of conventional GBM treatments, specifically Temozolomide and irradiation.
3. Implication of ferroptosis in Temozolomide-mediated cell death during Temozolomide therapy
4. Possible induction of ferroptosis in the C6 glioma model

3 Materials

3.1 Antibodies

Name	Manufacturer	Catalog Number
Anti-ALDH1A3 (321) ab129815	Abcam	GR3211979-3
Anti-ALDH1A3 (334)	NovusBio	NBP2-15339
Anti-rabbit igG Secondary Ab	Thermo Scientific	A10042
Anti-Vinculin Ab	CellSignaling	13901

3.2 Non-Reusable Laboratory Equipment

Name	Manufacturer	Catalog Number
6-Well Plates	Greiner Bio-One	10536952
96-Well Plates	Greiner Bio-One	10625821
Conical Flask, 15ml, 50ml	Cellstar	227261
Serological Pipettes 5ml,10ml, 25ml	Cellstar	Various
T-75 Flasks	Cellstar	658170
Reaction Tube, 1,5ml	Eppendorf	0030120086
Medical X-Ray Film	Fuji	47410 19289
Hemocytometer	Neubauer	Not applicable
Research Plus Pipettes	Eppendorf	Various

3.3 Machines and Devices

Name	Manufacturer	Catalog Number
Flexlid Mastercycler Nexus	Eppendorf	6333000014
NanoDrop™2000/2000c	Thermo Scientific	ND-2000
Ecotron Incubation Shaker	Infors HT	Not applicable
FACS sorter		
Research Plus Pipettes	Eppendorf	Various
InfiniteF200pro multifunctional reader	Tecan	IN-MNANO+
RM5 Conical Rotator	CAT	60207-0070
Centrifuge 5415D	Eppendorf	Not applicable

Centrifuge 5417R	Eppendorf	Not applicable
Centrifuge 4K15	Sigma	Not applicable
Herasafe Security Hood	Fisher	10213322
Heracell 150i CO2 Incubator	Thermo Scientific	50116048
TS100 Eclipse Microscope	Nikon	Not applicable
Gel Documentation System	Peqlab	Not applicable
PowerPac 300	Biorad	1645050
XStrahl RS 225	Life Science	

3.4 Kits

Name	Manufacturer	Catalog Number
GeneJET Gel Extraction Kit	Thermo Scientific	K0691
Aldefluor Assay Kit	Stemcell Technologies	01700
Plasmid Extraction MiniKit	QIAGEN	12125
peqGOLD Taq All Inclusive	Peqlab	PEQL01-1000
Lipofectamine 3000 Transfection	Thermo Fisher	2136964

3.5 Molecular Biology + Other Reagants

Name	Manufacturer	Catalog Number
T4 Ligation Buffer	New England Biolabs	B0202S
T4 Polynucleotide Kinase	New England Biolabs	M0201S
NE Buffer	New England Biolabs	B7001S
Bbsl Restriction Enzyme	New England Biolabs	R0539S
NEB® 5-alpha Competent E. coli	New England Biolabs	C2987H
Luria Broth Base	Invitrogen	12-795-027
Rotipherese Gel 30	Roth	3029.1
DMEM	Thermo Fisher	41965062
PBS	Thermo Fisher	70011044
Ampicillin	Sigma-Aldrich	A9618-5G
Trypsin	Sigma-Aldrich	T4549
10x RIPA Lysis Buffer	Sigma-Aldrich	20-188

Bradford Dye Reagant, 1x	Biorad	5000205
Acrylamide, 30%	Sigma-Aldrich	A3574
Ammonium persulfate (APS)	Sigma-Aldrich	A3678
TEMED	Sigma-Aldrich	T9281
TRIS	Roth	0188.4
SDS	Roth	0183.1
Hydrogen Peroxide	Roth	9681.4
Crystal Violet	Sigma	C0775
NaCl	Roth	P029.5
Glycine	Roth	0079.4
Temozolomide	Sigma	T2577-100MG
RSL-3	Sigma-Aldrich	SML2234-5MG
Liproxstatin-1	Sigma-Aldrich	SML1414-5MG
pSpCas9(BB)-2A-GFP plasmid	AddGene	48138
gRNA Sequences for rnALDH1A3	Sigma Aldrich GmbH	Not applicable
alamarBlue™HS Cell Viability Reagent	Thermo Scientific	A50100
LE Agarose	Biozym	840004
Prestained Protein Ladder	Thermo Fisher	11812124

4 Methods

4.1 Development of an ALDH1A3 Knockout Model using the CRISPR-CAS9-Technique

4.1.1 Design of Guide RNA for ALDH1A3 Knockout in R.norvegicus

In order to perform mutagenesis in the rnALDH1A3 gene located on Chromosome 1p, gRNA was created using the generator services of the Zhang Lab, Massachusetts Institute of Technology, Cambridge, MA, 02142. 250 base pair sections were chosen from the beginning of the coding sequence to ensure insertion of error from the very beginning; generated sequences were obtained commercially from Sigma-Aldrich (Sigma Aldrich Chemie GmbH, München).

4.1.2 Phosphorylation and Annealing of gRNA Oligo Sequences

gRNA was resuspended in distilled water (ddH20) to 100uM as recommended by the manufacturer's manual. The reaction mixture including the T4-DNA-ligase and the T4-Phosphonucleotidekinase was created as follows:

Component	**Amount(µL)**
sgRNA top (10µM)	1
sgRNA bottom (10µM)	1
10×T4 Ligation Buffer	1
ddH_2O	6.5
T4 PNK(Polynucleotide Kinase)	0.5
TOTAL	**10**

In a thermo cycler, the mixture was warmed to 37°C for 30 minutes, then to 95°C for 5 minutes, followed by incremental decrease of temperature to 25°C at a rate of 5°C/min, followed by a cooling phase at 25°C for 30 minutes.

1:200 Dilution of sgRNA oligos was then performed using 1µL of the oligo and 199µL of ddH_20.

4.1.3 Linearization of the Vector Plasmid

For introduction into the target cells' DNA, the pSpCas9(BB)-2A-GFP plasmid, containing the caspase 9 gene, a GFP gene, and a gene mediating resistance to Ampicillin, was used as commercially available. The plasmid was linearized in NEBuffer using BbsI restriction enzyme in the following concentrations:

Component	**Amount(µL)**
DNA (=100ng)	8 µg
BBsI Restriction Enzyme	≤5µl (2.5µL)
10X NEBuffer	5 µl (1X)
ddH2O	N
Total	50µL

The reaction mixture was incubated at 37°C for 4 hours.

4.1.4 Electrophoresis and DNA Gel Extraction

To confirm successful linearization of the vector, electrophoresis was performed.

The electrophoresis gel was prepared by dissolution of 3g Agarose in 150ml of 1x TBE buffer to create a 2% Agarose gel. The mixture was heated for 75 seconds with proper mixing; 15µl of 10000x Gel-Red solution for DNA staining and poured into an electrophoresis chamber. After a 2-hour cooling period, DNA was added to the proper chambers. The gel was run at 100V for 30 minutes.

Hereafter, DNA was extracted from electrophoresis gel using the Thermo Scientific GeneJet Gel Extraction Kit #K0692 and incubated at 60°C using 1:1 volume binding buffer. DNA concentration was measured using Thermo Scientific Nanodrop 2000 Photospectrometer. Concentration was recorded in ng/µl.

4.1.5 Ligation of Linearized Plasmid to sgRNA

sgRNA was ligated to the pSpCas9(BB)-2A-GFP plasmid after creation of a reaction mixture as shown below and incubated at 16°C for 30 minutes.

Component	Amount(µL)
Linearized DNA	0.5(50ng)
gRNA oligos	2
Solution 1	2.5
Total	5

4.1.6 NEB-5-α E.coli Transformation

A tube of NEB-5-α competent E. coli was thawed on ice until disappearance of all remaining crystals. 10ng of plasmid DNA were added to the tube containing the thawed bacterial culture and were mixed thoroughly by hand. The mixture was placed on ice for 30 minutes and consequently heat shocked at 42°C for 30 seconds. Hereafter, it was placed on ice for 5 minutes for proper cooling.

950 µl LB medium were added to the tube, subsequently the mixture was incubated on an incubation shaker at 100rpm for one hour. Meanwhile, LB Ampicillin agar plates were warmed to 37°C. After incubation, the mixture tube containing the ligated plasmid was centrifuged at 500rpm for 5 minutes; approximately 900µl of supernatant were discarded and the remaining mixture was applied to the selection plate using a conventional glass scraper until its top layer appeared to be dry. The selection plate was incubated at 37°C for 10 hours.

The growth plate was observed for formation of single bacterial colonies; three colonies were picked and inoculated into Erlenmeyer flasks containing LB medium at 25g LB base/l and Ampicillin at a working concentration of 100µl/ml. The flasks were incubated in the bacterial shaker at 180rpm and 37°C for 16 hours.

4.1.7 Confirmation of Successful Plasmid Expansion by PCR

Bacterial single cell colonies were picked and added each to its own Eppendorf vial containing 500ml of Ampicillin-infused LB growth medium and subsequently mixed by hand. As per lab protocol a PCR master mix was prepared for each own culture; bacterial PCR was performed on a Flexlid Master Cycler (annealing temperature 55°C). Meanwhile, extracted single cell colonies were shaken in the reaction tubes at 37°C and 100°C. Again, a 2% agarose gel was prepared, and electrophoresis was performed at 100V for 30 minutes. Clones with positive bands were kept.

4.1.8 Plasmid Isolation

Plasmid was isolated from successfully transformed bacterial colonies using the QIAGEN Plasmid Isolation Kit as per manufacturer's protocol. After successful plasmid elution, Plasmid DNA was stored at -20°C.

4.1.9 Lipofectamine 3000 Transfection of C6 cells

C6 cells were grown to approximately 70% confluence in 5% FBS Dulbecco's Modified Eagle Medium (DMEM) in conventional Cell Star 6-well-plates. For transfection, the ThermoFisher Invitrogen Lipofectamine 3000 ® Transfection kit was used. The following mixing protocol was using per 6 wells in a six-well setting.

Preparation of Transfection medium	
5% FBS DMEM	750µl
Lipofectamine 3000®	45µl
DNA-P3000-Complexes	
Plasmid DNA	15µg
P3000® Reagent	30µl
5% FBS DMEM	750 µl

As control, no plasmid and a plasmid containing solely GFP were used.

Transfected cells were incubated for 48 hours; initial microscopic analysis confirmed successful transfection in GFP- and ALDH1A3 groups. Successfully transmitted cells in ALDH1A3 groups were isolated using fluorescence-activated cell sorting (FACS).

4.1.10 Single Cell Dilution

GFP positive C6 cells were cultured in 5% FBS DMEM growth medium until 70% confluence and subsequently gently washed with PBS twice. Trypsin was used to detach cells from the growth surface and resuspended in 3ml of growth medium. To assess concentration, cells were counted using a Neubauer hemocytometer. To allow for single cell growth, a solution containing 0.5 cells/100µl was prepared. A ninety-six-well plate was inoculated with 100µl per well.

Cell growth was checked periodically every 24 hours for formation of single cell cultures. Those that were identified as such were grown to 70% confluence and moved to large growth wells until an amount large enough to continue culture and confirm positive knockout were grown.

4.1.11 Cell Lysis and Bradford Assay

Cells were grown to 70% confluence in a T-75 flask; medium was removed, and cells were washed gently with 2ml PBS twice. 500µl RIPA Buffer was added to the flask which was subsequently swirled to distribute the lysis buffer. Cells were removed from the growth surface using a conventional cell scraper and moved to a 15ml conical flask. The lysate was incubated on ice for 20 minutes and then sonicated twice for 3 seconds. Cells were then placed on ice for 15 minutes and centrifuged at 4°C and 15,000g for 5 minutes. Supernatant was collected, the remaining cell pellet was discarded.

Protein concentration was assessed using the Bradford Assay. Samples were tested in triplicates and standard controls were used as recommended. Samples were diluted 1:10 with ddH20 and added to their respective wells. The Bradford Protein Assay Dye reagent was diluted 1:5 with Millipore H20 and filtered through Whatman paper, then 200µl were added to all wells containing standards controls or samples using a multipette.

Samples were incubated at room temperature for 10 minutes and then moved to a TECAN Infinite F200pro multifunctional reader. Samples were measured at a wavelength of 595nm, transferred to a standardized Excel spreadsheet and adjusted for volume containing 25µg of protein.

4.1.12 Western Blot

4.1.12.1 Gel Preparation

Running Gel Preparation by Density, 2 Gels			
Gel Density	**8 %**	**10 %**	**12 %**
H_2O	6,9 ml	5,9 ml	4,9 ml
1,5 M Tris pH 8,8	3,8 ml	3,8 ml	3,8 ml
SDS 10 %	150 µl	150 µl	150 µl
Acrylamide 30 %	4 ml	5,0 ml	6,0 ml
APS 10%	150 µl	150 µl	150 µl
Temed	9 µl	9 µl	9 µl

Stacking Gel Preparation, 2 Gels	
Gel Density	**5 %**
H2o	5,5 ml
1.5 M Tris pH 6.8	1 ml
SDS 10 %	80 µl
Acrylamid 30 %	1,3 ml
APS 10 %	80 µl
Temed	8 µl

The above gel compositions were used to create gels for electrophoresis. 10% density gels were used in this case.

4.1.12.2 Sample Preparation and SDS Polyacrylamide Electrophoresis

5x Laemmli Buffer was added to the protein lysates for a final concentration of 1x Laemmli. Samples were boiled at 95°C for 5 minutes, then cooled down on ice for 5 minutes and spun down using an Eppendorf 5415D centrifuge.

Volumes representing 25µg of protein were added to each lane, as reference a prestained protein ladder was used. Samples were run in running buffer at 80V for 15 minutes, then voltage as increased to 180V for 45 minutes.

4.1.12.3 Wet Blotting

Gels were transferred to blotting chamber and layered with a Nitrocellulose blotting membrane and filter paper, then placed in a transfer cassette and inserted into the electrode module. Transfer buffer was prepared using the following protocol:

10x Transfer Buffer	
25 mM Tris	30,3 g
190 mM Glycine	142,6 g
ddH_2O	Ad 1 L

Transfer buffer was diluted to 1x concentration and ethanol was added at a concentration of 1:10 to increase transfer efficiency and prevent membrane swelling. Transfer was performed in a 4°C cool room at 100V for 1 hour. Cool packs were added to the transfer tank to prevent cooking of the membrane.

4.1.12.4 Antibody Staining

Membranes were blocked in 5% milk or 10% BSA as recommended for the respective antibodies for 1 hour. Vinculin was used as a control. ALDH1A3 (Abcam ab129815, polyclonal, rabbit) and Vinculin antibodies (CellSignaling, 13901, monoclonal, rabbit) were applied at factory recommended concentrations. Membranes were placed in a 50ml conical tube on a CAT RM-5 rotator at 4°C overnight.

Next day, membranes were washed in TBS-T buffer three times, for 10 minutes each. Then, membranes were incubated in secondary antibody (Abcam, Ab6721, goat to rabbit) at a concentration of 1:10.000 and placed on a RM-5 rotator for 1 hour.

Membranes were washed in TBS-T 5 times for 5 minutes each. 1ml HRS substrate was applied to each membrane. Plastic wrap was used to cover the membranes and membranes were visualized using a Fuji Medical X-Ray film.

4.2 Aldefluor Assay

To assess changes in the size of the ALDH1 positive stem cell population, C6 wild type and ALDH1A3ko cells were grown separately to 70% confluence; medium was removed, cells were washed with PBS, trypsinized, resuspended in 3ml growth medium and centrifuged at 300g for 5 minutes. Cells were resuspended in 1ml DMEM growth medium and supplemented with 50µM Verapamil; a control with Diethylaminobenzaldehyde (DEAB), a commercially available ALDH1 inhibitor, was prepared as well. 500ml of the cell suspensions were transferred to a new 1.5ml Eppendorf tube. 5µl Aldefluor Assay Buffer was added to each sample and mixed by slowly pipetting up and down. Samples were incubated at 37°C for 1 hour and wrapped in aluminum foil to prevent light interaction.

1ml FACS buffer (PBS + 5% FBS) were added to the suspensions which were subsequently spun down at 300g for 5 minutes. Pellets were resuspended in 500µl Aldefluor Assay Buffer at 4°C and assessed for ALDH1 activity in a FACS reader.

4.3 Viability Assays

4.3.1 Temozolomide

In order to assess changes in stemness, and therefore changes in resistance of tumor to conventional chemotherapy, viability of cell population in the ALDH1A3ko model after treatment with Temozolomide was assessed. Cells were seeded in quadruplicates in growth

plates and grown overnight. As controls, C6 wild type cells and C6 cells treated with DEAB were used. Cells were treated with TMZ at concentrations of 100µM and 200µM; as a cytotoxicity control, they were also treated with H_2O_2 at 20µM. Viability was assessed after 48 hours using the AlamarBlue Viability Assay.

4.3.2 Determination of In Vitro Concentration of Temozolomide for Cell Culture Experiments

Temozolomide (µM)	Temozolomide (µg/ml)
100	0.1
200	0.2
500	0.5
800	0.8

In vivo, Temozolomide is commonly administered at a dose of 150mg/m². Through intracerebral microdialysis (ICMD), it has been attempted to measure intracerebral drug concentration after oral administration. In 7 patients, Portnow et al. recorded an average peak concentration of Temozolomide after oral administration with dialysis catheters that had been placed in the brain peritumorally during GBM resection a day prior. Mean peak concentration in brain tissue was measured at 0.6 ± 0.3 µg/ml (Portnow et al., 2009). In brain tissue, peak concentrations are reached after 2.0 ± 0.8 hrs. Thus, concentrations used in this experimental setup are similar; bioavailability of Temozolomide is almost 100% (Newlands et al., 1992), similar presence of the drug can be assumed in in vitro drug application. For our experimental setup, Temozolomide was added to the growth medium to be administered to the cells, mixed carefully to account for even distribution and finally added to the growth wells in a manner designed to not disturb adherence of cells.

4.3.3 Irradiation

C6 wild type and ALDH1A3ko cells were seeded in 6-well plates at 150,000/well. On day 1, cells were irradiated in triplicates at 2, 4, 6, 8, and 10Gy, respectively using an X-Strahl RS 225 (Life Science). After irradiation cells were incubated for 48 hours. Cell viability was assessed using the AlamarBlue Assay.

4.4 Colony Forming Assay (CFA)

The Colony forming, or clonogenic assay, assesses the ability of a single cell to form a colony with or without exposure to a therapeutic agents (Franken et al., 2006). Initially used for radiation assays, it has since been uniformly used for a large variety of treatment options.

In this case, 150 cells were plated in 6-well plates for C6 WT, C6 WT/DEAB, and C6 ALDH1A3ko to allow assessment of clonogenic ability after exposure to TMZ at concentrations of 100µM, 200µM, 500µM, 800µM; 20µM of H_2O_2 was used as a cytotoxicity control.

Cells were plated in DMEM supplemented with 5% FBS overnight; treatment reagents were added to the medium; after 24 hours, medium was changed, and cells were incubated at 37°C for 7 days.

Subsequently, medium was removed and cells were washed with PBS; after removal of PBS, cells were incubated for fixation and stained using a mixture of 6.0% glutaraldehyde and 0.5% Crystal Violet for 30 minutes. The fixation mixture was then removed and discarded appropriately; wells were washed with tap water and dried for assessment at room temperature.

Data analysis was performed using the ImageJ Colony counter plugin to assess the amount of colonies in each well. To account for human error in counting, each well was counted three times and averages were calculated. For each cell population and treatment concentration, vessel Plating Efficiency (PE) and Surviving Fraction (SF) were calculated as follows:

$$Plating\ Efficiency\ (PE) = \frac{number\ of\ colonies\ formed}{number\ of\ colonies\ plated}\ x\ 100\%$$

$$Surviving\ Fraction\ (SF) = \frac{number\ of\ colonies\ formed\ after\ treatment}{number\ of\ cells\ \frac{seeded}{PE}}$$

4.5 Ferroptosis Assay

C6 wild type and ALDH1A3 KO cells were plated and cultured in DMEM + 5% FBS as described above (see 4.3.1). One C6 WT cohort was additionally treated with DEAB; to

assess effect of RSL-3 and Lip-1 on the different populations, the following study cohorts were established:

i. 200µM TMZ
ii. 200µM TMZ + 500nM Lip-1
iii. 400nM RSL-3
iv. 400nM RSL-3 + 500nM Lip-1
v. 500nM Lip-1

24 hours after treatment, viability of cells was analyzed using the AlamarBlue Viability Assay.

4.6 Statistical Analysis

All values are expressed as the mean ± SD. Differences between groups were compared using the Student's T Test/ANOVA. For the Colony Formation Assay, PE and SF were calculated. At least three independent experiments were performed to confirm the results. Statistical analysis and graphical presentation was performed using GraphPad Prism 5.0 (GraphPad Prism Software, CA, USA). A p-value < 0.05 was considered statistically significant.

5 Results

5.1 Establishment of Stable C6 ALDH1A3 Knockout Population

Table 1. GuideRNA primer sequences for ALDH1A3

gRNA Primer Name	Length	GC (%)	µL for 100 µM	Sequence (5' → 3')
rnALDH1A3_1F	24	79.1	302	CACCCAGGCCGAGCCGGTGCGTCG
rnALDH1A3_1R	24	70.8	358	AAACCGACGCACCGGCTCGGCCTG
rnALDH1A3_1F	24	75	420	CACCGCCGCGCCCCATCCGCAACT
rnALDH1A3_1R	24	66.6	372	AAACAGGTGCGGATGGGGCGCGGC
rnALDH1A3_1F	24	79.1	442	CACCCCAGGCCGAGCCGGTGCGTC
rnALDH1A3_1R	24	70.8	398	AAACGACGCACCGGCTCGGCCTGG

Potential gRNA sequences were chosen using the MIT CRISPR gRNA generation tool as provided by the Zhang lab (mit.crispr.edu); since, the Zhang lab has replaced this tool with a variety of commercial and free-to-use gRNA generation options. The three gRNA cassettes deemed most efficient by the design software were subsequently commercially ordered (Table 1), then phosphorylated and annealed as per protocol.

The pSpCas9(BB)-2A-GFP plasmid was linearized using the BbsI cutting enzyme; gel electrophoresis showed successful linearization of the plasmid (Figure 1, Exhibit A), with the linearized DNA travelling down the gel more slowly (Arrow) than the pSpCas9-Plasmid in its native, supercoiled DNA form.

After transformation, colonies were screened for inclusion and expansion of plasmid DNA using the in-house bacterial PCR protocol; positive clones are indicated (+, Exhibit B) and were subsequently kept for plasmid isolation. Following plasmid isolation and transfection, GFP positive cells were isolated from the general cell population using GFP + FACS cell sorting; transfection efficiency was indicated as 77.7%. The GFP + cell population was cultured for 7 days, subsequently a single cell dilution was created; single cell colonies were first cultivated in 96-well plates and were moved to larger vessel sizes after expansion.

Western Blot identified several ALDH1A3-deficient clones. Exhibit C shows Western Blot analysis of knockout clones used for subsequent experiments; Vinculin control bands at ~125kDa show comparable amount of protein used for analysis; bands at 55kDa account for ALDH expression, in this case stained for isotype 1A3. C6 wild type cells (left) show high expression of ALDH1A3, similar to human glioma cell line LN229 used a positive control. Two clones (middle left, middle right) show no expression of ALDH1A3; the latter was used as the clone of choice in the subsequent experiments. Because of the obvious nature of the knockout as seen in Western Blot, no sequencing of clonal DNA was performed.

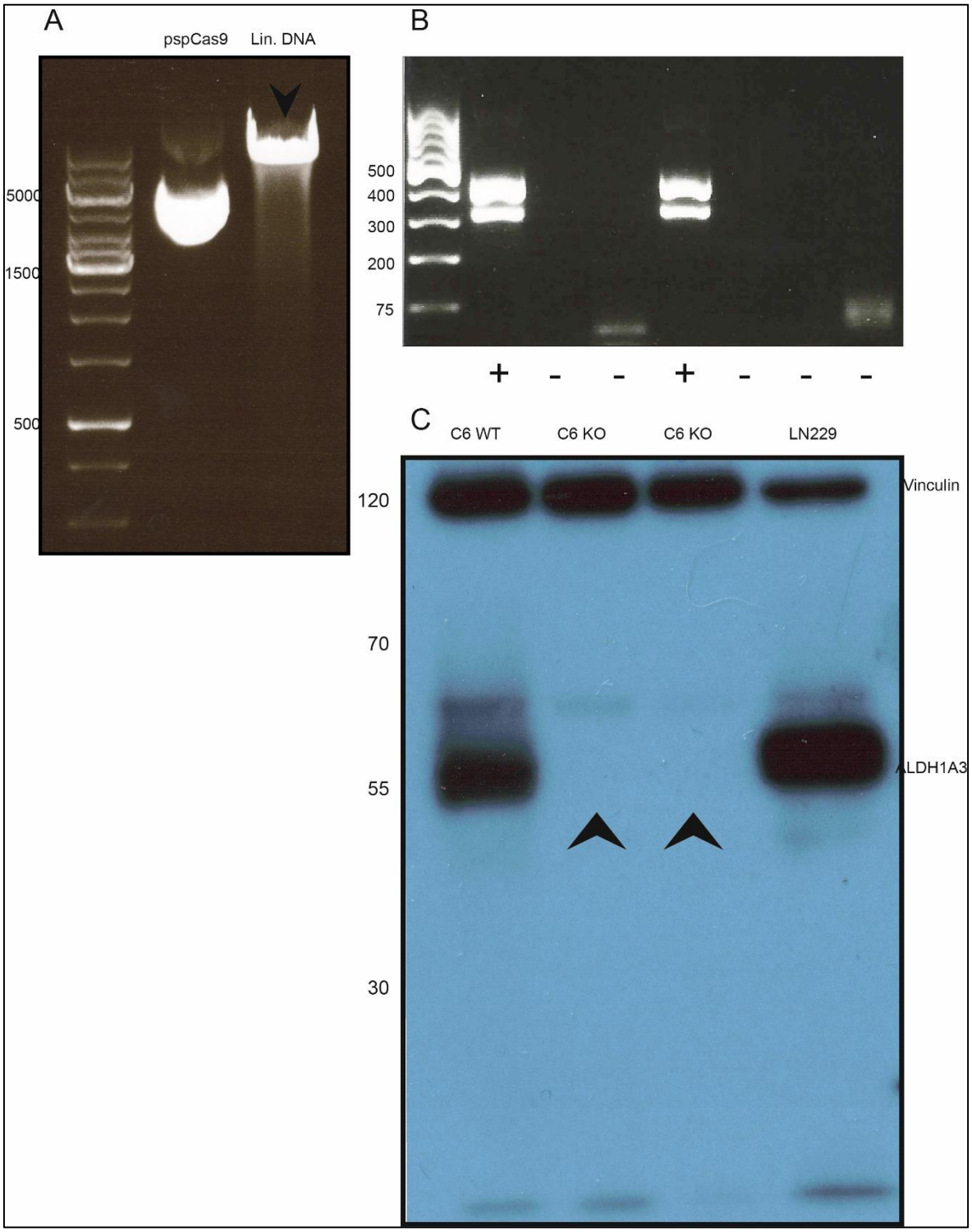

Figure 5. (A) Successful linearization of pSpCas9(BB)-2A-GFP plasmid as demonstrated by its migration time on a 2% Agarose Electrophoresis Gel. (B) PCR after bacterial plasmid expansion indicates successful expansion of mutant colonies in wells 1 + 4. (C) Western Blot confirms successful knockout of ALDH1A3 gene in C6 specimens in wells 2 + 3. C6 wild type (left, well 1) shows high ALDH1A3 content, human glioma cell line LN229 (right, well 4) shows high content as well. Wells 2 + 3 contain two separate C6 mutants grown from single cell suspension with no ALDH1A3 signal in WB, confirming successful knockout.

5.2 Aldefluor Assay Identifies ALDH1A3 as a Stem Cell Marker in C6 Glioma Model

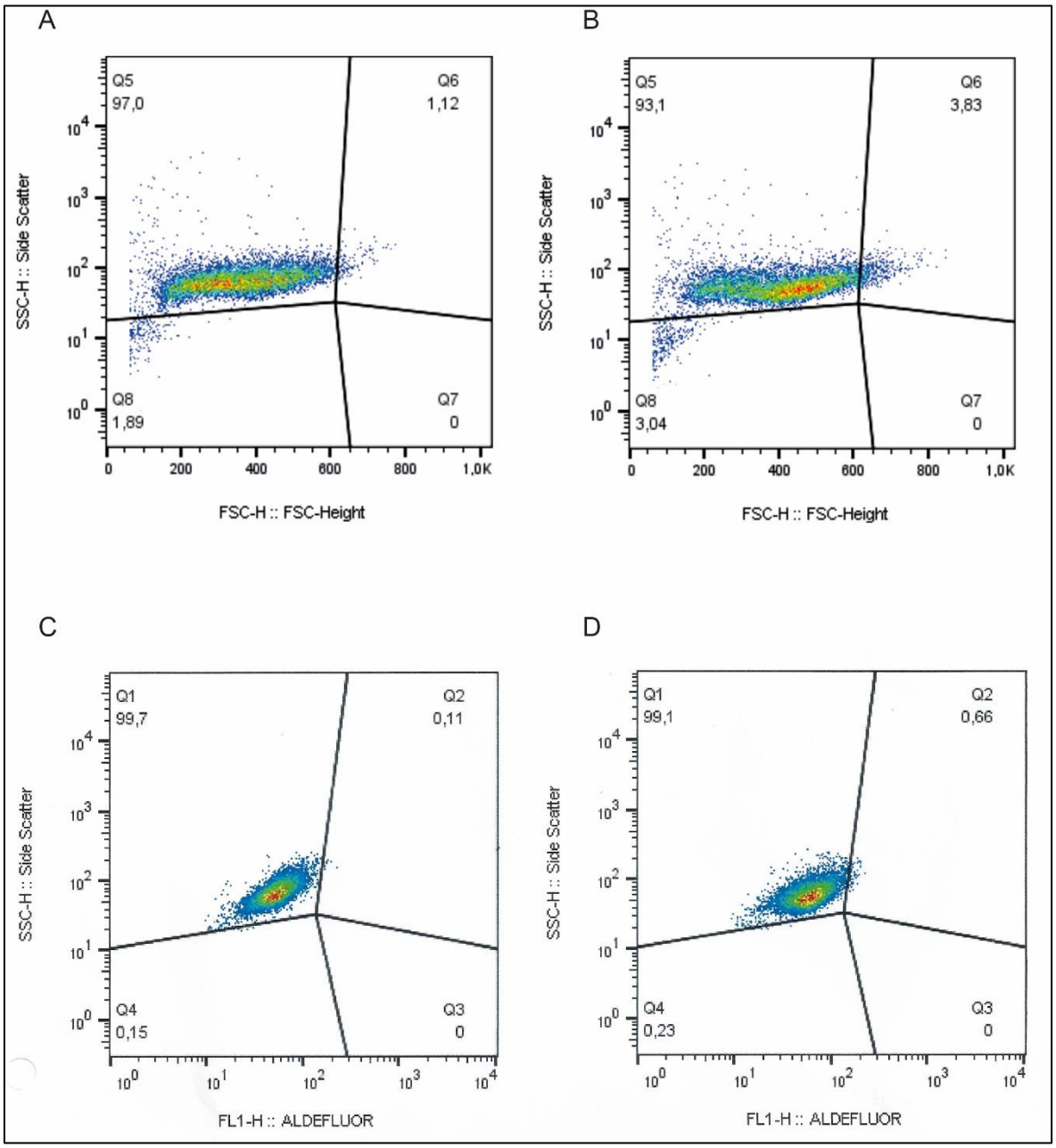

Figure 6. Aldefluor Assay shows ALDH1-bright cell populations in WT and KO. In a C6 wild type cell population, inhibition with DEAB results in residual population of 1.12% ALDH-bright stem cells (A, left). No inhibition (B, right) shows ALDH-bright stem cell population of 3.83%. ALDH1A3 knockout shows 0.11% ALDH-bright stem cell population in DEAB control (C, left) with ALDH1A3 sample showing residual 0.66% ALDH bright stem cells.

Aldefluor Assay can identify subpopulations of stems cell in the larger tumor cell population by their ALDH1 content. Used as a control for the efficacy of the assay is DEAB, marketed by the company as an effective ALDH1-inhibitor. Morgan et al. have indicated that the function of DEAB as an inhibitor is determined by the rate of reaction, meaning that while it

effectively behaves as a substrate for all ALDH isotypes, the speed at which it is hydrolyzed determines its effectiveness as an inhibitor; for ALDH1A1, ALDH1A2, ALDH2, ALDH1B1, ALDH1A3 (in that order), DEAB serves as a good to excellent inhibitor (Morgan et al., 2015).

FACS results for Aldefluor® Assay indicated a stem cell population as defined by ALDH1-bright ($ALDH_{br}$) cells of 3.83% for the C6 wild type general population; the control population accounted for 1.12% after ALDH1-inhibition by DEAB. For mutant ALDH1A3 knockout population, stem cell population size measured 0.11% for the DEAB-inhibited control population, the uninhibited mutant sample population showed a sub-population of 0.66% $ALDH_{br}$ stem cells.

5.3 7.3 ALDH1A3 Knockout Does not Increase Chemosensitivity in the C6 Model

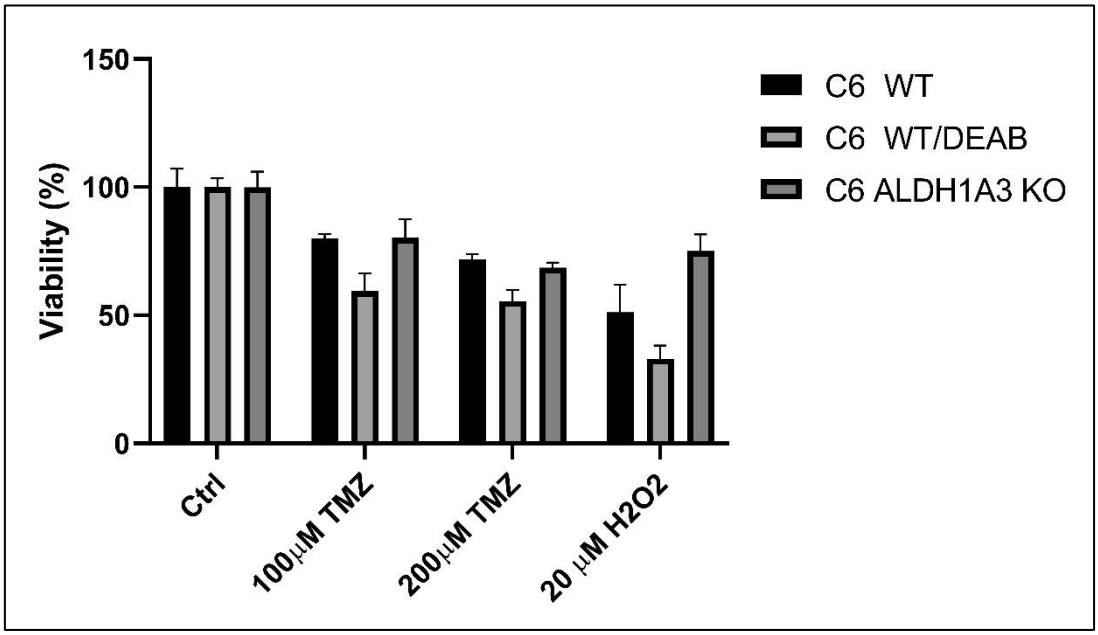

Figure 7. Viability of C6 WT, C6 WT + DEAB and C6 ALDH1A3 after treatment with Temozolomide at different concentrations. H_2O_2 was used as a Toxicity Control.

To assess whether changes in ALDH1A3 content produce palpable changes in viability during standard medical therapy for glioma, cells were seeded at low density (1000/well) in 96-well plates to account for rapid doubling time in our lab's C6 wild type cell population. The Deutsche Gesellschaft für Neurologie (DGN) recommends Temozolomide treatment in 24-hour intervals for 4 weeks („5 day on, 5 day off Regimen"), in concordance, Temozolomide was administered every 24 hours for 2 days after cells had grown to

adherence, and AlamarBlue Assay was performed after 48 hours to ensure cells were still in a linear growth phase.

As proof of principle, C6 cells treated with DEAB were also treated with Temozolomide. Doses chosen for this experiment were 100µM and 200µM TMZ, H_2O_2 (20µM) was used as a cytotoxicity control.

For C6 wild type and ALDH1A3 knockout cells, no difference could be observed at 100µM TMZ, 200µM TMZ or 20µM H_2O_2 (P-values for C6 wild type vs. C6 ALDH1A3 knockout 0.99, 0.32, 0.11 respectively); significant differences could be observed only between C6 WT + C6 WT/DEAB 100µM and 200µM TMZ groups (P-values 0.023, 0.017 respectively) and between C6 ALDH1A3KO + C6 WT/DEAB 100µM, 200µM TMZ and 20µM H_2O_2 groups (P-values 0.046, 0.029, 0.003 respectively). Mean Viability respective to the control at 100µM TMZ ranged from 80.03% (SD 1.605) for C6 WT, 80.23% (SD 7.24%) for C6 ALDH1A3KO to 59.41% (SD 7.035%) for the C6 DEAB Control. At 200 µM TMZ, mean viability clocked in at 71.78% (SD 2.02%), 68.51% (SD 2.11%) and 55.59% (SD 4.39%) respectively. Viability at 20µM H_2O_2 was calculated at 51.23% (SD 10.63%), 75.01% (SD 6.56%) and 33.11% (SD 5.09%) respectively. While these values indicate a level of statistical significance between the ALDH1A3KO group and the WT/DEAB group ($p=0.003$) and one barely missed between the C6 WT and the ALDH1A3KO ($p= 0.11$), these results must not be interpreted as discoveries but rather as measurement variance in the setting of the viability experiment.

Table 2. Statistical comparison of C6 wild type and C6 ALDH1A3KO in TMZ viability assay

TMZ (μM)	Wild type (mean, %)	ALDH1A3KO (mean, %)	Difference	p-value
100	80.03	80.23	-0.20	0.99
200	71.78	68.51	3.27	0.32
H_2O_2 (μM)				
20	51.23	75.00	-25.73	0.11

Table 3. Statistical comparison of C6 wild type and C6 wild type/DEAB in TMZ viability assay

TMZ (μM)	Wild type (mean, %)	WT + DEAB (mean, %)	Difference	p-value
100	80.03	59.41	20.62	**0.023**
200	71.78	55.59	16.19	**0.017**
H_2O_2 (μM)				
20	51.23	33.11	18.12	**0.003**

Table 4. Statistical comparison of C6 wild type/DEAB C6 ALDH1A3 KO in TMZ viability assay

TMZ (μM)	WT + DEAB (mean, %)	ALDH1A3KO (mean, %)	Difference	p-value
100	59.41	80.24	-20.83	**0.046**
200	55.59	68.51	-12.93	**0.029**
H_2O_2 (μM)				
20	33.11	75.00	-41.89	**0.003**

5.4 Radiotherapy is Equally Ineffective in C6 WT and ALDH1A3 Populations

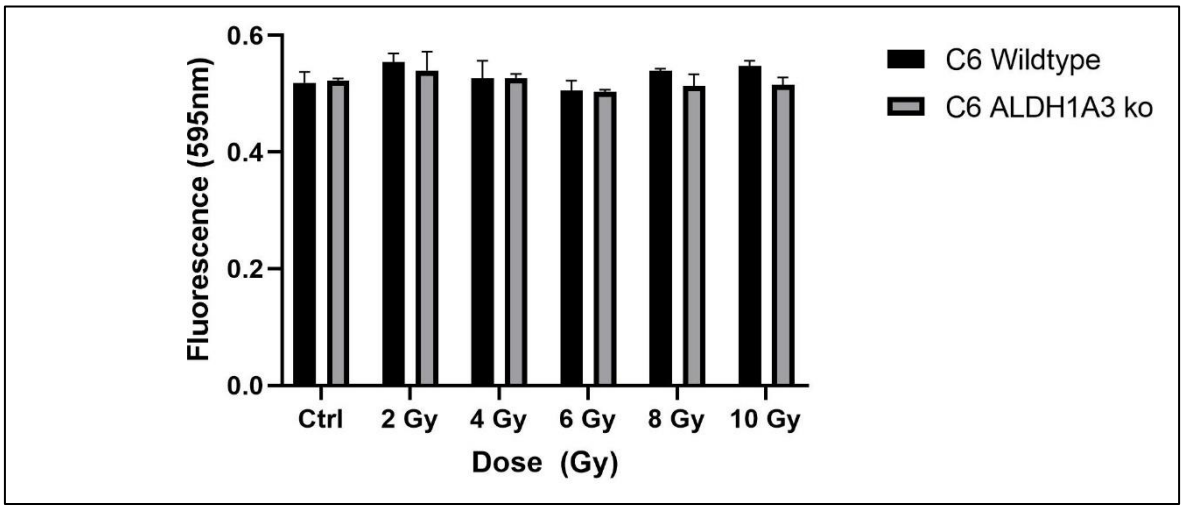

Figure 8. C6 wild type and C6 ALDH1A3KO after treatment with different doses of irradiation.

Despite the fact that radiotherapy under the DGN guidelines remains a recommended therapy option, glioma has proven radioresistant in vivo as well as in vitro. To investigate impact of reduction of ALDH1A3-expression of tumor stem cell population, C6 wild type and ALDH1A3 KO tumor populations were subjected to ionizing radiation at doses of 2,4,6,8, and 10 Gray (Gy). 48 hours after treatment, cell viability was assessed using the AlamarBlue Assay. Regardless of dose, p-values indicated no significant differences in viability between tumor populations (see Table below).

Dose (Gy)	Adjusted p-value
Ctrl	0.98
2	0.95
4	0.98
6	0.98
8	0.39
10	0.13

No significance can be attributed to apparent proliferative cell growth seen at different dosages with absolute values also at high dose radiation (8Gy + 10Gy) indicating such effect as these phenomena are non-significant and can be attributed to variance in cell seeding.

5.5 Temozolomide-Induced Cell Death Is Not Due to Ferroptosis

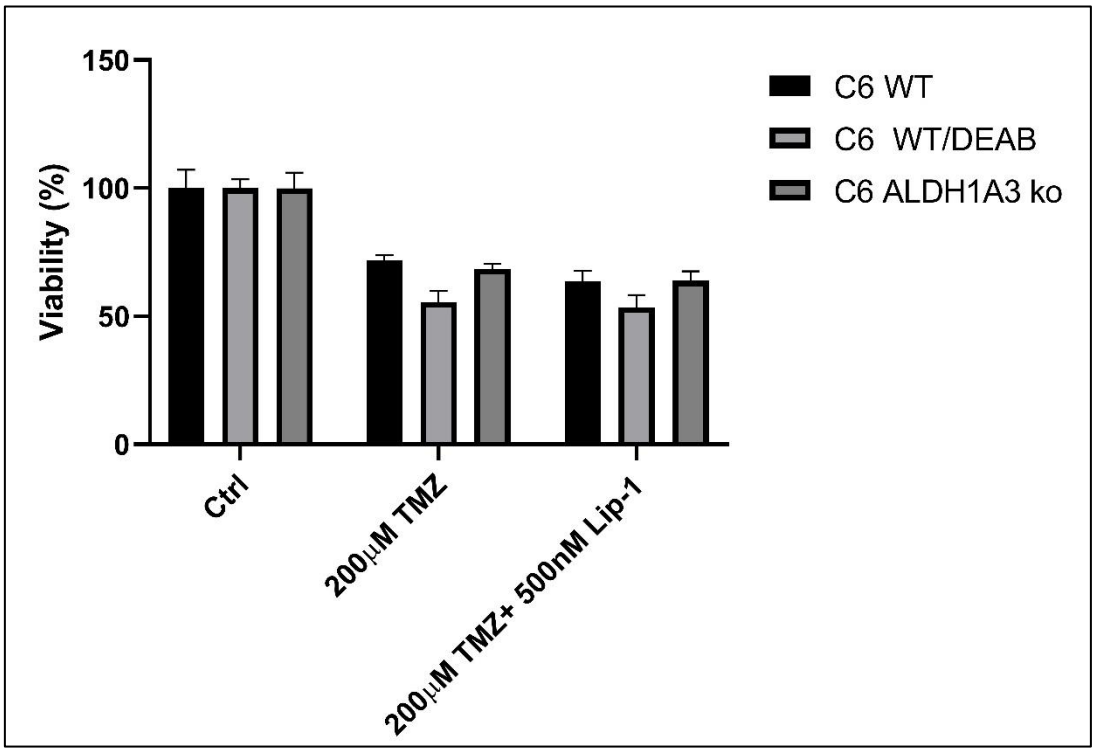

Figure 9. Addition of Liproxstatin-1 has no effect on viability after exposure to Temozolomide

At 200µM TMZ, viability relative to the control for C6 WT, C6 ALDH1A3KO and C6 WT/DEAB was 71.78% (SD 2.02%), 68.51% (SD 2.11%) and 55.59% (SD 4.39%) respectively. To assess whether ferroptosis contributed to this effect, Liproxstatin-1 was added to TMZ treatment. Liproxstatin-1 (Lip-1) is a potent ferroptosis inhibitor and does so by inhibiting lipid peroxidation through radical trapping (Zilka et al., 2017). Lip-1 was added to treatment medium at a concentration of 500nM.

Addition of Lip-1 results in no statistically significant changes in viability in either WT, chemical inhibition or mutant cell populations, with viability at 63.58% (SD 4.19%), 63.88% (SD 3.72%), and 53.60% (SD 4.67%) respectively.

Compared to the 200µM TMZ treatment group, a tentative decrease in viability could be observed after additional treatment with Lip-1, possibly indicating an additive cytotoxic effect of the combination of the two compounds.

While differences between C6 WT and C6 ALDH1A3KO populations bear no statistical significance (Adjusted p-values 200µM TMZ: 0.38; 200µM TMZ + 500nM Lip-1: 0.99), significance is partially observed between C6 WT and C6WT/DEAB (Adjusted p-values 200µM TMZ: 0.013; 200µM TMZ + 500nM Lip-1: 0.09); while the latter slightly misses

statistical significance as previously defined, a significant result can at least be assumed. Similarly, statistical significance is partially achieved between C6 WT/DEAB and C6 ALDH1A3KO significance (adjusted p-values 200µM TMZ: 0.030 ; 200µM TMZ + 500nM Lip-1: 0.079).

5.6 Ferroptosis Can be Induced in C6 WT and ALDH1A3KO and Reduces Viability

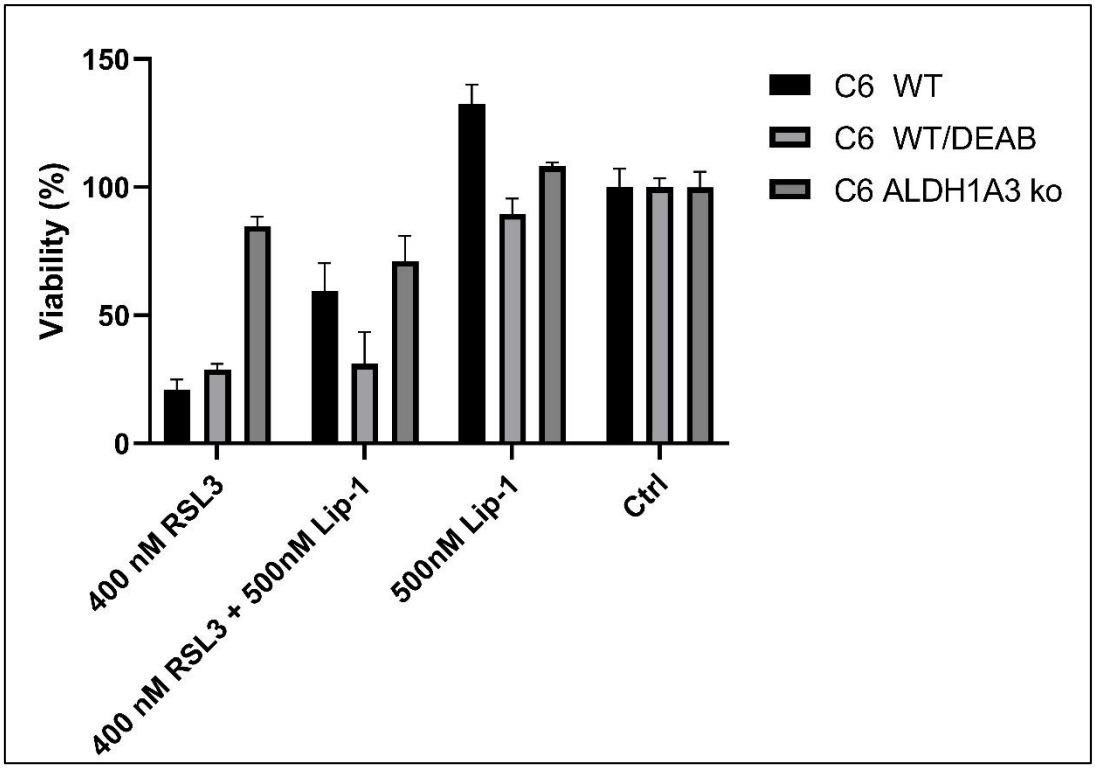

Figure 10. Ferroptosis is induced in C6 cell populations and is most pronounced in WT and WT/DEAB. Its effect is reversible with addition of Liproxstatin-1. Liproxstatin-1 alone has proliferative effect on wild type and ALDH1A3KO.

As previously stated, RSL-3 binds GPX-4, the only intracellular reductor of lipid hydroperoxides, and thus performs as a potent ferroptosis inducer.

Treatment of C6 WT, C6 WT/DEAB and C6 ALDH1A3KO populations with RSL-3 at a concentration of 400nM rendered reproducible decreases in viability for the first two groups, at 20.89% (SD 4.03%), 28.93% (SD 2.11%), while viabîlity for C6 ALDH1A3KO was surprisingly measured at 84.85% (SD 3.53%).

For C6 WT, this effect was antagonizable when cells were additionally treated with 500nM Lip-1 with viability measured at 59.41% (SD 10.9%; adjusted p-value 0.014). C6 ALDH1A3KO values after treatment with RSL-3 must be interpreted with caution as viability

with ferroptosis inhibitor Lip-1 indicates lower viability than with RSL-3 alone (84.85% vs. 71.20%).

As a control, cell populations were also treated with 500nM Lip-1 by itself; for C6 WT and C6 ALDH1A3KO this induced increased proliferation with viability values at 132.46% (SD 7.59%) and 108.23% (SD 1.43%), the C6 WT/DEAB population had a measured viability of 89.55% (SD 5.99%) compared to the control. These results could indicate that for treatment groups with sustained ALDH1 activity or mostly sustained ALDH1 activity (ALDH1A3KO showed only marginal changes in ALDH1-activity in ALDEFLUOR Assay) Lip-1 can inhibit background ferroptotic activity while in the setting of complete ALDH1-inhibition (WT/DEAB) the combination of not serviced aldehyde breakdown due to normal cell turnover in the setting of tumor tissue growth and another therapeutic agent in Lip-1 results in slightly reduced viability in comparison to the control group.

5.7 Reduced Colony Formation Can Be Attributed to ALDH1 but not Isotype ALDH1A3

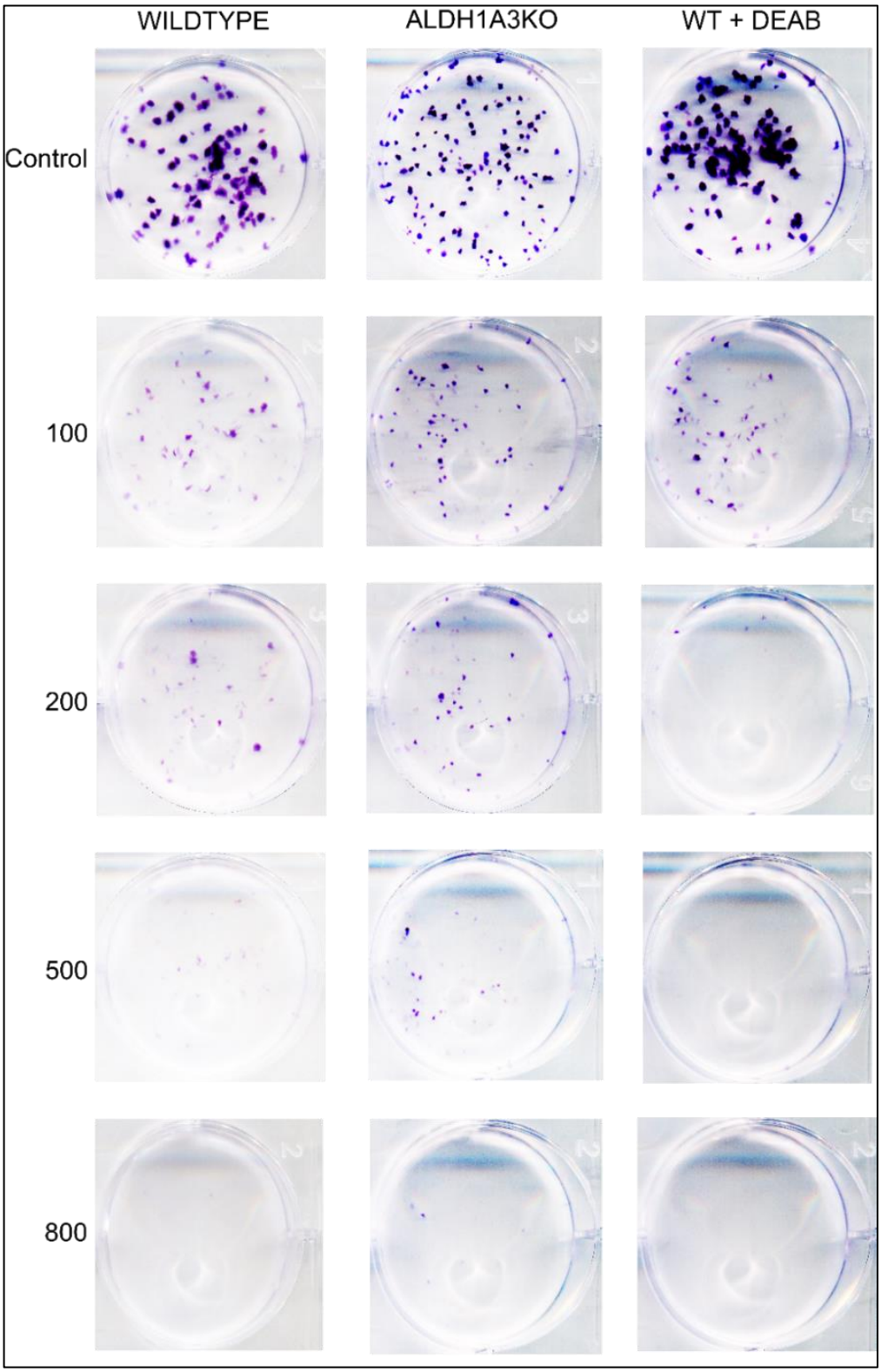

Figure 11. Colony formation in C6 wild type, C6 ALDH1A3 knockout and C6 Wild type + ALDH1 inhibitor DEAB after treatment with different concentrations of Temozolomide (in µM).

In order to avoid rapid confluence in C6 wild type cells, 150 cells were seeded in each well of plate before treatment. The experiments were performed in 6-well plates. After 12 hours, cells had grown to adherence and treatment was performed with TMZ at different concentrations (0, 100µM, 200µM, 500µM, 800µM). H_2O_2 was used as a toxicity control. After 24 hours, treatment medium was replaced with regular growth medium and plates were incubated for one week to allow for formation of cell colonies. Hereafter, cells were fixed for interpretation of results.

5.7.1 Plating Efficiency

	C6 WT	C6 ALDH1A3KO	C6 WT + DEAB
Colonies (n, mean)	99	124	97.6
Plating Efficiency (%)	66	82.6	65.1

Plating efficiency (PE) as a measurement of adherence of a comparatively low number of tumor cells showed comparative PE for C6 WT and C6 WT + DEAB treatment groups; C6 ALDH1A3 plating efficiency was calculated at 82.6%, higher than that of wild type treatment groups (WT at 66%, WT + DEAB 65.1%), indicating reproducably effective plating.

5.7.2 Temozolomide Inhibits Colony Formation for Chemically Inhibitor C6 Wild Type Cells but C6 ALDH1A3 Knockout Cells Only Show Minor Response.

5.7.2.1 C6 Wild Type Vs. C6 ALDH1A3 Knockout

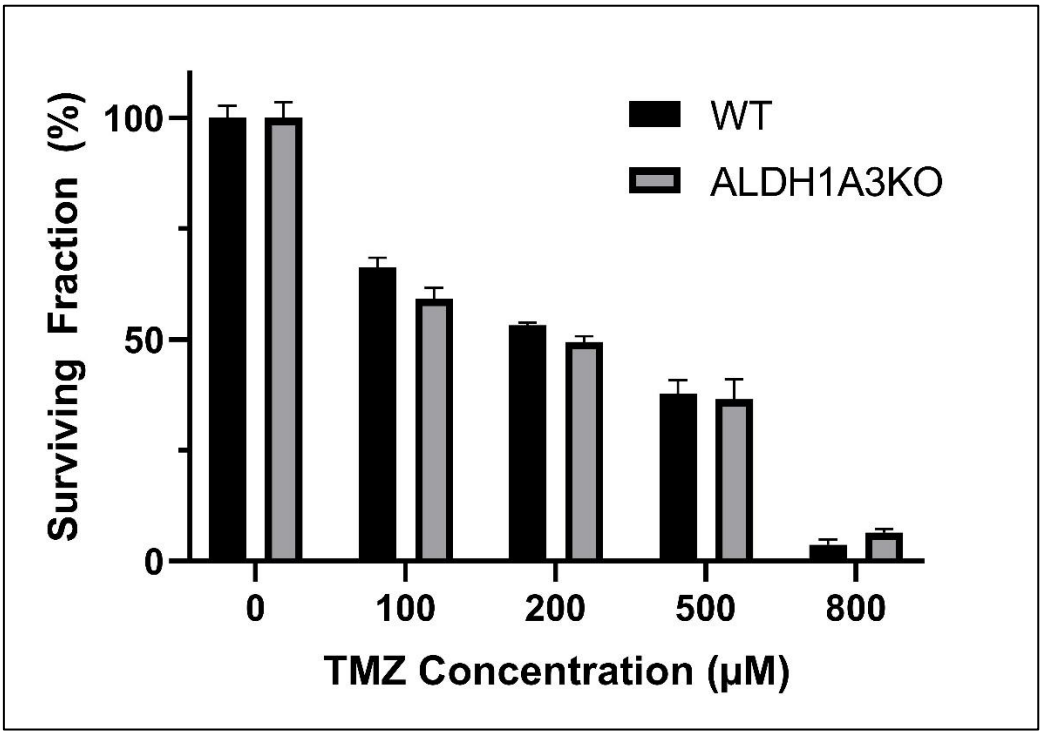

Figure 12. Colony formation after Temozolomide treatment shows no significant differences between C6 WT and ALDH1A3KO.

Throughout the different concentrations of Temozolomide, C6 wild type and C6 ALDH1A3 knockout cells show comparable colony forming behavior. In the 100/200µM treatment groups, a slight yet statistically significant difference can be assessed (100: 66.40% vs. 59.13%, p-value 0.032; 200: 52.23% vs. 49.48%, p value 0.038), yet one that, if it were to translate into an in vivo scenario, would likely not make a difference in tumor satellite growth. At higher concentrations, this gap between both cell types disappears and renders differences nonsignificant.

5.7.2.2 C6 Wild Type Vs. C6 Wild Type + Chemical ALDH1 Inhibition

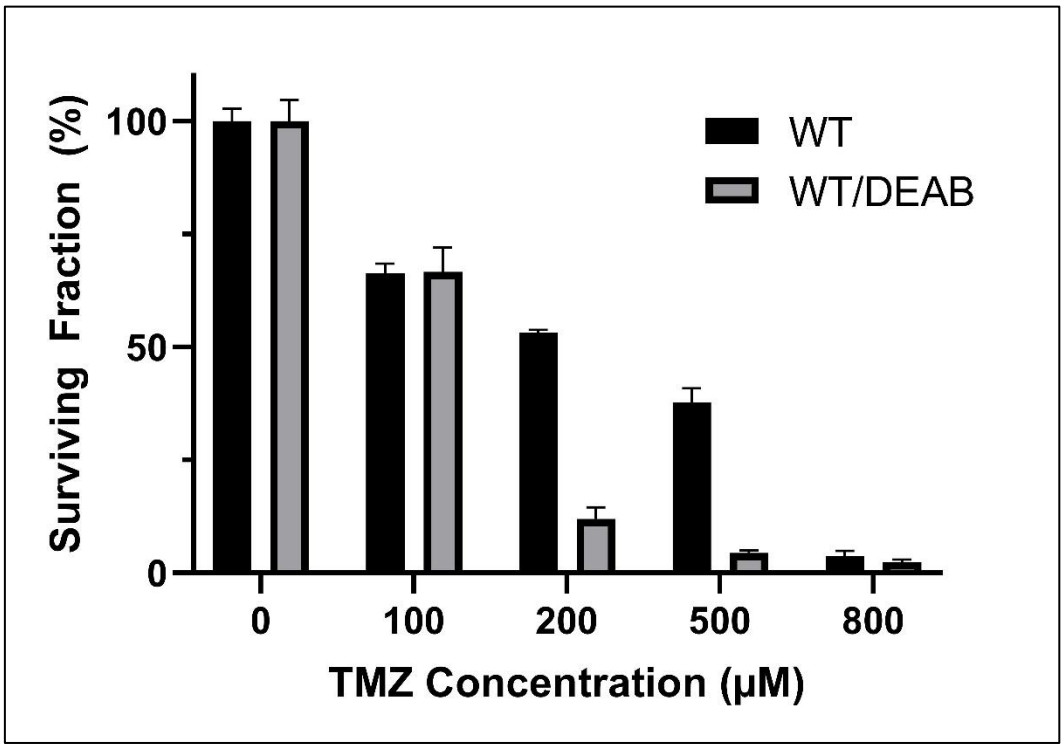

Figure 13. Colony formation is significantly impaired in C6 undergoing chemical ALDH1 inhibition compared to wild type.

DEAB inhibition shows reproducable decline in colony formation capabilities at medium and high TMZ concentrations; specifically, surviving fractions differ significantly at the 200/500 µM levels (200: 53.23% vs. 12.00%, p-value 0.004; 500: 37.67% vs. 4.442%, p value 0.002), indicative of a significant effect of unspecific ALDH1 inhibition through DEAB. This effect cannot be found at smaller or higher concentrations but appears to be specifically in range of what could be considered physiological TMZ concentrations.

5.7.2.3 C6 ALDH1A3 Knockout Vs. C6 Wild Type + Chemical ALDH1 Inhibition

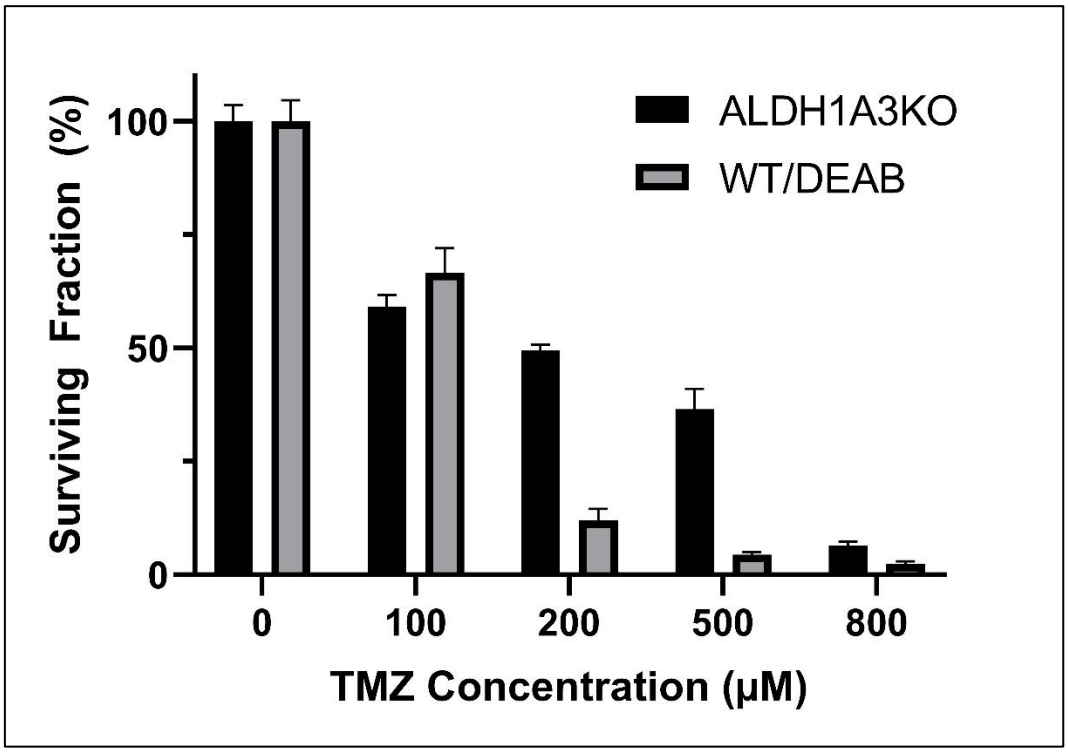

Figure 14. ALDH1A3 knockout results in more efficient colony formation that chemical inhibition of all ALDH1 isotypes

A similar effect can be acknowledged when comparing ALDH1A3 knockout to chemical inhibition; here as well, significant differences (200: 49.48% vs. 12.00%, p-value 0.004; 500: 36.50% vs. 4.442%, p-value 0.005) can be observed in the 200/500 µM treatment groups.

Table 5. Statistical comparison of C6 wild type and C6 ALDH1A3 KO in colony formation

TMZ (μM)	Wild type (mean)	ALDH1A3KO (mean)	Difference	p-value
100	66.40	59.13	7.265	**0.031979**
200	53.23	49.48	3.751	**0.037860**
500	37.67	36.50	1.178	0.632840
800	3.726	6.439	-2.713	0.029671

Table 6. Statistical comparison of C6 wild type and C6 wild type/DEAB in colony formation

TMZ (μM)	Wild type (mean)	WT + DEAB (mean)	Difference	p-value
100	66.40	66.63	-0.2348	0.970130
200	53.23	12.00	41.23	**0.004481**
500	37.67	4.442	33.23	**0.002034**
800	3.726	2.391	1.335	0.083018

Table 7. Statistical comparison of C6 wild type/DEAB C6 ALDH1A3 KO in colony formation

TMZ (μM)	WT + DEAB (mean)	ALDH1A3KO (mean)	Difference	p-value
100	66.63	59.13	-7.499	0.161636
200	12.00	49.48	37.48	**0.003684**
500	4.442	36.50	32.05	**0.004903**
800	2.391	6.439	4.049	**0.026276**

6 Discussion

6.1 In Viability Assays, Effect of ALDH1A3 Knockout in Human Glioma Cell Lines Cannot Be Reproduced in the C6 Rattus Norvegicus Model

An effect of ALDH1A3 knockout on viability of tumor cells in vitro has been demonstrated in a variety of laboratory setups, including our laboratory. In this experimental setup, this effect could not be replicated in the C6 cell line.

6.1.1 Knockout of ALDH1A3 Does Not Make C6 Tumor Population More Susceptible to Temozolomide

Effect of ALDH1A3 knockout has never been examined in C6 cells, one of the most commonly used in vitro glioma models in the last 50 years. Our experimental setup aimed to measure sensitivity to Temozolomide at different concentrations of the drug in order to find out whether 1A3 knockout would results in increased chemosensitivity, even though Aldefluor Assay had indicated that ALDH1^{hi} C6 population was relatively small compared to other, predominantly human, glioma cell modes. As other isotypes of ALDH, specifically ALDH1A1, had also been demonstrated to possess high protumoral capacity, this was an early indicator that ALDH1A3 knockout would not impact survival after TMZ treatment significantly.

Our experimental setup showed insignificantly decreased viability of C6 ALDH1A3 knockout at the chosen concentrations of 100 + 200µM TMZ in comparison to wild type population; the cytotoxicity control (20µM H_2O_2) mirrored those results but seems to indicate higher viability in the ALDH1A3 population. In comparison to ALDH1 chemical inhibition through DEAB, both assessed groups show higher survivability for TMZ and H_2O_2. For the C6 experimental setup, these findings seem to indicate that expression/overexpression of ALDH1 isotypes does convey a marked survival advantage in the face of current chemotherapeutical treatment; the DEAB inhibition, in all experiments, led to significantly decreased viability. In considering why this is, the results from the Aldefluor Assay should be acknowledged. Here, the C6 wild type population showed an ALDH^{br} population of 3.88% whereas ALDH^{br} population of ALDH1A3 knockout was measured at 0.66%. This indicates that C6 ALDH1 activity, while seemingly still conferring a survival advantage, is much lower than that in human glioma cells lines LN229 and U87 where ALDH1 activity has been shown in 43.1% and 14.3%, respectively, of control population (Li et al., 2018). It also indicates that ALDH1A3 knockout reduces ALDH^{br}

population significantly, so we can conclude that most of the ALDH^{br} population is in fact made up by ALDH1A3 positive cells. The size of the ALDH^{br} population is comparable to

other attempts to define stem cell populations within the C6 glioma models, so it is reasonable to assume that this population can be defined by ALDH1A3 positiveness; however, we can also conclude that its knockout is not mainly responsible for conveying a survival benefit.

6.1.2 ALDH1, but Not Isotype 1A3, Is Indicated in the Ability To Recommence Tumor Formation and Colony Growth in C6 Glioma Model

The Colony Forming Assay is a modality frequently used in tumor research to assess a cell population's ability to maintain proliferation capabilities after being exposed to treatment (Franken et al., 2006). More specifically, the experimental setup requires isolation of cells from one another to test one cell's ability to self-renew, differentiate and form a functioning colony from itself, tasks that are generally attributed only to a certain subset of cells within a tumor mass, the stem cell population (Yu et al., 2012). To account for rapid proliferation of the C6 cell line used for this experiment, we plated 150 cells from C6 wild type and ALDH1A3 knockout populations, an additional C6 wild type population was exposed to DEAB inhibition in the same manner as in other viability assays performed. Treatment with Temozolomide (TMZ) was done at concentrations of 100/200/500/800µM, H_2O_2 was used as cytotoxicity control.

Results obtained in this assay are similar to those obtained in the regular treatment assay. A significant difference can be observed between both C6 wild type and C6 ALDH1A3KO compared to DEAB-inhibited C6; this difference is most pronounced at medium to high concentrations (200/500µM TMZ) where DEAB inhibited C6 cells show significantly decreased survival fractions; 100µM and 800µM do not show significant differences compared to chemical inhibition. This suggests that in the colony formation setup, low concentrations do not sufficiently impact ALDH-mediated release of oxidative stress in the form of reactive oxygen species (ROS) even though low concentrations already affect overall survivability. What seems to be counterintuitive in this regard is that minor yet significant differences could be seem between wild type and ALDH1A3 populations at 100 + 200µM in these experiments. Whether this is an experimental artefact or an actual discovery is unclear; possibly, reduction of ALDH1 capacity results in lower survival whereas total ALDH1 inhibition triggers other systems to deal with oxidative stress. When interpreting results that attempt to investigate importance of ALDH impact on therapeutic resistance of cancer tissues, it is important to remember that other molecular compounds are also active in metabolizing aldehydes accumulating when cells deteriorate, namely Cytochrome P450 enzymatic complexes (Cyp450), Aldehyde oxidases (AO), aldo-ketoreductases and other short-chain reductases (Ahmed Laskar & Younus, 2019). These players could be activated in the setting of total ALDH1 inhibition and lower survivability

whereas partial ALDH1 knockout might not trigger supra-proportional involvement because the tissue can manage to survive at only marginally lower cell counts.

At high concentrations, effect of ALDH1A3 knockout and ALDH1 inhibition is marginalized again, resulting in non-significant differences in survival.

It is unclear in which order these different enzyme and enzyme complexes that are associated with aldehyde metabolism are activated. The interaction between these and other mechanisms by which drug resistance is mediated, i.e. ABC Transporters or the blood brain barrier itself (Drean et al., 2018), needs further investigation to explain why differences in survival dependent on single ALDH1 isotypes can only be visualized at certain drug concentrations and not at others.

6.1.3 The C6 Cell Line is Radioresistant Independent of ALDH1A3 Status and Radiation Dose

Radiation therapy remains an essential part of GBM therapy, having shown a limited but reproducible effect on overall survival alone or in combination with Temozolomide and either as primary therapy modality or post-operative (Stupp et al., 2005). Radiotherapy can be fractionated into 2Gy or 1.5Gy sessions dependent on performance status or age of the patient. In our experiment, we sought to elucidate whether ALDH1A3 knockout had any effect on efficacy of radiotherapy. Radiotherapy was performed at different dosages, a single treatment was admnistered.

Independent of ALDH1A3 knockout, C6 showed high radioresistance; even at high radio dosage, no effect could be seen. Compared to wild type population, ALDH1A3 knockout was inefficient at producing higher sensitivity to radiotherapy. Survival fractions were similar between control and even the highest administered radiation dose, 10Gy.

Radioresistance is common for glioma in vitro models. Specifically, C6 cells have been shown to show little reaction to single dose radiotherapy. Parthymou et al. were able to produce similar results; here, at doses of 5Gy and less, no effect on survival was shown; higher doses (in their experimental setup up to 40Gy) were able to produce marginally decreased survival in the remaining dosing overlap between the two experiments (5-10Gy), in this range only intermittently, as cell counts of C6 treated with 10 Gy reapproached those of the control within 15 days (Parthymou et al., 2004). While the exact mechanisms of in vitro radioresistance are still unclear, they have been attributed to several factors, including increased angiogenesis, hypoxia and other microenvironmental cues that enable survival of stem-like glioma cells (Bao et al., 2006; Lathia et al., 2015). As is shown in this experiment, ALDH1A3 knockout is not one of those mechanisms. It can be assumed that

compared to the cumulative effect of all other mechanisms that are induced in the setting of Radiotherapy-mediated DNA damage, the absence of ALDH1A3 is negligible. For a radioresistant cell population like the C6 glioma, lower radiation doses even seem to induce a proliferation benefit, possibly through angiogenetic cues in the perivascular niche where stemlike glioma cells are known to reside or by causing differentiation to mesenchymal glioblastoma subtypes that are associated with poor overall survival (Behnan et al., 2019; Bhat et al., 2013).

6.2 Ferroptosis Is Not the Mechanism of Cell Death in the Setting of Temozolomide Therapy

Mechanisms of cell death have been abundantly studied in GBM. Recently, studies have shown that in the setting of TMZ therapy, glioma cells undergo apoptosis, autophagy and enter a state of senescence while necrosis is only marginally induced (Knizhnik et al., 2013). With the discovery of the Fe^{2+} mediated cell death type Ferroptosis, much research aimed at further understanding the mechanisms and classify clinical scenarios in which it is present in disease, specifically cancer, has been done. In certain cancer entities, induction of ferroptosis in the setting of conventional therapy specific to the tumor tissue has resulted in increased sensitivity. Prominently, Sorafenib, a multikinase inhibitor readily used as a first line treatment for hepatocellular carcinoma, has shown an effect associated with ferroptotic cell death; induction of ferroptosis seemed to alleviate the effect of Sorafenib during cancer therapy and inhibition of ferroptosis marginalized it; specifically, co-administration of Defuroxamine (DFX), an iron chelator that effectively binds intracellular iron and thus functionally inhibits Ferroptosis, was able to marginalize Sorafenib efficacy; presaturation of DFX with Iron, on the other hand, resensitized hepatocellular carcinoma to its effect in vitro (Louandre et al., 2013).

Feng et al. were subsequently able to show that the response of in vitro HCC cell lines to treatment with Sorafenib (as quantified by the IC_{50} value) was inversely correlated with Acyl-CoA synthetase long-chain family member 4 (ACSL4) expression, an enzyme known as ferroptosis inducer, and that ACSL4 also served as an Sorafenib-independent biomarker of its treatment efficacy (Feng et al., 2020).

The relationship between gliomatous tumors and ferroptosis has not yet been as well investigated. Ferritin and Transferrin have been found to be upregulated in patients with gliomatous tissues compared to healthy controls (Legendre & Garcion, 2015) and the loss of appropriate iron storage capabilities by shRNA inhibition of Ferritin has even been shown to decrease the ability of glioma stem cells (GSC) to proliferate as evidenced by decreased

tumor sphere formation (Schonberg et al., 2015). On the other hand, the presence of reactive oxygen species in GSC has been associated with decreased overall survival (Singer et al., 2015), indicating that the presence and the role of iron, not just in glioma, is not one that cannot be easily summarized.

Our intention was to contribute to the growing pool of information about the role of ferroptosis in GBM in a treatment setting in the C6 cell setup; to evaluate whether ferroptosis can be induced in C6 cells and to assess whether TMZ-mediated cell death is associated with ferroptosis.

C6 WT, C6 ALDH1A3KO, and chemically ALDH1-inhibited C6 cells were subjected to TMZ (200uM); in addition, these cell populations were also treated with Lip-1 (500nM). TMZ treatment groups showed viability that was comparable to that shown in the TMZ viability assays. Additional treatment with Lip-1 showed nonsignificant differences compared to the TMZ controls, indicating that the manner of cell death under treatment with TMZ cannot not be categorized as ferroptotic. In light of the known mechanisms by which both TMZ and Lip-1 have been shown to propagate their effect, this is not unreasonable. Gluthathione peroxidase 4 (Gpx4) is a phospholipid peroxidase and catalyzes lipid peroxides in a reaction in which reduced Glutathione-sulfide is produced, thus protecting cells from radical oxygen species (ROS). Scenarios in which this mechanism is defective, i.e. loss of function mutations in the Gpx4 gene, otherwise Gpx4 inhibition or GSH depletion, lead to accumulation of ROS and induce damage to lipid membranes and subsequent cell death (Skouta et al., 2014). In this setting, Lip-1 can trap a variety of peroxyl radicals and prevent cell death in place of Gpx4 (Zilka et al., 2017).

Temozolomide, as has been discussed, acts as a prodrug alkylating DNA at purine bases, preferentially at O6-guanine and N7-guanine, but also N3-adenine without known production of ROS (Zhang et al., 2012). Thus, these results confirm that, during regular TMZ administration, ROS that arise in the cell can be effective taken care of by tumor-specific Glutathione activity, possibly augmented by gain of function mutations of the players involved, for example Gpx4.

An indication that these players are part of the hypermutated intratumoral machinery of GBM could be observed when C6 populations were treated with RSL-3. Compared to control, significantly decreased survival could be induced in WT and DEAB-inhibited cells; this effect was visible throughout, as surviving fractions in WT and DEAB-inhibited cells were reduced to 20.89% and 28.93%, respectively. Interestingly, ALDH1A3KO did not present equally RSL-3 sensitive with a survival fraction of 84.85%. Addition of Lip-1 was able to antagonize the RSL-3 effect, and increase survival in C6 WT and DEAB inhibition

significantly; C6 ALDH1A3KO showed nonsignificant differences to its sister population solely treated with RSL-3.

Additionally, sole treatment with Lip-1 resulted in increased viability in C6 WT, C6 ALDH1A3 populations, while the chemically inhibited DEAB C6 population showed slightly lower (non-significant) survival compared to its control. These effects seem inconclusive at first, yet can be explained when interpreting the results in light of observed growth doubling times of the respective population. C6 WT showed shortest doubling rates, thus creating a scenario in which the likelihood for intermittent hypoxia in the setting of ever increasing cell numbers is highest; thus, it is plausible that it has the highest chance for the creation of ROS through cell death and the highest potential for inhibited cell division that can be antagonized by Lip-1. With modestly decreased doubling time in the ALDH1A3 population this effect can be replicated, but not as pronounced as in the wild type population. Lastly, cells treated with DEAB are inherently more susceptible to baseline accumulation of aldehydes and ROS and this in itself should create some baseline growth inhibition which results in lower viability compared to the other two populations.

6.3 The Role of ALDH1A3 in Other Glioma Models

Wu et al. have demonstrated that in human glioma cell lines U87, T98G and LN229, ALDH1A3 is an adequate marker of the GSC population and have also shown that, compared to the control, knockout of ALDH1A3 expression led to significantly reduced viability in TMZ treatment settings at lower concentrations (specifically <300µM) (Wu et al., 2018). From our experimental setup, these results can only partially be confirmed. Aldefluor Assay showed that ALDH1A3 knockout can properly reduce the $ALDH1^{br}$ population to <1%, while C6 WT showed a $ALDH1^{br}$ population of 3.88%. Zhou et al. attempted to examine the C6 GSC population through expression of Nestin, a popular stem cell marker, and thus estimated it at around 4%; this resonates well with our current results (Zhou et al., 2009). In Wu's experimental setup, ALDH1A3 knockout was similarly successful but cell lines differed significantly in ALDH1A3 proportion with LN229, U87, and T98G was measured at 24.7%, 8.57%, and 3.05%, respectively. Their TMZ treatments indicated significant difference between treatment groups, the effect being most pronounced at lower TMZ concentrations and most pronounced in LN229, the cell line with the highest original ALDH1A3 content (Wu et al., 2018); in line with this, LN229 also showed highest relative reduction in viability compared to the control. T98G, the cell line with the lowest original ALDH1A3 content, however, showed lower relative reduction compared to the control; the relative reduction in viability is somewhat in line with what we were able to observe in the

C6 cell line (C6 viability at 100 µM TMZ: 80.03% ± 1.65%; T98G viability at 100µM TMZ: 80-90%). Compared to these values, LN229 showed viability values at 100µM TMZ of ~40%. These results seem suggestive for several important observations: while ALDH1A3 seems a potent stem cell marker (or rather a marker of overall ALDH1 activity) we cannot presume it to be prognostic of sensitivity to TMZ treatment. Wu et al. were able to observe that it does in fact convey some sort of survival benefit for treated cells in vitro (whether a relative reduction of 20-40% is enough end up actually impacting overall survival in vivo remains to be seen) but that the overall treatment effect of TMZ seems to be heavily impacted by other factors as $ALDH1A3^{hi}$ cells showed significantly higher baseline sensitivity to TMZ than $ALDH1A3^{lo}$ cells. These results are corroborated in our experimental setup with the distinction that C6, overall presenting as a highly TMZ-resistant specimen, do not show significantly elevated sensitivity with additional knockout of ALDH1A3.

As stated, System X_c^- (SLC7A11) is an essential regulator of the antioxidant capacity of glial cells by providing Cysteine in exchange for Glutamate, thus driving Gluthathione activity by supplying it with the rate limiting factor Cysteine; its pivotal role in the maintenance of an ROS-free environment within tumor tissues through different mechanism has been well documented (Jiang et al., 2015; Lei et al., 2020). In cell lines F98 and U251, Sehm et al. used overexpression and knockdown of SLC7A11 to gather insight about the role of ferroptosis in glioma cells undergoing treatment; their results showed, similarly to ours, that simple TMZ therapy does not lead to ferroptotic but rather apoptotic and autophagic cell death. Furthermore, they were able to show that SLC7A11 knockdown could induce TMZ-mediated cell death, thus leading to decreased viability relative to the overexpressing treatment control; here, efficacy of ferroptosis induction depended on SLC7A11 levels. Combined Erastin/TMZ treatment, however, was only able to produce statistically significant results in U251 (Sehm et al., 2016). We can now confirm that TMZ-related cell death in C6 occurs similarly in an ferroptosis-independent manner, but that ferroptosis can be induced and results in reduced viability that is more pronounced in a ALDH1-native cell population. Whether combined treatment increases the TMZ effect and how knockout/-down of important players in its pathway affect that therapeutic capacity in the C6 glioma cell line requires more investigation.

Wu et al. took another step at bridging the gap to ALDH1A3 as a stem cell marker and active contributor of TMZ-related therapy resistance by identifying oxidative stress as a significant component of TMZ-mediated cell death in cell lines LN229, T98G and U87 (Wu et al., 2020). While interesting, we suggest that, given the lack of effect of ALDH1A3 knockout on TMZ sensitivity in C6 glioma cells, an investigation of this would not lead to results that show palpable impact on tumor viability.

Lastly, in the radiation (IR) setting, Lei at al. were able to show in lung cancer cell lines that, similarly to the treatment of TMZ in C6, while IR induction induces DNA damage and repair mechanism, it it not associated with ferroptotic cell death; ferroptosis was able to be induced however by a variety of mechanisms including chemical inhibition and knockout of ferroptosis-inhibiting mechanisms, resensitizing the tumor tissue to IR (Lei et al., 2020).

6.4 Is it Time for ALDH Inhibitors In Vivo?

As an understanding of the role of various ALDH isotypes in a variety of cancer tissues has been gained over the last 10 years, and their use as prognostic markers and markers of stem-like subpopulations has been well investigated, there has been increasing research focused on identifying molecules that can act as ALDH inhibitors in therapy settings.

For development of ALDH inhibitors, three subsites have been identified as potential targets: the aldehyde substrate binding site, the polymerization site, and lastly the Co-Factor NAD+ binding site (Dinavahi et al., 2019). ALDH inhibitors can be most successfully created as multiform inhibitors, most prominently inhibiting the enzyme at the ALDH-unique NAD+ binding site or,isotype-specific at the isotype-unique polymerization site (Dinavahi et al., 2019).

The best known multiform ALDH inhibitors include DEAB and 4-dimethylamino-4-methyl-pent-2-ynthioic acid-S-methylester (DIMATE). DEAB presents as an irreversible inhibitor of ALDH1A2, ALDH2 and a competitive inhibitor of ALDH1A1, ALDH1A3, ALDH5A1, and ALDH1B1 (Morgan et al., 2015); DIMATE, an amino thiolester has been reported as a capable ALDH1A1 and ALDH1A3 inhibitor with high efficacy in prostate cancer cell lines and also in vivo in melanoma models (Fournet et al., 2013). Whether it can be used in a clinical trial setting has not yet been reported.

Citral is a natural compound occurring in a variety of plants including lemon, orange, lemongrass and certain tomato species and has also been found in the pheromonal concoctions of several insects, including the Leafcutter Ant. It has been found to have anti-tumor activity in breast cancer cell lines with high ALDH1 activity and, if delivered by nano-particle encapsulation, to reduce ALDH1A3-mediated tumor growth (Thomas et al., 2016). Unfortunately, its heritage as a natural agent produces a variety of off-target effects, making it largely unsuitable as an anti-cancer agent.

Various isotype-specific ALDH inhibitors have been investigated. CM037, a competitive ALDH1A1 inhibitor, inhibited ovarian cancer cell lines in combination with Cisplatin but proved to have low solibility in water and thus ineffective in vivo (Morgan & Hurley, 2015).

NCT-501, also a selective ALDH1A1 inhibitor, showed effectiveness in monotherapy of squamous head and neck carcinoma (Yang et al., 2015) and its chemically optimized siblings NCT-505 and NCT-506 were competent in inhibiting ovarian cancer cell lines in combination with Paclitaxel with the added benefit of oral bioavailability (Yang et al., 2018). Lastly, 13g and 13h showed anti-tumor capacity in ovarian cancer cell lines alone and in combination with cisplatin and were able to be administered in vivo through the intraperitoneal route (Huddle et al., 2018).

While the search is ongoing for ALDH inhibitors, isotype specific or not, few have been shown to be suitable for in vivo administration. Advancing these compounds to become treatment options will require an interdisciplinary approach and collaboration of chemists, foundational researchers and clinical scientists.

7 Limitations

Experimental setup was intermittently hampered by growth rate of C6 wild type cells; experimental setup had to be adjusted to allow for all treated cell variations to remain in logarithmic growth phases so that comparability was preserved. In vivo, Temozolomide is administered 5 days per cycle. Initially, the experimental setup attempted to copy in vivo administration of the chemotherapeutic agent, however C6 wild type grew to confluence within 72 hours, thus the interpretation of results was concluded with data obtained after 48 hours.

We only give an introductory overview of the impact of ferroptotic cell death on decreased viability in the C6 cell model. In order to investigate further, there should be an evaluation of the presence of other components of intracellular ferroptosis pathways, for example baseline Gpx4 expression, changes in Gpx4 expression under treatment with TMZ and IR. As RSL-3 proved to exhibit cytotoxic effects, most pronounced in C6 WT and DEAB inhibited C6 cells, combined treatment with RSL-3 and TMZ needs to be performed in regular viability assays and CFA to assess whether the combination increases cytotoxicity further.

Combined treatment with TMZ and IR was not performed in this experimental setup; furthermore, for the radiation treatments, DEAB inhibited C6 cells were excluded since radiation chambers are in high demand at our institution and thus usage time was limited; a more pronounced effect in the DEAB-inhibited cell population would have indicated ALDH1 isotypes other than 1A3 in play to mediate IR resistance. As it has been identified as a stem cell tumor marker in a variety of cell lines, ALDH1A1 needs further investigation in the C6 cell model.

Lastly, we identified ALDH1A3 as a stem cell marker in the C6 cells; $ALDH^{hi}$ cells in the C6 population (and its subsequent reduction by ALDH1A3 knockout) are comparative to previous experiments attempting to identify stem cell populations within the cell line with traditional stem cell markers Nestin and CD133. Using these markers for FACS analysis in this case would have acted as proof of principle.

8 Conclusion

Treatment of Glioblastoma multiforme remains a challenging task. In times in which immunotherapy has changed the landscape of cancer therapy and significantly increased overall and progression free survival, therapy options in the GBM landscape remain scarce. Characterizing neoplasms at the molecular level has led to the generation of a variety of therapeutic agents. However, many tumor entities, and Glioblastoma especially so, present as heterogeneous tissues. Next Generation Sequencing allows for fast identification of of potential molecular targets. Especially the characterization of therapy-reisistant subpopulations with stem-like capacities could enable clinician scientists to improve outcome of current therapy regimens. For this, it is important that experiments look not only at selected cell lines or tumor models but come to a comprehensive understanding of all those in use, identifying similarities and differences and the underlying mechanisms.

We are contributing to the breadth of information by identifying ALDH1A3 as an appropriate stem cell marker in C6 cells, however cannot underscore its knockout as an effect contributing to Temozolomide or IR resensitization. We also show that in C6 cells ferroptosis can be induced and is effective in decreasing viability. Interestingly, since in the absence of ALDH1A3, RSL-3 seems to be losing its ability to induce ferroptosis in the C6 glioma model, more investigative work must be done to illucidate its specific role in this novel form of cell death.

It remains to be seen whether induction of ferroptosis can be incorporated in current treatment strategy or whether further characterization of ALDH isotypic make up in the C6 population can serve to identify other target strategies; they are needed to provided GBM patients with an improved prognostic perspective in the setting of one of the most lethal cancer entities known.

9 Bibliography

Aguirre-Ghiso, J. A. (2007). Models, mechanisms and clinical evidence for cancer dormancy. *Nature Reviews Cancer*, *7*(11), 834-846. https://doi.org/10.1038/nrc2256

Ahmed Laskar, A., & Younus, H. (2019). Aldehyde toxicity and metabolism: the role of aldehyde dehydrogenases in detoxification, drug resistance and carcinogenesis. *Drug Metab Rev*, *51*(1), 42-64. https://doi.org/10.1080/03602532.2018.1555587

Alexander, B. M., & Cloughesy, T. F. (2017). Adult Glioblastoma. *J Clin Oncol*, *35*(21), 2402-2409. https://doi.org/10.1200/JCO.2017.73.0119

Arita, H., Narita, Y., Fukushima, S., Tateishi, K., Matsushita, Y., Yoshida, A., Miyakita, Y., Ohno, M., Collins, V. P., Kawahara, N., Shibui, S., & Ichimura, K. (2013). Upregulating mutations in the TERT promoter commonly occur in adult malignant gliomas and are strongly associated with total 1p19q loss. *Acta Neuropathol*, *126*(2), 267-276. https://doi.org/10.1007/s00401-013-1141-6

Arita, H., Yamasaki, K., Matsushita, Y., Nakamura, T., Shimokawa, A., Takami, H., Tanaka, S., Mukasa, A., Shirahata, M., Shimizu, S., Suzuki, K., Saito, K., Kobayashi, K., Higuchi, F., Uzuka, T., Otani, R., Tamura, K., Sumita, K., Ohno, M., Miyakita, Y., Kagawa, N., Hashimoto, N., Hatae, R., Yoshimoto, K., Shinojima, N., Nakamura, H., Kanemura, Y., Okita, Y., Kinoshita, M., Ishibashi, K., Shofuda, T., Kodama, Y., Mori, K., Tomogane, Y., Fukai, J., Fujita, K., Terakawa, Y., Tsuyuguchi, N., Moriuchi, S., Nonaka, M., Suzuki, H., Shibuya, M., Maehara, T., Saito, N., Nagane, M., Kawahara, N., Ueki, K., Yoshimine, T., Miyaoka, E., Nishikawa, R., Komori, T., Narita, Y., & Ichimura, K. (2016). A combination of TERT promoter mutation and MGMT methylation status predicts clinically relevant subgroups of newly diagnosed glioblastomas. *Acta Neuropathol Commun*, *4*(1), 79. https://doi.org/10.1186/s40478-016-0351-2

Ashkenazi, A., & Salvesen, G. (2014). Regulated cell death: signaling and mechanisms. *Annu Rev Cell Dev Biol*, *30*, 337-356. https://doi.org/10.1146/annurev-cellbio-100913-013226

Bao, S., Wu, Q., McLendon, R. E., Hao, Y., Shi, Q., Hjelmeland, A. B., Dewhirst, M. W., Bigner, D. D., & Rich, J. N. (2006). Glioma stem cells promote radioresistance by preferential activation of the DNA damage response. *Nature*, *444*(7120), 756-760. https://doi.org/10.1038/nature05236

Barth, R. F., & Kaur, B. (2009). Rat brain tumor models in experimental neuro-oncology: the C6, 9L, T9, RG2, F98, BT4C, RT-2 and CNS-1 gliomas. *J Neurooncol*, *94*(3), 299-312. https://doi.org/10.1007/s11060-009-9875-7

Behnan, J., Finocchiaro, G., & Hanna, G. (2019). The landscape of the mesenchymal signature in brain tumours. *Brain*, *142*(4), 847-866. https://doi.org/10.1093/brain/awz044

Benda, P., Lightbody, J., Sato, G., Levine, L., & Sweet, W. (1968). Differentiated rat glial cell strain in tissue culture. *Science*, *161*(3839), 370-371. https://doi.org/10.1126/science.161.3839.370

Beutler, A. S., Banck, M. S., Wedekind, D., & Hedrich, H. J. (1999). Tumor gene therapy made easy: allogeneic major histocompatibility complex in the C6 rat glioma model. *Hum Gene Ther*, *10*(1), 95-101. https://doi.org/10.1089/10430349950019228

Bhat, K. P. L., Balasubramaniyan, V., Vaillant, B., Ezhilarasan, R., Hummelink, K., Hollingsworth, F., Wani, K., Heathcock, L., James, J. D., Goodman, L. D., Conroy, S., Long, L., Lelic, N., Wang, S., Gumin, J., Raj, D., Kodama, Y., Raghunathan, A., Olar, A., Joshi, K., Pelloski, C. E., Heimberger, A., Kim, S. H., Cahill, D. P., Rao, G., Den Dunnen, W. F. A., Boddeke, H., Phillips, H. S., Nakano, I., Lang, F. F., Colman, H., Sulman, E. P., & Aldape, K. (2013). Mesenchymal differentiation mediated by NF-kappaB promotes radiation resistance in glioblastoma. *Cancer Cell*, *24*(3), 331-346. https://doi.org/10.1016/j.ccr.2013.08.001

Bloch, O., Han, S. J., Cha, S., Sun, M. Z., Aghi, M. K., McDermott, M. W., Berger, M. S., & Parsa, A. T. (2012). Impact of extent of resection for recurrent glioblastoma on overall survival: clinical article. *J Neurosurg*, *117*(6), 1032-1038. https://doi.org/10.3171/2012.9.JNS12504

Bonnet, D., & Dick, J. E. (1997). Human acute myeloid leukemia is organized as a hierarchy that originates from a primitive hematopoietic cell. *3*(7), 730-737. https://doi.org/10.1038/nm0797-730

Brandes, A. A., Franceschi, E., Tosoni, A., Blatt, V., Pession, A., Tallini, G., Bertorelle, R., Bartolini, S., Calbucci, F., Andreoli, A., Frezza, G., Leonardi, M., Spagnolli, F., & Ermani, M. (2008). MGMT promoter methylation status can predict the incidence and outcome of pseudoprogression after concomitant radiochemotherapy in newly diagnosed glioblastoma patients. *J Clin Oncol*, *26*(13), 2192-2197. https://doi.org/10.1200/JCO.2007.14.8163

Brennan, C. W., Verhaak, R. G., McKenna, A., Campos, B., Noushmehr, H., Salama, S. R., Zheng, S., Chakravarty, D., Sanborn, J. Z., Berman, S. H., Beroukhim, R., Bernard, B., Wu, C. J., Genovese, G., Shmulevich, I., Barnholtz-Sloan, J., Zou, L., Vegesna, R., Shukla, S. A., Ciriello, G., Yung, W. K., Zhang, W., Sougnez, C., Mikkelsen, T., Aldape, K., Bigner, D. D., Van Meir, E. G., Prados, M., Sloan, A., Black, K. L., Eschbacher, J., Finocchiaro, G., Friedman, W., Andrews, D. W., Guha, A., Iacocca, M., O'Neill, B. P., Foltz, G., Myers, J., Weisenberger, D. J., Penny, R., Kucherlapati, R., Perou, C. M., Hayes, D. N., Gibbs, R., Marra, M., Mills, G. B., Lander, E., Spellman, P., Wilson, R., Sander, C., Weinstein, J., Meyerson, M., Gabriel, S., Laird, P. W., Haussler, D., Getz, G., Chin, L., & Network, T. R. (2013). The somatic genomic landscape of glioblastoma. *Cell*, *155*(2), 462-477. https://doi.org/10.1016/j.cell.2013.09.034

Brown, T. J., Brennan, M. C., Li, M., Church, E. W., Brandmeir, N. J., Rakszawski, K. L., Patel, A. S., Rizk, E. B., Suki, D., Sawaya, R., & Glantz, M. (2016). Association of the Extent of Resection With Survival in Glioblastoma. *JAMA Oncology*, *2*(11), 1460. https://doi.org/10.1001/jamaoncol.2016.1373

Burger, P. E., Gupta, R., Xiong, X., Ontiveros, C. S., Salm, S. N., Moscatelli, D., & Wilson, E. L. (2009). High aldehyde dehydrogenase activity: a novel functional marker of murine prostate stem/progenitor cells. *Stem Cells*, *27*(9), 2220-2228. https://doi.org/10.1002/stem.135

Cancer Genome Atlas Research, N. (2008). Comprehensive genomic characterization defines human glioblastoma genes and core pathways. *Nature*, *455*(7216), 1061-1068. https://doi.org/10.1038/nature07385

Chamberlain, M. C., Glantz, M. J., Chalmers, L., Van Horn, A., & Sloan, A. E. (2007). Early necrosis following concurrent Temodar and radiotherapy in patients with glioblastoma. *J Neurooncol*, *82*(1), 81-83. https://doi.org/10.1007/s11060-006-9241-y

Chinot, O. L., Wick, W., Mason, W., Henriksson, R., Saran, F., Nishikawa, R., Carpentier, A. F., Hoang-Xuan, K., Kavan, P., Cernea, D., Brandes, A. A., Hilton, M., Abrey, L., & Cloughesy, T. (2014). Bevacizumab plus Radiotherapy–Temozolomide for Newly Diagnosed Glioblastoma. *New England Journal of Medicine*, *370*(8), 709-722. https://doi.org/10.1056/nejmoa1308345

Clarke, M. F., Dick, J. E., Dirks, P. B., Eaves, C. J., Jamieson, C. H. M., Jones, D. L., Visvader, J., Weissman, I. L., & Wahl, G. M. (2006). Cancer Stem Cells—Perspectives on Current Status and Future Directions: AACR Workshop on Cancer Stem Cells. *Cancer Research*, *66*(19), 9339-9344. https://doi.org/10.1158/0008-5472.can-06-3126

Cloughesy, T. F., Mochizuki, A. Y., Orpilla, J. R., Hugo, W., Lee, A. H., Davidson, T. B., Wang, A. C., Ellingson, B. M., Rytlewski, J. A., Sanders, C. M., Kawaguchi, E. S., Du, L., Li, G., Yong, W. H., Gaffey, S. C., Cohen, A. L., Mellinghoff, I. K., Lee, E. Q., Reardon, D. A., O'Brien, B. J., Butowski, N. A., Nghiemphu, P. L., Clarke, J. L., Arrillaga-Romany, I. C., Colman, H., Kaley, T. J., de Groot, J. F., Liau, L. M., Wen, P. Y., & Prins, R. M. (2019). Neoadjuvant anti-PD-1

immunotherapy promotes a survival benefit with intratumoral and systemic immune responses in recurrent glioblastoma. *Nat Med*, *25*(3), 477-486. https://doi.org/10.1038/s41591-018-0337-7

Creighton, C. J., Li, X., Landis, M., Dixon, J. M., Neumeister, V. M., Sjolund, A., Rimm, D. L., Wong, H., Rodriguez, A., Herschkowitz, J. I., Fan, C., Zhang, X., He, X., Pavlick, A., Gutierrez, M. C., Renshaw, L., Larionov, A. A., Faratian, D., Hilsenbeck, S. G., Perou, C. M., Lewis, M. T., Rosen, J. M., & Chang, J. C. (2009). Residual breast cancers after conventional therapy display mesenchymal as well as tumor-initiating features. *Proc Natl Acad Sci U S A*, *106*(33), 13820-13825. https://doi.org/10.1073/pnas.0905718106

Croker, A. K., Goodale, D., Chu, J., Postenka, C., Hedley, B. D., Hess, D. A., & Allan, A. L. (2009). High aldehyde dehydrogenase and expression of cancer stem cell markers selects for breast cancer cells with enhanced malignant and metastatic ability. *J Cell Mol Med*, *13*(8B), 2236-2252. https://doi.org/10.1111/j.1582-4934.2008.00455.x

de Wit, M. C., de Bruin, H. G., Eijkenboom, W., Sillevis Smitt, P. A., & van den Bent, M. J. (2004). Immediate post-radiotherapy changes in malignant glioma can mimic tumor progression. *Neurology*, *63*(3), 535-537. https://www.ncbi.nlm.nih.gov/pubmed/15304589

Deng, S., Yang, X., Lassus, H., Liang, S., Kaur, S., Ye, Q., Li, C., Wang, L. P., Roby, K. F., Orsulic, S., Connolly, D. C., Zhang, Y., Montone, K., Butzow, R., Coukos, G., & Zhang, L. (2010). Distinct expression levels and patterns of stem cell marker, aldehyde dehydrogenase isoform 1 (ALDH1), in human epithelial cancers. *PLOS ONE*, *5*(4), e10277. https://doi.org/10.1371/journal.pone.0010277

Dinavahi, S. S., Bazewicz, C. G., Gowda, R., & Robertson, G. P. (2019). Aldehyde Dehydrogenase Inhibitors for Cancer Therapeutics. *Trends Pharmacol Sci*, *40*(10), 774-789. https://doi.org/10.1016/j.tips.2019.08.002

Dixon, S. J., Lemberg, K. M., Lamprecht, M. R., Skouta, R., Zaitsev, E. M., Gleason, C. E., Patel, D. N., Bauer, A. J., Cantley, A. M., Yang, W. S., Morrison, B., 3rd, & Stockwell, B. R. (2012). Ferroptosis: an iron-dependent form of nonapoptotic cell death. *Cell*, *149*(5), 1060-1072. https://doi.org/10.1016/j.cell.2012.03.042

Doblas, S., He, T., Saunders, D., Pearson, J., Hoyle, J., Smith, N., Lerner, M., & Towner, R. A. (2010). Glioma morphology and tumor-induced vascular alterations revealed in seven rodent glioma models by in vivo magnetic resonance imaging and angiography. *J Magn Reson Imaging*, *32*(2), 267-275. https://doi.org/10.1002/jmri.22263

Doll, S., Proneth, B., Tyurina, Y. Y., Panzilius, E., Kobayashi, S., Ingold, I., Irmler, M., Beckers, J., Aichler, M., Walch, A., Prokisch, H., Trumbach, D., Mao, G., Qu, F., Bayir, H., Fullekrug, J., Scheel, C. H., Wurst, W., Schick, J. A., Kagan, V. E., Angeli, J. P., & Conrad, M. (2017). ACSL4 dictates ferroptosis sensitivity by shaping cellular lipid composition. *Nat Chem Biol*, *13*(1), 91-98. https://doi.org/10.1038/nchembio.2239

Dolma S, L. S., Hahn WC, Stockwell BR. (2003). Identification of genotype-selective antitumor agents using synthetic lethal chemical screening in engineered human tumor cells. *Cancer Cell*, *Mar*(3), 285-296. https://doi.org/10.1016/S1535-6108(03)00050-3

Drean, A., Rosenberg, S., Lejeune, F. X., Goli, L., Nadaradjane, A. A., Guehennec, J., Schmitt, C., Verreault, M., Bielle, F., Mokhtari, K., Sanson, M., Carpentier, A., Delattre, J. Y., & Idbaih, A. (2018). ATP binding cassette (ABC) transporters: expression and clinical value in glioblastoma. *J Neurooncol*, *138*(3), 479-486. https://doi.org/10.1007/s11060-018-2819-3

Feng, J., Lu, P. Z., Zhu, G. Z., Hooi, S. C., Wu, Y., Huang, X. W., Dai, H. Q., Chen, P. H., Li, Z. J., Su, W. J., Han, C. Y., Ye, X. P., Peng, T., Zhou, J., & Lu, G. D. (2020). ACSL4 is a predictive biomarker of sorafenib sensitivity in hepatocellular carcinoma. *Acta Pharmacol Sin*. https://doi.org/10.1038/s41401-020-0439-x

Fialkow, P. J., Jacobson, R. J., & Papayannopoulou, T. (1977). Chronic myelocytic leukemia: clonal origin in a stem cell common to the granulocyte, erythrocyte, platelet and monocyte/macrophage. *Am J Med*, *63*(1), 125-130.

Filipp, F. V., Scott, D. A., Ronai, Z. A., Osterman, A. L., & Smith, J. W. (2012). Reverse TCA cycle flux through isocitrate dehydrogenases 1 and 2 is required for lipogenesis in hypoxic melanoma cells. *Pigment Cell Melanoma Res*, *25*(3), 375-383. https://doi.org/10.1111/j.1755-148X.2012.00989.x

Fournet, G., Martin, G., & Quash, G. (2013). alpha,beta-Acetylenic amino thiolester inhibitors of aldehyde dehydrogenases 1&3: suppressors of apoptogenic aldehyde oxidation and activators of apoptosis. *Curr Med Chem*, *20*(4), 527-533. https://doi.org/10.2174/0929867311320040004

Franken, N. A., Rodermond, H. M., Stap, J., Haveman, J., & van Bree, C. (2006). Clonogenic assay of cells in vitro. *Nat Protoc*, *1*(5), 2315-2319. https://doi.org/10.1038/nprot.2006.339

Friedman, H. S., Prados, M. D., Wen, P. Y., Mikkelsen, T., Schiff, D., Abrey, L. E., Yung, W. K. A., Paleologos, N., Nicholas, M. K., Jensen, R., Vredenburgh, J., Huang, J., Zheng, M., & Cloughesy, T. (2009). Bevacizumab Alone and in Combination With Irinotecan in Recurrent Glioblastoma. *27*(28), 4733-4740. https://doi.org/10.1200/jco.2008.19.8721

Friedmann Angeli, J. P., Schneider, M., Proneth, B., Tyurina, Y. Y., Tyurin, V. A., Hammond, V. J., Herbach, N., Aichler, M., Walch, A., Eggenhofer, E., Basavarajappa, D., Radmark, O., Kobayashi, S., Seibt, T., Beck, H., Neff, F., Esposito, I., Wanke, R., Forster, H., Yefremova, O., Heinrichmeyer, M., Bornkamm, G. W., Geissler, E. K., Thomas, S. B., Stockwell, B. R., O'Donnell, V. B., Kagan, V. E., Schick, J. A., & Conrad, M. (2014). Inactivation of the ferroptosis regulator Gpx4 triggers acute renal failure in mice. *Nat Cell Biol*, *16*(12), 1180-1191. https://doi.org/10.1038/ncb3064

Fuentealba, L. C., Obernier, K., & Alvarez-Buylla, A. (2012). Adult neural stem cells bridge their niche. *Cell Stem Cell*, *10*(6), 698-708. https://doi.org/10.1016/j.stem.2012.05.012

Gao, M., Monian, P., Quadri, N., Ramasamy, R., & Jiang, X. (2015). Glutaminolysis and Transferrin Regulate Ferroptosis. *Mol Cell*, *59*(2), 298-308. https://doi.org/10.1016/j.molcel.2015.06.011

Gerson, S. L. (2004). MGMT: its role in cancer aetiology and cancer therapeutics. *Nat Rev Cancer*, *4*(4), 296-307. https://doi.org/10.1038/nrc1319

Giakoumettis, D., Kritis, A., & Foroglou, N. (2018). C6 cell line: the gold standard in glioma research. *Hippokratia*, *22*(3), 105-112. https://www.ncbi.nlm.nih.gov/pubmed/31641331

Gieryng, A., Pszczolkowska, D., Bocian, K., Dabrowski, M., Rajan, W. D., Kloss, M., Mieczkowski, J., & Kaminska, B. (2017). Immune microenvironment of experimental rat C6 gliomas resembles human glioblastomas. *Sci Rep*, *7*(1), 17556. https://doi.org/10.1038/s41598-017-17752-w

Gilbert, M. R., Dignam, J. J., Armstrong, T. S., Wefel, J. S., Blumenthal, D. T., Vogelbaum, M. A., Colman, H., Chakravarti, A., Pugh, S., Won, M., Jeraj, R., Brown, P. D., Jaeckle, K. A., Schiff, D., Stieber, V. W., Brachman, D. G., Werner-Wasik, M., Tremont-Lukats, I. W., Sulman, E. P., Aldape, K. D., Curran, W. J., & Mehta, M. P. (2014). A Randomized Trial of Bevacizumab for Newly Diagnosed Glioblastoma. *New England Journal of Medicine*, *370*(8), 699-708. https://doi.org/10.1056/nejmoa1308573

Gilbertson, R. J., & Rich, J. N. (2007). Making a tumour's bed: glioblastoma stem cells and the vascular niche. *7*(10), 733-736. https://doi.org/10.1038/nrc2246

Gundersen, S., Aamdal, S., & Fodstad, O. (1987). Mitozolomide (NSC 353451), a new active drug in the treatment of malignant melanoma. Phase II trial in patients with advanced disease. *British journal of cancer*, *55*(4), 433-435. https://www.ncbi.nlm.nih.gov/pubmed/3580266

Hanahan, D., & Weinberg, R. A. (2000). The hallmarks of cancer. *Cell*, *100*(1), 57-70. https://doi.org/Doi 10.1016/S0092-8674(00)81683-9

Hanahan, D., & Weinberg, R. A. (2011). Hallmarks of cancer: the next generation. *Cell*, *144*(5), 646-674. https://doi.org/10.1016/j.cell.2011.02.013

Haraguchi, N., Ishii, H., Mimori, K., Tanaka, F., Ohkuma, M., Kim, H. M., Akita, H., Takiuchi, D., Hatano, H., Nagano, H., Barnard, G. F., Doki, Y., & Mori, M. (2010). CD13 is a therapeutic

target in human liver cancer stem cells. *The Journal of clinical investigation*, *120*(9), 3326-3339. https://doi.org/10.1172/JCI42550

Hardwick, J. M., & Youle, R. J. (2009). SnapShot: BCL-2 proteins. *Cell*, *138*(2), 404, 404 e401. https://doi.org/10.1016/j.cell.2009.07.003

Hegi, M. E., Diserens, A. C., Gorlia, T., Hamou, M. F., de Tribolet, N., Weller, M., Kros, J. M., Hainfellner, J. A., Mason, W., Mariani, L., Bromberg, J. E., Hau, P., Mirimanoff, R. O., Cairncross, J. G., Janzer, R. C., & Stupp, R. (2005). MGMT gene silencing and benefit from temozolomide in glioblastoma. *N Engl J Med*, *352*(10), 997-1003. https://doi.org/10.1056/NEJMoa043331

Hemmati, H. D., Nakano, I., Lazareff, J. A., Masterman-Smith, M., Geschwind, D. H., Bronner-Fraser, M., & Kornblum, H. I. (2003). Cancerous stem cells can arise from pediatric brain tumors. *Proc Natl Acad Sci U S A*, *100*(25), 15178-15183. https://doi.org/10.1073/pnas.2036535100

Huddle, B. C., Grimley, E., Buchman, C. D., Chtcherbinine, M., Debnath, B., Mehta, P., Yang, K., Morgan, C. A., Li, S., Felton, J., Sun, D., Mehta, G., Neamati, N., Buckanovich, R. J., Hurley, T. D., & Larsen, S. D. (2018). Structure-Based Optimization of a Novel Class of Aldehyde Dehydrogenase 1A (ALDH1A) Subfamily-Selective Inhibitors as Potential Adjuncts to Ovarian Cancer Chemotherapy. *J Med Chem*, *61*(19), 8754-8773. https://doi.org/10.1021/acs.jmedchem.8b00930

Ishimoto, T., Nagano, O., Yae, T., Tamada, M., Motohara, T., Oshima, H., Oshima, M., Ikeda, T., Asaba, R., Yagi, H., Masuko, T., Shimizu, T., Ishikawa, T., Kai, K., Takahashi, E., Imamura, Y., Baba, Y., Ohmura, M., Suematsu, M., Baba, H., & Saya, H. (2011). CD44 variant regulates redox status in cancer cells by stabilizing the xCT subunit of system xc(-) and thereby promotes tumor growth. *Cancer Cell*, *19*(3), 387-400. https://doi.org/10.1016/j.ccr.2011.01.038

Jiang, L., Kon, N., Li, T., Wang, S. J., Su, T., Hibshoosh, H., Baer, R., & Gu, W. (2015). Ferroptosis as a p53-mediated activity during tumour suppression. *Nature*, *520*(7545), 57-62. https://doi.org/10.1038/nature14344

Jiang, Z., Pore, N., Cerniglia, G. J., Mick, R., Georgescu, M. M., Bernhard, E. J., Hahn, S. M., Gupta, A. K., & Maity, A. (2007). Phosphatase and tensin homologue deficiency in glioblastoma confers resistance to radiation and temozolomide that is reversed by the protease inhibitor nelfinavir. *Cancer Res*, *67*(9), 4467-4473. https://doi.org/10.1158/0008-5472.CAN-06-3398

Kabbinavar, F., Hurwitz, H. I., Fehrenbacher, L., Meropol, N. J., Novotny, W. F., Lieberman, G., Griffing, S., & Bergsland, E. (2003). Phase II, randomized trial comparing bevacizumab plus fluorouracil (FU)/leucovorin (LV) with FU/LV alone in patients with metastatic colorectal cancer. *J Clin Oncol*, *21*(1), 60-65. https://doi.org/10.1200/JCO.2003.10.066

Kelly, P. N., Dakic, A., Adams, J. M., Nutt, S. L., & Strasser, A. (2007). Tumor Growth Need Not Be Driven by Rare Cancer Stem Cells. *Science*, *317*(5836), 337-337. https://doi.org/10.1126/science.1142596

Kerr, J. F., Wyllie, A. H., & Currie, A. R. (1972). Apoptosis: a basic biological phenomenon with wide-ranging implications in tissue kinetics. *Br J Cancer*, *26*(4), 239-257. https://doi.org/10.1038/bjc.1972.33

Kirson, E. D., Dbaly, V., Tovarys, F., Vymazal, J., Soustiel, J. F., Itzhaki, A., Mordechovich, D., Steinberg-Shapira, S., Gurvich, Z., Schneiderman, R., Wasserman, Y., Salzberg, M., Ryffel, B., Goldsher, D., Dekel, E., & Palti, Y. (2007). Alternating electric fields arrest cell proliferation in animal tumor models and human brain tumors. *Proceedings of the National Academy of Sciences*, *104*(24), 10152-10157. https://doi.org/10.1073/pnas.0702916104

Knizhnik, A. V., Roos, W. P., Nikolova, T., Quiros, S., Tomaszowski, K. H., Christmann, M., & Kaina, B. (2013). Survival and death strategies in glioma cells: autophagy, senescence and

apoptosis triggered by a single type of temozolomide-induced DNA damage. *PLOS ONE*, *8*(1), e55665. https://doi.org/10.1371/journal.pone.0055665

Koh, H. J., Lee, S. M., Son, B. G., Lee, S. H., Ryoo, Z. Y., Chang, K. T., Park, J. W., Park, D. C., Song, B. J., Veech, R. L., Song, H., & Huh, T. L. (2004). Cytosolic NADP+-dependent isocitrate dehydrogenase plays a key role in lipid metabolism. *J Biol Chem*, *279*(38), 39968-39974. https://doi.org/10.1074/jbc.M402260200

Kondo, T., Setoguchi, T., & Taga, T. (2004). Persistence of a small subpopulation of cancer stem-like cells in the C6 glioma cell line. *Proc Natl Acad Sci U S A*, *101*(3), 781-786. https://doi.org/10.1073/pnas.0307618100

Lane, D. P. (1992). Cancer. p53, guardian of the genome. *Nature*, *358*(6381), 15-16. https://doi.org/10.1038/358015a0

Lathia, J. D., Mack, S. C., Mulkearns-Hubert, E. E., Valentim, C. L., & Rich, J. N. (2015). Cancer stem cells in glioblastoma. *Genes Dev*, *29*(12), 1203-1217. https://doi.org/10.1101/gad.261982.115

Lazebnik, Y. (2010). What are the hallmarks of cancer? [Comment]. *Nature Reviews Cancer*, *10*, 232. https://doi.org/10.1038/nrc2827

Legendre, C., & Garcion, E. (2015). Iron metabolism: a double-edged sword in the resistance of glioblastoma to therapies. *Trends Endocrinol Metab*, *26*(6), 322-331. https://doi.org/10.1016/j.tem.2015.03.008

Lei, G., Zhang, Y., Koppula, P., Liu, X., Zhang, J., Lin, S. H., Ajani, J. A., Xiao, Q., Liao, Z., Wang, H., & Gan, B. (2020). The role of ferroptosis in ionizing radiation-induced cell death and tumor suppression. *Cell Res*, *30*(2), 146-162. https://doi.org/10.1038/s41422-019-0263-3

Lenting, K., Verhaak, R., Ter Laan, M., Wesseling, P., & Leenders, W. (2017). Glioma: experimental models and reality. *Acta Neuropathol*, *133*(2), 263-282. https://doi.org/10.1007/s00401-017-1671-4

Li, G., Li, Y., Liu, X., Wang, Z., Zhang, C., Wu, F., Jiang, H., Zhang, W., Bao, Z., Wang, Y., Cai, J., Zhao, L., Kahlert, U. D., Jiang, T., & Zhang, W. (2018). ALDH1A3 induces mesenchymal differentiation and serves as a predictor for survival in glioblastoma. *Cell Death Dis*, *9*(12), 1190. https://doi.org/10.1038/s41419-018-1232-3

Li, J., Cao, F., Yin, H. L., Huang, Z. J., Lin, Z. T., Mao, N., Sun, B., & Wang, G. (2020). Ferroptosis: past, present and future. *Cell Death Dis*, *11*(2), 88. https://doi.org/10.1038/s41419-020-2298-2

Li, K., Guo, X., Wang, Z., Li, X., Bu, Y., Bai, X., Zheng, L., & Huang, Y. (2016). The prognostic roles of ALDH1 isoenzymes in gastric cancer. *Onco Targets Ther*, *9*, 3405-3414. https://doi.org/10.2147/OTT.S102314

Li, X., Lewis, M. T., Huang, J., Gutierrez, C., Osborne, C. K., Wu, M. F., Hilsenbeck, S. G., Pavlick, A., Zhang, X., Chamness, G. C., Wong, H., Rosen, J., & Chang, J. C. (2008). Intrinsic resistance of tumorigenic breast cancer cells to chemotherapy. *J Natl Cancer Inst*, *100*(9), 672-679. https://doi.org/10.1093/jnci/djn123

Li, X., Wu, C., Chen, N., Gu, H., Yen, A., Cao, L., Wang, E., & Wang, L. (2016). PI3K/Akt/mTOR signaling pathway and targeted therapy for glioblastoma. *Oncotarget*, *7*(22), 33440-33450. https://doi.org/10.18632/oncotarget.7961

Louandre, C., Ezzoukhry, Z., Godin, C., Barbare, J. C., Maziere, J. C., Chauffert, B., & Galmiche, A. (2013). Iron-dependent cell death of hepatocellular carcinoma cells exposed to sorafenib. *Int J Cancer*, *133*(7), 1732-1742. https://doi.org/10.1002/ijc.28159

Louis, D. N., Perry, A., Reifenberger, G., von Deimling, A., Figarella-Branger, D., Cavenee, W. K., Ohgaki, H., Wiestler, O. D., Kleihues, P., & Ellison, D. W. (2016). The 2016 World Health Organization Classification of Tumors of the Central Nervous System: a summary. *Acta Neuropathol*, *131*(6), 803-820. https://doi.org/10.1007/s00401-016-1545-1

Louis, D. N., Perry, A., Wesseling, P., Brat, D. J., Cree, I. A., Figarella-Branger, D., Hawkins, C., Ng, H. K., Pfister, S. M., Reifenberger, G., Soffietti, R., von Deimling, A., & Ellison, D. W. (2021).

The 2021 WHO Classification of Tumors of the Central Nervous System: a summary. *Neuro Oncol*, *23*(8), 1231-1251. https://doi.org/10.1093/neuonc/noab106

Lu, S. C. (2009). Regulation of glutathione synthesis. *Mol Aspects Med*, *30*(1-2), 42-59. https://doi.org/10.1016/j.mam.2008.05.005

Ma, Y. M., & Zhao, S. (2016). Prognostic values of aldehyde dehydrogenase 1 isoenzymes in ovarian cancer. *Onco Targets Ther*, *9*, 1981-1988. https://doi.org/10.2147/OTT.S101063

Mabray, M. C., Barajas, R. F., & Cha, S. (2015). Modern Brain Tumor Imaging. *3*(1), 8. https://doi.org/10.14791/btrt.2015.3.1.8

MacDonald, M. J., Brown, L. J., Longacre, M. J., Stoker, S. W., Kendrick, M. A., & Hasan, N. M. (2013). Knockdown of both mitochondrial isocitrate dehydrogenase enzymes in pancreatic beta cells inhibits insulin secretion. *Biochim Biophys Acta*, *1830*(11), 5104-5111. https://doi.org/10.1016/j.bbagen.2013.07.013

Marcato, P., Dean, C. A., Giacomantonio, C. A., & Lee, P. W. (2011). Aldehyde dehydrogenase: its role as a cancer stem cell marker comes down to the specific isoform. *Cell Cycle*, *10*(9), 1378-1384. https://doi.org/10.4161/cc.10.9.15486

Marchitti, S. A., Brocker, C., Stagos, D., & Vasiliou, V. (2008). Non-P450 aldehyde oxidizing enzymes: the aldehyde dehydrogenase superfamily. *Expert Opinion on Drug Metabolism & Toxicology*, *4*(6), 697-720. https://doi.org/10.1517/17425255.4.6.697

Miraglia, S., Godfrey, W., Yin, A. H., Atkins, K., Warnke, R., Holden, J. T., Bray, R. A., Waller, E. K., & Buck, D. W. (1997). A novel five-transmembrane hematopoietic stem cell antigen: isolation, characterization, and molecular cloning. *Blood*, *90*(12), 5013-5021. https://www.ncbi.nlm.nih.gov/pubmed/9389721

Mirzadeh, Z., Merkle, F. T., Soriano-Navarro, M., Garcia-Verdugo, J. M., & Alvarez-Buylla, A. (2008). Neural stem cells confer unique pinwheel architecture to the ventricular surface in neurogenic regions of the adult brain. *Cell Stem Cell*, *3*(3), 265-278. https://doi.org/10.1016/j.stem.2008.07.004

Morgan, C. A., & Hurley, T. D. (2015). Characterization of two distinct structural classes of selective aldehyde dehydrogenase 1A1 inhibitors. *J Med Chem*, *58*(4), 1964-1975. https://doi.org/10.1021/jm501900s

Morgan, C. A., Parajuli, B., Buchman, C. D., Dria, K., & Hurley, T. D. (2015). N,N-diethylaminobenzaldehyde (DEAB) as a substrate and mechanism-based inhibitor for human ALDH isoenzymes. *Chem Biol Interact*, *234*, 18-28. https://doi.org/10.1016/j.cbi.2014.12.008

Nabors, L. B., Fink, K. L., Mikkelsen, T., Grujicic, D., Tarnawski, R., Nam, D. H., Mazurkiewicz, M., Salacz, M., Ashby, L., Zagonel, V., Depenni, R., Perry, J. R., Hicking, C., Picard, M., Hegi, M. E., Lhermitte, B., & Reardon, D. A. (2015). Two cilengitide regimens in combination with standard treatment for patients with newly diagnosed glioblastoma and unmethylated MGMT gene promoter: results of the open-label, controlled, randomized phase II CORE study. *17*(5), 708-717. https://doi.org/10.1093/neuonc/nou356

Newlands, E. S., Blackledge, G. R., Slack, J. A., Rustin, G. J., Smith, D. B., Stuart, N. S., Quarterman, C. P., Hoffman, R., Stevens, M. F., & Brampton, M. H. (1992). Phase I trial of temozolomide (CCRG 81045: M&B 39831: NSC 362856). *British journal of cancer*, *65*(2), 287-291. https://www.ncbi.nlm.nih.gov/pubmed/1739631

Newlands, E. S., Stevens, M. F. G., Wedge, S. R., Wheelhouse, R. T., & Brock, C. (1997). Temozolomide: a review of its discovery, chemical properties, pre-clinical development and clinical trials. *Cancer Treatment Reviews*, *23*(1), 35-61. https://doi.org/10.1016/s0305-7372(97)90019-0

Nie, J., Lin, B., Zhou, M., Wu, L., & Zheng, T. (2018). Role of ferroptosis in hepatocellular carcinoma. *J Cancer Res Clin Oncol*, *144*(12), 2329-2337. https://doi.org/10.1007/s00432-018-2740-3

O'Brien, P. J., Siraki, A. G., & Shangari, N. (2005). Aldehyde sources, metabolism, molecular toxicity mechanisms, and possible effects on human health. *Crit Rev Toxicol*, *35*(7), 609-662. https://www.ncbi.nlm.nih.gov/pubmed/16417045

Oh, T., Sayegh, E. T., Fakurnejad, S., Oyon, D., Lamano, J. B., DiDomenico, J. D., Bloch, O., & Parsa, A. T. (2015). Vaccine therapies in malignant glioma. *Current neurology and neuroscience reports*, *15*(1), 508-508. https://doi.org/10.1007/s11910-014-0508-y

Okada, M., Sato, A., Shibuya, K., Watanabe, E., Seino, S., Suzuki, S., Seino, M., Narita, Y., Shibui, S., Kayama, T., & Kitanaka, C. (2014). JNK contributes to temozolomide resistance of stem-like glioblastoma cells via regulation of MGMT expression. *Int J Oncol*, *44*(2), 591-599. https://doi.org/10.3892/ijo.2013.2209

Omuro, A., & DeAngelis, L. M. (2013). Glioblastoma and other malignant gliomas: a clinical review. *JAMA*, *310*(17), 1842-1850. https://doi.org/10.1001/jama.2013.280319

Omuro, A., Vlahovic, G., Lim, M., Sahebjam, S., Baehring, J., Cloughesy, T., Voloschin, A., Ramkissoon, S. H., Ligon, K. L., Latek, R., Zwirtes, R., Strauss, L., Paliwal, P., Harbison, C. T., Reardon, D. A., & Sampson, J. H. (2018). Nivolumab with or without ipilimumab in patients with recurrent glioblastoma: results from exploratory phase I cohorts of CheckMate 143. *Neuro Oncol*, *20*(5), 674-686. https://doi.org/10.1093/neuonc/nox208

Ostrom, Q. T., Gittleman, H., Truitt, G., Boscia, A., Kruchko, C., & Barnholtz-Sloan, J. S. (2018). CBTRUS Statistical Report: Primary Brain and Other Central Nervous System Tumors Diagnosed in the United States in 2011–2015. *Neuro-Oncology*, *20*(suppl_4), iv1-iv86. https://doi.org/10.1093/neuonc/noy131

Parsons, D. W., Jones, S., Zhang, X., Lin, J. C., Leary, R. J., Angenendt, P., Mankoo, P., Carter, H., Siu, I. M., Gallia, G. L., Olivi, A., McLendon, R., Rasheed, B. A., Keir, S., Nikolskaya, T., Nikolsky, Y., Busam, D. A., Tekleab, H., Diaz, L. A., Jr., Hartigan, J., Smith, D. R., Strausberg, R. L., Marie, S. K., Shinjo, S. M., Yan, H., Riggins, G. J., Bigner, D. D., Karchin, R., Papadopoulos, N., Parmigiani, G., Vogelstein, B., Velculescu, V. E., & Kinzler, K. W. (2008). An integrated genomic analysis of human glioblastoma multiforme. *Science*, *321*(5897), 1807-1812. https://doi.org/10.1126/science.1164382

Parthymou, A., Kardamakis, D., Pavlopoulos, I., & Papadimitriou, E. (2004). Irradiated C6 glioma cells induce angiogenesis in vivo and activate endothelial cells in vitro. *Int J Cancer*, *110*(6), 807-814. https://doi.org/10.1002/ijc.20188

Pelloski, C. E., Ballman, K. V., Furth, A. F., Zhang, L., Lin, E., Sulman, E. P., Bhat, K., McDonald, J. M., Yung, W. K. A., Colman, H., Woo, S. Y., Heimberger, A. B., Suki, D., Prados, M. D., Chang, S. M., Barker, F. G., Buckner, J. C., James, C. D., & Aldape, K. (2007). Epidermal Growth Factor Receptor Variant III Status Defines Clinically Distinct Subtypes of Glioblastoma. *Journal of Clinical Oncology*, *25*(16), 2288-2294. https://doi.org/10.1200/jco.2006.08.0705

Ponten, J., & Macintyre, E. H. (1968). Long term culture of normal and neoplastic human glia. *Acta Pathol Microbiol Scand*, *74*(4), 465-486. https://doi.org/10.1111/j.1699-0463.1968.tb03502.x

Portnow, J., Badie, B., Chen, M., Liu, A., Blanchard, S., & Synold, T. W. (2009). The neuropharmacokinetics of temozolomide in patients with resectable brain tumors: potential implications for the current approach to chemoradiation. *Clin Cancer Res*, *15*(22), 7092-7098. https://doi.org/10.1158/1078-0432.CCR-09-1349

Posti, J. P., Bori, M., Kauko, T., Sankinen, M., Nordberg, J., Rahi, M., Frantzen, J., Vuorinen, V., & Sipila, J. O. (2015). Presenting symptoms of glioma in adults. *Acta Neurol Scand*, *131*(2), 88-93. https://doi.org/10.1111/ane.12285

Qu, X. (2003). Promotion of tumorigenesis by heterozygous disruption of the beclin 1 autophagy gene. *Journal of Clinical Investigation*, *112*(12), 1809-1820. https://doi.org/10.1172/jci20039

Rasper, M., Schafer, A., Piontek, G., Teufel, J., Brockhoff, G., Ringel, F., Heindl, S., Zimmer, C., & Schlegel, J. (2010). Aldehyde dehydrogenase 1 positive glioblastoma cells show brain

tumor stem cell capacity. *Neuro Oncol*, *12*(10), 1024-1033. https://doi.org/10.1093/neuonc/noq070

Reardon, D. A., Brandes, A. A., Omuro, A., Mulholland, P., Lim, M., Wick, A., Baehring, J., Ahluwalia, M. S., Roth, P., Bahr, O., Phuphanich, S., Sepulveda, J. M., De Souza, P., Sahebjam, S., Carleton, M., Tatsuoka, K., Taitt, C., Zwirtes, R., Sampson, J., & Weller, M. (2020). Effect of Nivolumab vs Bevacizumab in Patients With Recurrent Glioblastoma: The CheckMate 143 Phase 3 Randomized Clinical Trial. *JAMA Oncol*, *6*(7), 1003-1010. https://doi.org/10.1001/jamaoncol.2020.1024

Rock, K. L., & Kono, H. (2008). The inflammatory response to cell death. *Annu Rev Pathol*, *3*, 99-126. https://doi.org/10.1146/annurev.pathmechdis.3.121806.151456

Schafer, A., Teufel, J., Ringel, F., Bettstetter, M., Hoepner, I., Rasper, M., Gempt, J., Koeritzer, J., Schmidt-Graf, F., Meyer, B., Beier, C. P., & Schlegel, J. (2012). Aldehyde dehydrogenase 1A1--a new mediator of resistance to temozolomide in glioblastoma. *Neuro Oncol*, *14*(12), 1452-1464. https://doi.org/10.1093/neuonc/nos270

Schonberg, D. L., Miller, T. E., Wu, Q., Flavahan, W. A., Das, N. K., Hale, J. S., Hubert, C. G., Mack, S. C., Jarrar, A. M., Karl, R. T., Rosager, A. M., Nixon, A. M., Tesar, P. J., Hamerlik, P., Kristensen, B. W., Horbinski, C., Connor, J. R., Fox, P. L., Lathia, J. D., & Rich, J. N. (2015). Preferential Iron Trafficking Characterizes Glioblastoma Stem-like Cells. *Cancer Cell*, *28*(4), 441-455. https://doi.org/10.1016/j.ccell.2015.09.002

Schwartzentruber, J., Korshunov, A., Liu, X. Y., Jones, D. T., Pfaff, E., Jacob, K., Sturm, D., Fontebasso, A. M., Quang, D. A., Tonjes, M., Hovestadt, V., Albrecht, S., Kool, M., Nantel, A., Konermann, C., Lindroth, A., Jager, N., Rausch, T., Ryzhova, M., Korbel, J. O., Hielscher, T., Hauser, P., Garami, M., Klekner, A., Bognar, L., Ebinger, M., Schuhmann, M. U., Scheurlen, W., Pekrun, A., Fruhwald, M. C., Roggendorf, W., Kramm, C., Durken, M., Atkinson, J., Lepage, P., Montpetit, A., Zakrzewska, M., Zakrzewski, K., Liberski, P. P., Dong, Z., Siegel, P., Kulozik, A. E., Zapatka, M., Guha, A., Malkin, D., Felsberg, J., Reifenberger, G., von Deimling, A., Ichimura, K., Collins, V. P., Witt, H., Milde, T., Witt, O., Zhang, C., Castelo-Branco, P., Lichter, P., Faury, D., Tabori, U., Plass, C., Majewski, J., Pfister, S. M., & Jabado, N. (2012). Driver mutations in histone H3.3 and chromatin remodelling genes in paediatric glioblastoma. *Nature*, *482*(7384), 226-231. https://doi.org/10.1038/nature10833

Sehm, T., Rauh, M., Wiendieck, K., Buchfelder, M., Eyupoglu, I. Y., & Savaskan, N. E. (2016). Temozolomide toxicity operates in a xCT/SLC7a11 dependent manner and is fostered by ferroptosis. *Oncotarget*, *7*(46), 74630-74647. https://doi.org/10.18632/oncotarget.11858

Seifert, L., & Miller, G. (2017). Molecular Pathways: The Necrosome-A Target for Cancer Therapy. *Clin Cancer Res*, *23*(5), 1132-1136. https://doi.org/10.1158/1078-0432.CCR-16-0968

Shen, Q., Wang, Y., Kokovay, E., Lin, G., Chuang, S. M., Goderie, S. K., Roysam, B., & Temple, S. (2008). Adult SVZ stem cells lie in a vascular niche: a quantitative analysis of niche cell-cell interactions. *Cell Stem Cell*, *3*(3), 289-300. https://doi.org/10.1016/j.stem.2008.07.026

Sherr, C. J., & McCormick, F. (2002). The RB and p53 pathways in cancer. *Cancer Cell*, *2*(2), 103-112. https://doi.org/10.1016/s1535-6108(02)00102-2

Singer, E., Judkins, J., Salomonis, N., Matlaf, L., Soteropoulos, P., McAllister, S., & Soroceanu, L. (2015). Reactive oxygen species-mediated therapeutic response and resistance in glioblastoma. *Cell Death Dis*, *6*, e1601. https://doi.org/10.1038/cddis.2014.566

Singh, S., Brocker, C., Koppaka, V., Chen, Y., Jackson, B. C., Matsumoto, A., Thompson, D. C., & Vasiliou, V. (2013). Aldehyde dehydrogenases in cellular responses to oxidative/electrophilic stress. *Free Radic Biol Med*, *56*, 89-101. https://doi.org/10.1016/j.freeradbiomed.2012.11.010

Singh, S. K., Clarke, I. D., Terasaki, M., Bonn, V. E., Hawkins, C., Squire, J., & Dirks, P. B. (2003). Identification of a cancer stem cell in human brain tumors. *Cancer Res*, *63*(18), 5821-5828.

Skouta, R., Dixon, S. J., Wang, J., Dunn, D. E., Orman, M., Shimada, K., Rosenberg, P. A., Lo, D. C., Weinberg, J. M., Linkermann, A., & Stockwell, B. R. (2014). Ferrostatins inhibit oxidative lipid damage and cell death in diverse disease models. *J Am Chem Soc*, *136*(12), 4551-4556. https://doi.org/10.1021/ja411006a

Stepanenko, A. A., & Chekhonin, V. P. (2018). Recent Advances in Oncolytic Virotherapy and Immunotherapy for Glioblastoma: A Glimmer of Hope in the Search for an Effective Therapy? *Cancers (Basel)*, *10*(12). https://doi.org/10.3390/cancers10120492

Stupp, R., Mason, W. P., Van Den Bent, M. J., Weller, M., Fisher, B., Taphoorn, M. J. B., Belanger, K., Brandes, A. A., Marosi, C., Bogdahn, U., Curschmann, J., Janzer, R. C., Ludwin, S. K., Gorlia, T., Allgeier, A., Lacombe, D., Cairncross, J. G., Eisenhauer, E., & Mirimanoff, R. O. (2005). Radiotherapy plus Concomitant and Adjuvant Temozolomide for Glioblastoma. *New England Journal of Medicine*, *352*(10), 987-996. https://doi.org/10.1056/nejmoa043330

Stupp, R., Taillibert, S., Kanner, A., Read, W., Steinberg, D. M., Lhermitte, B., Toms, S., Idbaih, A., Ahluwalia, M. S., Fink, K., Di Meco, F., Lieberman, F., Zhu, J.-J., Stragliotto, G., Tran, D. D., Brem, S., Hottinger, A. F., Kirson, E. D., Lavy-Shahaf, G., Weinberg, U., Kim, C.-Y., Paek, S.-H., Nicholas, G., Bruna, J., Hirte, H., Weller, M., Palti, Y., Hegi, M. E., & Ram, Z. (2017). Effect of Tumor-Treating Fields Plus Maintenance Temozolomide vs Maintenance Temozolomide Alone on Survival in Patients With Glioblastoma. *JAMA*, *318*(23), 2306. https://doi.org/10.1001/jama.2017.18718

Sulman, E. P., Ismaila, N., Armstrong, T. S., Tsien, C., Batchelor, T. T., Cloughesy, T., Galanis, E., Gilbert, M., Gondi, V., Lovely, M., Mehta, M., Mumber, M. P., Sloan, A., & Chang, S. M. (2017). Radiation Therapy for Glioblastoma: American Society of Clinical Oncology Clinical Practice Guideline Endorsement of the American Society for Radiation Oncology Guideline. *Journal of Clinical Oncology*, *35*(3), 361-369. https://doi.org/10.1200/jco.2016.70.7562

Sun, X., Ou, Z., Chen, R., Niu, X., Chen, D., Kang, R., & Tang, D. (2016). Activation of the p62-Keap1-NRF2 pathway protects against ferroptosis in hepatocellular carcinoma cells. *Hepatology*, *63*(1), 173-184. https://doi.org/10.1002/hep.28251

Tang, D., Chen, X., Kang, R., & Kroemer, G. (2020). Ferroptosis: molecular mechanisms and health implications. *Cell Res*. https://doi.org/10.1038/s41422-020-00441-1

Thomas, M. L., de Antueno, R., Coyle, K. M., Sultan, M., Cruickshank, B. M., Giacomantonio, M. A., Giacomantonio, C. A., Duncan, R., & Marcato, P. (2016). Citral reduces breast tumor growth by inhibiting the cancer stem cell marker ALDH1A3. *Mol Oncol*, *10*(9), 1485-1496. https://doi.org/10.1016/j.molonc.2016.08.004

Waitkus, M. S., Diplas, B. H., & Yan, H. (2016). Isocitrate dehydrogenase mutations in gliomas. *Neuro Oncol*, *18*(1), 16-26. https://doi.org/10.1093/neuonc/nov136

Walker, M. D., Green, S. B., Byar, D. P., Alexander, E., Batzdorf, U., Brooks, W. H., Hunt, W. E., MacCarty, C. S., Mahaley, M. S., Mealey, J., Owens, G., Ransohoff, J., Robertson, J. T., Shapiro, W. R., Smith, K. R., Wilson, C. B., & Strike, T. A. (1980). Randomized Comparisons of Radiotherapy and Nitrosoureas for the Treatment of Malignant Glioma after Surgery. *303*(23), 1323-1329. https://doi.org/10.1056/nejm198012043032303

Wang, C., Xie, J., Guo, J., Manning, H. C., Gore, J. C., & Guo, N. (2012). Evaluation of CD44 and CD133 as cancer stem cell markers for colorectal cancer. *Oncology reports*, *28*(4), 1301-1308. https://doi.org/10.3892/or.2012.1951

Weller, M., Butowski, N., Tran, D. D., Recht, L. D., Lim, M., Hirte, H., Ashby, L., Mechtler, L., Goldlust, S. A., Iwamoto, F., Drappatz, J., O'Rourke, D. M., Wong, M., Hamilton, M. G., Finocchiaro, G., Perry, J., Wick, W., Green, J., He, Y., Turner, C. D., Yellin, M. J., Keler, T., Davis, T. A., Stupp, R., Sampson, J. H., & investigators, A. I. t. (2017). Rindopepimut with temozolomide for patients with newly diagnosed, EGFRvIII-expressing glioblastoma (ACT

IV): a randomised, double-blind, international phase 3 trial. *Lancet Oncol*, *18*(10), 1373-1385. https://doi.org/10.1016/S1470-2045(17)30517-X

Weller, M., van den Bent, M., Preusser, M., Le Rhun, E., Tonn, J. C., Minniti, G., Bendszus, M., Balana, C., Chinot, O., Dirven, L., French, P., Hegi, M. E., Jakola, A. S., Platten, M., Roth, P., Ruda, R., Short, S., Smits, M., Taphoorn, M. J. B., von Deimling, A., Westphal, M., Soffietti, R., Reifenberger, G., & Wick, W. (2020). EANO guidelines on the diagnosis and treatment of diffuse gliomas of adulthood. *Nat Rev Clin Oncol*. https://doi.org/10.1038/s41571-020-00447-z

Westermark, B., Ponten, J., & Hugosson, R. (1973). Determinants for the establishment of permanent tissue culture lines from human gliomas. *Acta Pathol Microbiol Scand A*, *81*(6), 791-805. https://doi.org/10.1111/j.1699-0463.1973.tb03573.x

Wolpaw, A. J., Shimada, K., Skouta, R., Welsch, M. E., Akavia, U. D., Pe'er, D., Shaik, F., Bulinski, J. C., & Stockwell, B. R. (2011). Modulatory profiling identifies mechanisms of small molecule-induced cell death. *Proc Natl Acad Sci U S A*, *108*(39), E771-780. https://doi.org/10.1073/pnas.1106149108

Wu, W., Schecker, J., Wurstle, S., Schneider, F., Schonfelder, M., & Schlegel, J. (2018). Aldehyde dehydrogenase 1A3 (ALDH1A3) is regulated by autophagy in human glioblastoma cells. *Cancer Lett*, *417*, 112-123. https://doi.org/10.1016/j.canlet.2017.12.036

Wu, W., Wu, Y., Mayer, K., von Rosenstiel, C., Schecker, J., Baur, S., Wurstle, S., Liesche-Starnecker, F., Gempt, J., & Schlegel, J. (2020). Lipid Peroxidation Plays an Important Role in Chemotherapeutic Effects of Temozolomide and the Development of Therapy Resistance in Human Glioblastoma. *Transl Oncol*, *13*(3), 100748. https://doi.org/10.1016/j.tranon.2020.100748

Yang, S. M., Martinez, N. J., Yasgar, A., Danchik, C., Johansson, C., Wang, Y., Baljinnyam, B., Wang, A. Q., Xu, X., Shah, P., Cheff, D., Wang, X. S., Roth, J., Lal-Nag, M., Dunford, J. E., Oppermann, U., Vasiliou, V., Simeonov, A., Jadhav, A., & Maloney, D. J. (2018). Discovery of Orally Bioavailable, Quinoline-Based Aldehyde Dehydrogenase 1A1 (ALDH1A1) Inhibitors with Potent Cellular Activity. *J Med Chem*, *61*(11), 4883-4903. https://doi.org/10.1021/acs.jmedchem.8b00270

Yang, S. M., Yasgar, A., Miller, B., Lal-Nag, M., Brimacombe, K., Hu, X., Sun, H., Wang, A., Xu, X., Nguyen, K., Oppermann, U., Ferrer, M., Vasiliou, V., Simeonov, A., Jadhav, A., & Maloney, D. J. (2015). Discovery of NCT-501, a Potent and Selective Theophylline-Based Inhibitor of Aldehyde Dehydrogenase 1A1 (ALDH1A1). *J Med Chem*, *58*(15), 5967-5978. https://doi.org/10.1021/acs.jmedchem.5b00577

Yang, W. S., SriRamaratnam, R., Welsch, M. E., Shimada, K., Skouta, R., Viswanathan, V. S., Cheah, J. H., Clemons, P. A., Shamji, A. F., Clish, C. B., Brown, L. M., Girotti, A. W., Cornish, V. W., Schreiber, S. L., & Stockwell, B. R. (2014). Regulation of ferroptotic cancer cell death by GPX4. *Cell*, *156*(1-2), 317-331. https://doi.org/10.1016/j.cell.2013.12.010

Yang, W. S., & Stockwell, B. R. (2008). Synthetic lethal screening identifies compounds activating iron-dependent, nonapoptotic cell death in oncogenic-RAS-harboring cancer cells. *Chem Biol*, *15*(3), 234-245. https://doi.org/10.1016/j.chembiol.2008.02.010

Yang, W. S., & Stockwell, B. R. (2016). Ferroptosis: Death by Lipid Peroxidation. *Trends Cell Biol*, *26*(3), 165-176. https://doi.org/10.1016/j.tcb.2015.10.014

Yang, Z. L., Yang, L., Zou, Q., Yuan, Y., Li, J., Liang, L., Zeng, G., & Chen, S. (2013). Positive ALDH1A3 and negative GPX3 expressions are biomarkers for poor prognosis of gallbladder cancer. *Dis Markers*, *35*(3), 163-172. https://doi.org/10.1155/2013/187043

Yu, Z., Pestell, T. G., Lisanti, M. P., & Pestell, R. G. (2012). Cancer stem cells. *Int J Biochem Cell Biol*, *44*(12), 2144-2151. https://doi.org/10.1016/j.biocel.2012.08.022

Zhang, J., Stevens, M. F., & Bradshaw, T. D. (2012). Temozolomide: mechanisms of action, repair and resistance. *Curr Mol Pharmacol*, *5*(1), 102-114. https://doi.org/10.2174/1874467211205010102

Zhang, L., Zhang, S., Yao, J., Lowery, F. J., Zhang, Q., Huang, W. C., Li, P., Li, M., Wang, X., Zhang, C., Wang, H., Ellis, K., Cheerathodi, M., McCarty, J. H., Palmieri, D., Saunus, J., Lakhani, S., Huang, S., Sahin, A. A., Aldape, K. D., Steeg, P. S., & Yu, D. (2015). Microenvironment-induced PTEN loss by exosomal microRNA primes brain metastasis outgrowth. *Nature*, *527*(7576), 100-104. https://doi.org/10.1038/nature15376

Zhang, Y., Dube, C., Gibert, M., Cruickshanks, N., Wang, B., Coughlan, M., Yang, Y., Setiady, I., Deveau, C., Saoud, K., Grello, C., Oxford, M., Yuan, F., & Abounader, R. (2018). The p53 Pathway in Glioblastoma. *Cancers*, *10*(9), 297. https://doi.org/10.3390/cancers10090297

Zheng, X., Shen, G., Yang, X., & Liu, W. (2007). Most C6 cells are cancer stem cells: evidence from clonal and population analyses. *Cancer Res*, *67*(8), 3691-3697. https://doi.org/10.1158/0008-5472.CAN-06-3912

Zhou, X. D., Wang, X. Y., Qu, F. J., Zhong, Y. H., Lu, X. D., Zhao, P., Wang, D. H., Huang, Q. B., Zhang, L., & Li, X. G. (2009). Detection of cancer stem cells from the C6 glioma cell line. *J Int Med Res*, *37*(2), 503-510. https://doi.org/10.1177/147323000903700226

Zilka, O., Shah, R., Li, B., Friedmann Angeli, J. P., Griesser, M., Conrad, M., & Pratt, D. A. (2017). On the Mechanism of Cytoprotection by Ferrostatin-1 and Liproxstatin-1 and the Role of Lipid Peroxidation in Ferroptotic Cell Death. *ACS Cent Sci*, *3*(3), 232-243. https://doi.org/10.1021/acscentsci.7b00028

Zussman, B. M., & Engh, J. A. (2015). Outcomes of the ACT III Study: Rindopepimut (CDX-110) Therapy for Glioblastoma. *Neurosurgery*, *76*(6), N17. https://doi.org/10.1227/01.neu.0000465855.63458.0c

10 Tables

11 Figures